Real-Time Dynamics of Open Quantum Systems

and

Anyonic Statistics in Doubled-Chern-Simons Theories

Inauguraldissertation
der Philosophisch-naturwissenschaftlichen Fakultät
der Universität Bern

vorgelegt von

Stephan Caspar

von Klosters-Serneus GR

Leiter der Arbeit:

Prof. Dr. U.-J. Wiese

Albert Einstein Center for Fundamental Physics
Institut für Theoretische Physik, Universität Bern

Abstract

In the first part of this thesis we investigate real-time evolution of open quantum systems. We derive the Lindblad equation, as the Markovian master equation for their evolution. The Lindblad equation can be expressed by a series of jump operators. We then derive conditions on these jump operators under which closed hierarchies of observables arise. The real-time evolution can then be expressed as a set of coupled differential equations, which grows only polynomially with the size of the system. In particular we were able to apply this to a process that drives hardcore bosons (or spins 1/2) into a Bose-Einstein condensate. The polynomial size of the problem allowed us to investigate this process free from any approximations, thus enabling us to obtain reliable information for large systems and arbitrarily long evolution periods. Furthermore we studied the stability of the condensation process under competing thermal and non-thermal effects.

Under suitable conditions, the Lindblad equation is also solvable using Monte Carlo techniques. We present an algorithm for a specific case of hardcore boson condensation that is also solvable with the closed hierarchy approach. This allowed us to verify the statistical approach as a potentially useful complementary method to study real-time dynamics.

The second part is dedicated to the construction of doubled lattice Chern-Simons theories with discrete non-Abelian gauge groups. The two gauge fields live on a lattice and its dual. The Chern-Simons nature is implemented locally on a cross of links from both lattices by a non-commuting operator algebra of the two gauge fields. Gauge invariance requires that the deformed algebra fulfills a consistency condition. We provide a classification of all consistent theories in terms of the structure of the gauge group. We investigate the topological structure of these theories in terms of the braiding statistics of external charges and we show that they exhibit mutual Abelian statistics akin to Kitaev's toric code. All these theories have a finite dimensional Hilbert space and are thus, at least in principle, implementable on a quantum simulator.

Contents

Part I

Real-Time Dynamics of Open Quantum Systems

1 Introduction

The real-time-evolution of a quantum system is notoriously difficult to study, both analytically and numerically. The main reason lies, of course, in the intractability of the dimension of the Hilbert space, which contains all possible states of the quantum system, and typically grows exponentially with the size of the system. In practice it is therefore impossible to keep track of all possible states throughout the entire time-evolution of the system. We are therefore in need of a guiding principle in order to decide which states are important, and which can be neglected. Two standard approaches dominate theoretical quantum physics today: Perturbation theory and stochastic methods. Perturbation theory relies on the fact that, starting from a simple initial state of low energy and particle density, large parts of the Hilbert space are inaccessible due to conservation laws. Furthermore, the interaction strength between different particles allows one to preselect the most probable final states among the accessible ones. The problem then reduces to calculating a handful of transitions amplitudes, which can be done order by order in the number of interactions, thus also restricting the intermediate states. Statistical quantum mechanics, on the other hand, can be applied in the regime of high energy and particle density. The complexity of the Hilbert space is reduced by only looking at a representative sample of the thermal density matrix, using importance sampling methods. Neither approach gives a solution to the question of real-time-evolution of a quantum system. They both yield information about the most likely final state after an infinite amount of time has passed. Perturbation theory enables us to identify the most likely final states long after the interaction of a few initial state particles collided and allows us to calculate their likelihood. Statistical quantum mechanics allows one to describe the final state in terms of a representative sample of states with similar energy and particle density, thus assuming the system reaches a thermal equilibrium. But what about high density states, far from thermal equilibrium? Perturbative methods cannot help us since the conservation laws do not significantly reduce the accessible Hilbert space. Stochastic methods face an insurmountable obstacle in unitary time-evolution, since transition amplitudes carry complex phases. Thus different intermediate states interfere with each other, prohibiting a direct probabilistic interpretation of the time-evolution and therefore the use of importance sampling. A third method employed in the study of real-time dynamics is the density matrix renormalization group (DMRG) [1, 2], it is, however, only applicable to gapped one-dimensional systems and growing entanglement makes it unreliable after a short period of time [3–6].

In this part of the thesis we circumvent the difficulties of unitary evolution of closed systems and consider the time-evolution of open quantum systems. There the time-evolution of the density matrix is given by the Lindblad master equation [7]. In addition to the familiar Hamiltonian contributions, the Lindblad equation contains a series of jump operators, which describe interactions between the system and its environment. By engineering the coupling to the environment [8], open systems can be used to prepare specific quantum states [9–13], simulation of quantum systems [14–16] and even quantum computing [9, 17–19]. These concepts have proven to be viable in experiments with ultracold gases and trapped ions [20–22] and the recent progress is promising a better understanding of quantum real-time dynamics with the help of quantum simulators [23, 24].

By going to the Heisenberg picture of evolving operators, one can derive coupled differential equations for all observables. The number of coupled observables is again exponentially large. However, the system of differential equations typically provides a hierarchy among the observables. Assuming only bi-local operators contributing to the time-evolution, one can show that the time-evolution of n-point functions depends at most on all $(n+1)$-point functions. This provides a natural separation of all observables and a truncation above some n can be introduced, when studying the time-evolution of a typical 2-point function. However, truncating the hierarchy limits the reliability of the method to short time intervals. Here we investigate conditions under which the hierarchy closes exactly [25], such that the evolution of a set of low-order n-point functions is independent from all other observables. While this is usually not possible in Hamiltonian systems, several examples have been found for open, dissipative systems [26–31], where the evolution can be studied for an arbitrarily long time. The closure conditions for bosonic and fermionic models

have been derived in [32].

In particular we are interested in the generation of a condensate in spin-1/2 systems, which can also be reinterpreted by a mapping to hard-core bosons. This can be achieved with bilocal jump operators only [33, 34], while multilocal operators provide a way to generate states with non-trivial topology [35–38]. It is a quite common in dissipative systems that the nonequilibrium steady state (NESS) is known exactly and a wide variety of states and processes are described in the literature, from condensed bosons and η states of fermions [39, 40], to states with topological order [41–44] or even fermionic d-wave pairing [45, 46]. This is also true for the condensation of hardcore bosons or quantum spins [34] considered here. The real-time-evolution, however, is a much more complicated problem, and the dynamics of approaching these final states are not well understood. Due to the closure of the hierarchy, the real-time solution can be derived semi-analytically with manageable effort, even for large systems. We investigate the approach to a steady state, in particular the slowest decay rate, the dissipative gap, which sets the time scale for reaching the steady state of the system. Its finite size scaling has been studied in several one-dimensional systems before [26–30, 32, 47–50], but our method is directly applicable to higher-dimensional lattices as well and we will find that the scaling behavior varies in a nontrivial way with the dimensionality of the system [51, 52].

2 The Lindblad Equation

2.1 Density Matrix

In quantum mechanics the state of a system is described by a vector $|\psi\rangle \in \mathcal{H}$ in the Hilbert space. Any observable then corresponds to a Hermitian operator $O = O^\dagger$, and its expectation value is given by

$$\langle O \rangle = \langle \psi | O | \psi \rangle,$$

assuming that the state vector is properly normalized to $\langle \psi | \psi \rangle = 1$. The invariance of the normalization then restricts the time-evolution operator to be unitary

$$|\psi(t)\rangle = U(t)|\psi(0)\rangle \quad \Rightarrow \quad 1 = \langle \psi(t)|\psi(t)\rangle = \langle \psi(0)|U(t)^\dagger U(t)|\psi(0)\rangle \quad \Rightarrow \quad U(t)^\dagger U(t) = \mathbb{1},$$

which in turn fixes the Schrödinger equation for both the state and the time-evolution operator ($\hbar = 1$)

$$\partial_t |\psi(t)\rangle = -iH(t)|\psi(t)\rangle, \qquad \partial_t U(t) = -iH(t)U(t),$$

in terms of a (possibly time-dependent) Hermitian Hamiltonian $H(t)$. Observables can be computed at any instant in time using

$$\langle O \rangle(t) = \langle \psi(t)|O|\psi(t)\rangle = \langle \psi(0)|U(t)^\dagger O U(t)|\psi(0)\rangle = \langle \psi(0)|O(t)|\psi(0)\rangle,$$

yielding the Heisenberg equation for the evolution of observables

$$\partial_t O(t) = \partial_t (U(t)^\dagger O U(t)) = iU(t)^\dagger [H(t), O] U(t) = i[H_H(t), O(t)], \tag{1}$$

where the Hamiltonian in the Heisenberg picture is given by $H_H(t) = U(t)^\dagger H(t) U(t)$. All of this requires that we know the initial state $|\psi(0)\rangle$ of the system exactly. In case we only have probabilistic information, namely that the initial state was one of an orthonormal set $\{|\psi_i\rangle\}$, each with probability $0 \leq p_i \leq 1$ ($\sum_i p_i = 1$) we can rewrite the expectation value of an observable as

$$\langle O \rangle = \sum_i p_i \langle O \rangle_i = \sum_i p_i \langle \psi_i | O | \psi_i \rangle = \sum_i p_i \mathrm{Tr}\left[O |\psi_i\rangle\langle\psi_i| \right] = \mathrm{Tr}\left[O\rho \right],$$

in terms of the density matrix

$$\rho = \sum_i p_i |\psi_i\rangle\langle\psi_i|, \tag{2}$$

and the trace, which is nothing but a sum over a complete set of states of the Hilbert space (or the subspace spanned by the $|\psi_i\rangle$).

2.2 Superoperators

Similar to state vectors $|\psi\rangle$, the dynamics of density matrices ρ is described by linear operators $\mathcal{A}, \mathcal{B}$ acting on the vector space of density matrices

$$\mathcal{A}(\rho + \rho') = \mathcal{A}\rho + \mathcal{A}\rho', \qquad (\mathcal{A} + \mathcal{B})\rho = \mathcal{A}\rho + \mathcal{B}\rho.$$

In order to avoid confusion with the linear operators O acting on the Hilbert space $\mathcal{H}$, they are sometimes called superoperators, as we will in this thesis. The operators O can be embedded into the space of superoperators in two nonequivalent ways, either linearly or anti-linearly

$$\mathcal{O}\rho = O\rho, \qquad \overline{\mathcal{O}}\rho = \rho O^\dagger,$$

and any superoperator can be decomposed in terms of operators B_i, C_i

$$\mathcal{A}\rho = \sum_i B_i \rho C_i^\dagger.$$

This is a direct consequence of the fact that the density matrices are by construction elements of the product space of two copies of the Hilbert space $\mathcal{H} \otimes \overline{\mathcal{H}}$ and any operator in the product space can be written as

$$\mathcal{A} = \sum_i B_i \otimes \overline{C}_i.$$

Unitary evolution of density matrices is then described by the superoperator

$$\rho(t) = \mathcal{O}(t)\rho = U(t)\rho U(t)^\dagger, \tag{3}$$

and thus fulfills the Liouville-von Neumann equation

$$\partial_t \rho(t) = \mathcal{H}(t)\rho(t) = -i[H(t), \rho(t)]. \tag{4}$$

Again the Schrödinger picture, given by the evolving density matrix according to (4), is completely equivalent to the Heisenberg picture (1) when calculating expectation values

$$\langle O \rangle(t) = \mathrm{Tr}\left[O\rho(t)\right] = \mathrm{Tr}\left[O(t)\rho\right].$$

However, the density matrix is not restricted to unitary evolution, since the normalization condition $\langle\psi|\psi\rangle = 1$ is replaced by the more general trace

$$\mathrm{Tr}\left[\rho\right] = \sum_i p_i \mathrm{Tr}\left[|\psi_i\rangle\langle\psi_i|\right] = \sum_i p_i = 1,$$

and positivity conditions (which also implies hermiticity $\rho = \rho^\dagger$)

$$\langle\psi|\rho|\psi\rangle = \sum_{i,j} \alpha_i^* \alpha_j \langle\psi_i|\rho|\psi_j\rangle = \sum_{i,j} \alpha_i^* \alpha_j p_i \delta_{ij} = \sum_i |\alpha_i|^2 p_i \geq 0.$$

2.3 Time Evolution of Density Matrices

How can we generalize the time-evolution of a density matrix? First of all, time-evolution is nothing but a map that takes the density matrix of an earlier time ρ as input and produces the density matrix ρ' at a later time as an output. This map should be linear (a component contributing p_i to the initial state should also produce a fraction p_i of the final state). Abandoning unitarity implies that the system can transfer information to its environment, which means we are studying open quantum systems. However we assume the evolution to be Markovian, which means that the environment does not keep a memory of the information it receives. This assumption is well motivated if one considers the environment to be infinitely large, such that the information received by the environment is spread so thinly, that the system itself is unable to feel its effect. The Markovian assumption excludes memory effects, making the evolution equation local in time. The future state ρ' thus only depends on the current state ρ, but is indifferent to its past. Taken together, the Markovian and linear constraint imply that we can write the map as a superoperator $\rho' = \mathcal{A}\rho$. In a basis $|\psi_i\rangle$ we can write this superoperator explicitly [53]

$$\rho'_{ij} = \langle\psi_i|\rho'|\psi_j\rangle = \langle\psi_i|\mathcal{A}\rho|\psi_j\rangle = \sum_{k,l} A_{ik,jl}\langle\psi_k|\rho|\psi_l\rangle = \sum_{k,l} A_{ik,jl}\rho_{kl} \tag{5}$$

which is nothing but a matrix operation in the vector-space of density matrices. We start constraining the components $A_{ik,jl}$ by using Hermiticity

$$\rho' = \rho'^\dagger \qquad \Leftrightarrow \qquad \sum_{k,l}(A_{ik,jl} - A^*_{jl,ik})\rho_{kl} = 0 \qquad \Leftrightarrow \qquad A_{ik,jl} = A^*_{jl,ik}.$$

The last equality follows since the Hermiticity constraint has to be full-filled for any density matrix ρ. This means that the matrix $A_{ik,jl}$ is Hermitian, which implies that it can be described by a set of orthonormal vectors E^α_{ik} (in the vector space of matrices)

$$\sum_{i,k} E^\alpha_{ik} E^{\beta *}_{ik} = \delta^{\alpha\beta} \qquad \Leftrightarrow \qquad \mathrm{Tr}\left[E^\alpha E^{\beta\dagger}\right] = \delta^{\alpha\beta},$$

and the corresponding real eigenvalues λ^α, such that inserting this into (5) yields

$$\rho'_{ij} = \sum_{k,l} \sum_\alpha E^\alpha_{ik} \lambda^\alpha E^{\alpha *}_{jl} \rho_{kl} = \sum_\alpha \lambda^\alpha (E^\alpha \rho E^{\alpha\dagger})_{ij}. \tag{6}$$

Next we try to fulfill the trace constraint, which (using the cyclicity of the trace) we write as

$$\mathrm{Tr}\left[\rho' - \rho\right] = \mathrm{Tr}\left[\left(\sum_\alpha \lambda^\alpha E^{\alpha\dagger} E^\alpha - \mathbb{1}\right)\rho\right] = \sum_{i,j}\left(\sum_\alpha \lambda^\alpha (E^{\alpha\dagger}E^\alpha)_{ij} - \delta_{ij}\right)\rho_{ji},$$

from which we again conclude

$$\sum_\alpha \lambda^\alpha (E^{\alpha\dagger}E^\alpha)_{ij} = \delta_{ij} \qquad \Leftrightarrow \qquad \sum_\alpha \lambda^\alpha E^{\alpha\dagger}E^\alpha = \mathbb{1}.$$

The final constraint comes from positivity

$$\langle\psi|\rho'|\psi\rangle = \sum_\alpha \lambda^\alpha \langle\psi|E^\alpha \rho E^{\alpha\dagger}|\psi\rangle = \sum_\alpha \lambda^\alpha (\langle\psi|E^\alpha)\rho(E^{\alpha\dagger}|\psi\rangle) \geq 0.$$

This is certainly fulfilled, if all $\lambda^\alpha \geq 0$. This condition is not necessary in order to have positivity and counter-examples can be found easily. However, there is a stronger requirement than positivity which enforces $\lambda^\alpha \geq 0$ and is still physically motivated.

2.4 Complete Positivity

The constraint which enforces $\lambda^\alpha \geq 0$ is known as complete positivity and is defined as follows. Suppose that the quantum system is part of a larger quantum system it has previously interacted with. Thus the joint initial state is in general an entangled state of the system and its environment. Then the evolution of the complete system given by (6), where all operators $E^\alpha \to E^\alpha \otimes \mathbb{1}$ act trivially on the environment, should respect positivity as well. To simplify the derivation of $\lambda^\alpha \geq 0$ we now assume that the full Hilbert space consists of two copies of the initial system, with basis vectors $|\psi_i\rangle \otimes |\chi_j\rangle$, then a general state $|\Psi\rangle$ and an independent pure density matrix $\mathcal{P}$ can be written as

$$\begin{aligned} |\Psi\rangle &= \sum_{i,j} D_{ij} |\psi_i\rangle|\chi_j\rangle, \\ \mathcal{P} &= \sum_{i,j,k,l} C_{ij} C^*_{kl} |\psi_i\rangle|\chi_j\rangle\langle\psi_k|\langle\chi_l|, \end{aligned} \tag{7}$$

with the single constraint $\mathrm{Tr}[\mathcal{P}] = \mathrm{Tr}[C^\dagger C] = 1$. Complete positivity is then given by the inequality

$$\begin{aligned} \langle\Psi|\mathcal{P}'|\Psi\rangle &= \sum_\alpha \lambda^\alpha \langle\Psi|E^\alpha \mathcal{P} E^{\alpha\dagger}|\Psi\rangle \\ &= \sum_\alpha \lambda^\alpha \sum_{i,j,k,l} D^*_{ij}\langle\psi_i|\langle\chi_j|E^\alpha|\psi_k\rangle|\chi_l\rangle C_{kl} \sum_{m,n,o,p} C^*_{mn}\langle\psi_m|\langle\chi_n|E^{\alpha\dagger}|\psi_o\rangle|\chi_p\rangle D_{op} \\ &= \sum_\alpha \lambda^\alpha \sum_{i,j,k,l} D^*_{ij} E^\alpha_{ik} \delta_{jl} C_{kl} \sum_{m,n,o,p} C^*_{mn} E^{\alpha\dagger}_{mo} \delta_{np} D_{op} \\ &= \sum_\alpha \lambda^\alpha \mathrm{Tr}\left[E^\alpha C D^\dagger\right] \mathrm{Tr}\left[D C^\dagger E^{\alpha\dagger}\right] \geq 0 \\ &= \sum_\alpha \lambda^\alpha \left|\mathrm{Tr}\, E^\alpha C D^\dagger\right|^2 \geq 0. \end{aligned} \tag{8}$$

To conclude the proof we need to choose C, D in order to isolate a single eigenvalue λ^β. The pair $D = \mathbb{1}, C = E^{\beta\dagger}$ fulfills the trace constraint $\mathrm{Tr}[C^\dagger C] = \mathrm{Tr}\left[E^\beta E^{\beta\dagger}\right] = 1$ and reduces the complete positivity inequality to

$$\sum_\alpha \lambda^\alpha \left|\mathrm{Tr}\, E^\alpha C D^\dagger\right|^2 = \sum_\alpha \lambda^\alpha (\delta^{\alpha\beta})^2 = \lambda^\beta \geq 0,$$

for any choice of β. In conclusion we have shown that $\lambda^\beta \geq 0$ is a necessary condition for complete positivity. It is also sufficient, as (8) is also valid for Hilbert spaces of arbitrary dimension and positivity for general density matrices follows directly from the positivity of all pure density matrices $\mathcal{P}$.

2.5 The Kraus Representation

We have shown that completely positive and trace preserving linear maps $\rho' = \mathcal{A}\rho$ always have a Kraus representation [54], which means that they can be described by set of Kraus operators $M^\alpha = \sqrt{\lambda^\alpha} E^\alpha$ obeying

$$\rho' = \sum_\alpha M^\alpha \rho M^{\alpha\dagger}, \qquad \sum_\alpha M^{\alpha\dagger} M^\alpha = \mathbb{1}, \qquad \mathrm{Tr}\left[M^\alpha M^{\beta\dagger}\right] = \lambda^\alpha \delta^{\alpha\beta}.$$

However, one can show that the third (orthogonality) condition is not necessary and any set of Kraus operators defines a map with the desired properties (even overcomplete sets). Trace preservation follows directly from the second condition. Complete positivity can be shown for every Kraus operator individually. Choosing an arbitrary basis $|\chi_i\rangle$ for the environment and state $|\psi\rangle$ as in equation (7), complete positivity reduces to the statement

$$\begin{aligned}\langle\Psi|\left(M^\alpha \rho M^{\alpha\dagger} \otimes |\chi_1\rangle\langle\chi_1|\right)|\Psi\rangle &= \sum_{i,j} D^*_{i1} D_{j1} \langle\psi_i|M^\alpha \rho M^{\alpha\dagger}|\psi_j\rangle \\ &= \left(\sum_i D^*_{i1}\langle\psi_i|M^\alpha\right) \rho \left(\sum_j D_{j1} M^{\alpha\dagger}|\psi_j\rangle\right) \geq 0,\end{aligned}$$

since any initial density matrix $\mathcal{P}$ can be written as a sum of terms of this form.

2.6 Infinitesimal Time-Evolution

Now that we have formulated the generalization of the unitary map (3) we would like to derive a differential equation for a continuous family of maps $\rho(t) = \mathcal{A}(t)\rho$ which generalizes the Liouville-von Neumann equation (4). Time-dependent maps can be described by a time-dependent set $M^\alpha(t)$ of Kraus operators. The initial condition $\rho(0) = \rho$ can be written as

$$\rho = \mathbb{1}\rho\mathbb{1}$$

and can thus be described by a single Kraus operator $M^0 = \mathbb{1}$. The map to $\rho(\delta t)$ for an infinitesimal δt can therefore be described by the set of Kraus operators

$$M^0(\delta t) = \mathbb{1} + B\delta t, \qquad M^\alpha(\delta t) = K^\alpha\sqrt{\delta t}, \quad \alpha > 0,$$

where B, K^α are arbitrary operators. The Kraus operators M^α with $\alpha > 0$ scale with the square root of δt, since they only appear quadratically in the infinitesimal map

$$\rho(\delta t) = (\mathbb{1} + B\delta t)\rho(\mathbb{1} + B^\dagger\delta t) + \delta t \sum_\alpha K^\alpha \rho K^{\alpha\dagger} + \mathcal{O}(\delta t^2).$$

Taking the limit $\delta t \to 0$ we obtain the differential equation

$$\partial_t \rho(t) = B\rho(t) + \rho(t)B^\dagger + \sum_\alpha K^\alpha \rho(t) K^{\alpha\dagger}.$$

The trace constraint $\mathrm{Tr}[\partial_t\rho(t)] = 0$ becomes

$$\mathrm{Tr}\left[\left(B + B^\dagger + \sum_\alpha K^{\alpha\dagger}K^\alpha\right)\rho(t)\right] = 0 \qquad \Rightarrow \qquad B + B^\dagger + \sum_\alpha K^{\alpha\dagger}K^\alpha = 0. \tag{9}$$

Reinserting this into the differential equation to eliminate the symmetric combination $B + B^\dagger$ yields the Lindblad equation [7]

$$\begin{aligned}\partial_t \rho(t) &= [\frac{1}{2}(B - B^\dagger), \rho(t)] + \sum_\alpha \left[K^\alpha \rho(t) K^{\alpha\dagger} - \frac{1}{2}\{K^{\alpha\dagger} K^\alpha, \rho(t)\}\right] \\ &= -i[H, \rho(t)] + \sum_\alpha \left[L^\alpha \rho(t) L^{\alpha\dagger} - \frac{1}{2}\{L^{\alpha\dagger} L^\alpha, \rho(t)\}\right] \\ &= \mathcal{H}\rho(t) + \mathcal{L}\rho(t),\end{aligned} \tag{10}$$

with Hermitian Hamiltonian $H = \frac{i}{2}(B - B^\dagger)$ and Lindblad operators $L^\alpha = K^\alpha$. The trace constraint (9) has eliminated the symmetric combination $B + B^\dagger$ and thus no longer constrains the Hamiltonian H or the Lindblad operators L^α at all, as it now just trivially identifies $\sum_\alpha L^{\alpha\dagger} L^\alpha$ with an arbitrary Hermitian operator. Although we have not explicitly written it this way, no step in the above derivation is an obstruction to making $H(t)$ and $L^\alpha(t)$ time-dependent. As we have derived it from an infinitesimal Kraus representation, the Lindblad equation (10) itself is thus the most general differential equation for trace preserving, completely positive maps of density matrices.

2.7 Physics of the Lindblad Equation

We have shown how the Liouville-von Neumann equation (4) for the evolution of quantum systems described by a density matrix can be generalized to the Lindblad equation

$$\partial_t \rho(t) = -i[H, \rho(t)] + \sum_\alpha \left[L^\alpha \rho(t) L^{\alpha\dagger} - \frac{1}{2}\{L^{\alpha\dagger} L^\alpha, \rho(t)\}\right]. \tag{11}$$

So what are the physical consequences of adding Lindblad operators to the evolution equation? The primary difference is the loss of reversibility. While completely positive and trace preserving maps form a semi-group under composition

$$\mathcal{A}_1 \mathcal{A}_2 \rho = \sum_{\alpha,\beta} M_1^\alpha M_2^\beta \rho M_2^{\beta\dagger} M_1^{\alpha\dagger} = \sum_{\alpha\beta} M^{\alpha\beta} \rho M^{\alpha\beta\dagger} = \mathcal{A}\rho, \qquad M^{\alpha\beta} = M_1^\alpha M_2^\beta,$$

it is in general not possible to define an inverse (especially one that is completely positive as well). For instance, the map defined by a complete set of projection operators $M^\alpha M^\beta = \delta^{\alpha\beta} M^\alpha, \sum_\alpha M^\alpha = \mathbb{1}$ acts on a general density matrix as

$$\rho = \begin{pmatrix} \rho_{11} & \rho_{12} & \cdots \\ \rho_{21} & \rho_{22} & \\ \vdots & & \ddots \end{pmatrix} \qquad \rightarrow \qquad \rho' = \begin{pmatrix} \rho_{11} & 0 & \cdots \\ 0 & \rho_{22} & \\ \vdots & & \ddots \end{pmatrix}.$$

The complete loss of information about the off-diagonal correlations $\rho_{\alpha\beta}, \alpha \neq \beta$ clearly makes this map irreversible. Although the Lindblad equation (11) only generates such maps asymptotically, the (finite) suppression of matrix elements can not be reversed through the Lindblad equation and highly different initial states may converge to the same final state. A second important feature is the transition from pure to mixed state density matrices (and vice versa). Although, from a mathematical standpoint, the Lindblad equation defines a deterministic evolution of the density matrix, mixed density matrices still have the physical interpretation of uncertainty with respect to the true current state of the system described by the wave function $|\psi\rangle$. Thus the Lindblad equation describes a probabilistic evolution of the quantum system, with discrete jumps $|\psi\rangle \rightarrow L^\alpha |\psi\rangle$ happening at a characteristic rate $\langle\psi| L^{\alpha\dagger} L^\alpha |\psi\rangle$. The Lindblad equation thus describes an open quantum system, which interacts with its environment under appropriate conditions (large bath, fast relaxation times, weak interaction). It is thus a good candidate to model decoherence and measurement effects, for instance in experiments. We will now discuss two examples of how the Lindblad equation arises for systems with decoherence and systems which undergo continued and unsupervised measurement, before we show how it can be derived as an approximation to a unitary interaction of system and bath.

2.7.1 Decoherence

Imagine that the phases of the two states $|0\rangle, |1\rangle$ get repeatedly shoved independently of each other, thus effectively performing a random walk. Then the total acquired phase after time t follows a normal distribution

$$\theta_i(t) \sim N(0, \lambda_i t),$$

with different rates $\lambda_{0,1}$. The density matrix then evolves as ($P_i = |i\rangle\langle i|$)

$$\rho(t) = \int \frac{d^2\theta}{2\pi\sqrt{\lambda_0\lambda_1 t}} e^{-\frac{\theta_0^2}{2\lambda_0 t} - \frac{\theta_1^2}{2\lambda_1 t}} e^{i(\theta_0 P_0 + \theta_1 P_1)} \rho(0) e^{-i(\theta_0 P_0 + \theta_1 P_1)},$$

which is already in Kraus form (although with a continuous set of operators). Performing the integrals we obtain

$$\begin{aligned}\rho(t) &= P_0\rho(0)P_0 + e^{-\frac{\lambda_0+\lambda_1}{2}t} P_0\rho(0)P_1 + e^{-\frac{\lambda_0+\lambda_1}{2}t} P_1\rho(0)P_0 + P_1\rho(0)P_1 \\ &= (P_0 + e^{-\frac{\lambda_0+\lambda_1}{2}t}P_1)\rho(0)(P_0 + e^{-\frac{\lambda_0+\lambda_1}{2}t}P_1) + (1 - e^{-(\lambda_0+\lambda_1)t})P_1\rho(0)P_1,\end{aligned}$$

which show exponential decay of the off-diagonal correlations ρ_{01}, ρ_{10}. Taking the derivative provides us with the Lindblad equation

$$\begin{aligned}\partial_t\rho(t) &= -\frac{\lambda_0+\lambda_1}{2}\left[e^{-\frac{\lambda_0+\lambda_1}{2}t} P_0\rho(0)P_1 + e^{-\frac{\lambda_0+\lambda_1}{2}t} P_1\rho(0)P_0\right] \\ &= -\frac{\lambda_0+\lambda_1}{2}\left[\rho(t) - P_0\rho(t)P_0 - P_1\rho(t)P_1\right] \\ &= \frac{\lambda_0+\lambda_1}{2}\sum_{i=0,1}\left[P_i\rho(t)P_i - \frac{1}{2}\{P_i, \rho(t)\}\right],\end{aligned}$$

with Lindblad operators $L^i = \sqrt{(\lambda_0+\lambda_1)/2}P_i$.

2.7.2 Continuous Unsupervised Measurement

Measuring an observable O of a quantum system collapses the wave function $|\psi\rangle$ into the subspace $P_\lambda(O)^2 = P_\lambda(O)$ of the measured eigenvalue λ. The probability for measuring λ is given by $p_\lambda = \langle\psi|P_\lambda(O)|\psi\rangle$. The density matrix describing all possible measurement outcomes is thus given by

$$\rho' = \mathcal{O}\rho = \sum_\lambda P_\lambda(O)\rho P_\lambda(O), \qquad \sum_\lambda P_\lambda(O)P_\lambda(O) = \mathbb{1},$$

and is obviously of Kraus from. We use the notation where $\mathcal{O}$ denotes the map of density matrices under measurement, and not the operator which is used to determine expectation values. Since we are not interested in the result λ of the measurement process, the map itself contains the complete information about this process. Now we are interested in the process where multiple measurements are performed at random instances of time. The average time separation between consecutive measurements is governed by a rate ν and we assume that they occur independent of each other, thus the number of measurements per time interval follows a Poisson distribution. In between two measurements the system evolves according to the Liouville-von Neumann equation

$$\partial_t\rho(t) = -i[H, \rho(t)], \qquad \rho(t) = \mathcal{U}(t,t')\rho(t') = e^{-iH(t-t')}\rho(t')e^{iH(t-t')}.$$

The full time-evolution is then given by the infinite sum

$$\begin{aligned}\rho(t) &= \sum_{n=0}^{\infty} e^{-\nu t}\nu^n \int_0^t dt_n \int_0^{t_n} dt_{n-1} \cdots \int_0^{t_2} dt_1 \mathcal{U}(t,t_n)\mathcal{O}\mathcal{U}(t_n,t_{n-1})\cdots\mathcal{O}\mathcal{U}(t_2,t_1)\mathcal{O}\mathcal{U}(t_1,t_0)\rho(t_0) \\ &= \mathcal{V}(t,t_0)\rho(t_0).\end{aligned}$$

Since $\mathcal{O}$ and $\mathcal{U}$ are both completely positive trace-preserving maps, it is straightforward to show that the full map $\mathcal{V}$ is also completely positive and preserves the trace

$$\mathrm{Tr}\rho(t) = \sum_{n=0}^{\infty} e^{-\nu t}\nu^n \int_0^t dt_n \int_0^{t_n} dt_{n-1} \cdots \int_0^{t_2} dt_1 \mathrm{Tr}\rho(t_0) = \sum_n e^{-\nu t}\frac{(\nu t)^n}{n!} = 1.$$

To show that this family of maps obeys the Lindblad equation, we simplify it to an iterated equation

$$\rho(t) = e^{-\nu t}\left[\mathcal{U}(t,t_0)\rho(t_0) + \nu\int_0^t dt_n e^{\nu t_n}\mathcal{U}(t,t_n)\mathcal{O}\mathcal{V}(t_n,t_0)\rho(t_0)\right], \tag{12}$$

before simply taking the derivative with respect to t to obtain

$$\begin{aligned}\partial_t\rho(t) &= -\nu\rho(t) - i[H,\rho(t)] + \nu\mathcal{U}(t,t)\mathcal{O}\mathcal{V}(t,t_0)\rho(t_0)\\ &= -i[H,\rho(t)] + \nu\left[\mathcal{O}\rho(t) - \rho(t)\right]\\ &= -i[H,\rho(t)] + \nu\sum_\lambda\left[P_\lambda(O)\rho(t)P_\lambda(O) - \frac{1}{2}\{P_\lambda(O)^2,\rho(t)\}\right].\end{aligned}$$

This derivation neatly interprets the Lindblad equation as the evolution under randomly occurring measurements (or generalized measurements if the Lindblad operators are not projection operators). The rate of measurement ν dictates the exponential decay of the contributions from an undisturbed (unmeasured) system (12), while the full evolution can be broken down as a series of $\sim \nu t$ measurements with intermediate unitary evolution.

2.8 Lindblad Equation from Unitary Interactions with a Thermal Bath

The derivation of the Lindblad equation from the joint von Neumann equation of system and bath rests upon three key assumptions. The first is that the initial state has no correlations between system and bath, therefore the density matrix is separable and can be written as a product

$$\rho = \rho_S \otimes \rho_B, \qquad\qquad \rho_B \sim e^{-\beta H_B},$$

where ρ_S is an arbitrary initial state of the system and ρ_B describes a thermal state of the bath Hamiltonian H_B. Second we have the Markov condition which removes memory effects from the bath. By introducing the projection superoperators $\mathcal{P} + \mathcal{Q} = \mathbb{1}$ defined by

$$\mathcal{P}\rho = \mathrm{Tr}_B(\rho)\otimes\rho_B,$$

we immediately identify $\mathcal{P}\rho$ as the part of ρ, which carries all relevant information about the reduced system $\mathrm{Tr}_B\rho = \mathrm{Tr}_B\mathcal{P}\rho$ and fulfills the Markov condition. Finally, we assume the system and bath to be weakly coupled

$$H = H_S + H_B + \lambda V = H_S\otimes\mathbb{1} + \mathbb{1}\otimes H_B + \lambda V,$$

through an interaction λV, such that we can expand in powers of λ. For the derivation it is practical to go to the interaction picture

$$\begin{aligned}\tilde\rho(t) &= e^{i(H_S+H_B)t}\rho(t)e^{-i(H_S+H_B)t}, &\qquad \partial_t\tilde\rho(t) &= -i\lambda[\tilde V(t),\tilde\rho(t)] = -i\lambda\mathcal{V}(t)\tilde\rho(t),\\ \tilde V(t) &= e^{i(H_S+H_B)t}Ve^{-i(H_S+H_B)t}, &\qquad \mathcal{P}\tilde\rho(t) &= e^{i(H_S+H_B)t}[\mathcal{P}\rho(t)]e^{-i(H_S+H_B)t}.\end{aligned} \tag{13}$$

The last equation shows that the projection superoperator commutes with the interaction transformations, since H_S, H_B commute and H_B commutes with its thermal state density matrix ρ_B. Furthermore we have introduced the interaction superoperator $\mathcal{V}(t)\cdot = [\tilde V(t),\cdot]$ to simplify the notation. We now split the von Neumann equation into two parts by inserting the projection operators $\mathbb{1} = \mathcal{P} + \mathcal{Q}$

$$\partial_t\mathcal{P}\tilde\rho(t) = -i\lambda\mathcal{P}\mathcal{V}(t)\mathcal{P}\tilde\rho(t) - i\lambda\mathcal{P}\mathcal{V}(t)\mathcal{Q}\tilde\rho(t), \tag{14}$$

$$\partial_t\mathcal{Q}\tilde\rho(t) = -i\lambda\mathcal{Q}\mathcal{V}(t)\mathcal{Q}\tilde\rho(t) - i\lambda\mathcal{Q}\mathcal{V}(t)\mathcal{P}\tilde\rho(t). \tag{15}$$

Before we attempt to solve the coupled equations, we quickly remark that we can drop the first term in (14)

$$\mathcal{P}\mathcal{V}(t)\mathcal{P}\tilde{\rho}(t) = [\mathrm{Tr}_B\{\tilde{V}(t)\rho_B\}, \mathrm{Tr}_B\{\tilde{\rho}(t)\}] \otimes \rho_B = 0.$$

We can always make this contribution vanish, by redefining

$$V' = V - \mathrm{Tr}_B\{V\rho_B\} \otimes \mathbb{1}, \qquad\qquad H'_S = H_S + \lambda \mathrm{Tr}_B\{V\rho_B\} \otimes \mathbb{1}.$$

All we need now is an approximate solution of (15) for $\mathcal{Q}\tilde{\rho}(t)$ in order to insert it into (14). A formal solution of (15) can be written with the help of the propagator of the homogeneous equation $\mathcal{G}(t,t') = \mathcal{T} \exp -i\lambda \int_{t'}^{t} d\tau\, \mathcal{Q}\mathcal{V}(\tau)$

$$\mathcal{Q}\tilde{\rho}(t) = \mathcal{G}(t,0)\mathcal{Q}\tilde{\rho}(0) - i\lambda \int_0^t d\tau\, \mathcal{G}(t,\tau)\mathcal{Q}\mathcal{V}(\tau)\mathcal{P}\tilde{\rho}(\tau),$$

which can be shown to solve (15) by simply taking the derivative on both sides. This formal solution is remarkable as it only depends on the initial value of $\mathcal{Q}\tilde{\rho}$ at time $t = 0$. However our initial condition is separable and thus an eigenstate of $\mathcal{P}\rho(0) = \rho(0)$. Therefore the homogeneous term vanishes and we can insert the remainder into (14)

$$\partial_t \mathcal{P}\tilde{\rho}(t) = -\lambda^2 \int_0^t d\tau\, \mathcal{P}\mathcal{V}(t)\mathcal{G}(t,\tau)\mathcal{Q}\mathcal{V}(\tau)\mathcal{P}\tilde{\rho}(\tau),$$

to obtain an integro-differential equation for $\mathcal{P}\tilde{\rho}$. To proceed we would like to remove the dependence on intermediate times $0 \leq \tau \leq t$. This we do by introducing the unitary propagator for the full von Neumann equation (13) in the interaction picture $\mathcal{U}(t,t') = \mathcal{T} \exp -i\lambda \int_{t'}^{t} d\tau\, \mathcal{V}(\tau)$, to back propagate

$$\mathcal{U}(t,t')\tilde{\rho}(t') = \tilde{\rho}(t) \qquad \Rightarrow \qquad \tilde{\rho}(t') = \mathcal{U}(t,t')^\dagger \tilde{\rho}(t) = \mathcal{T}^* e^{i\lambda \int_{t'}^{t} d\tau\, \mathcal{V}(\tau)} \tilde{\rho}(t),$$

where $\mathcal{T}^*$ denotes anti-time-ordering. Thus we finally arrive at a differential equation for $\mathcal{P}\tilde{\rho}(t)$ in terms of the density matrix at t only

$$\partial_t \mathcal{P}\tilde{\rho}(t) = -\lambda^2 \int_0^t d\tau\, \mathcal{P}\mathcal{V}(t)\mathcal{G}(t,\tau)\mathcal{Q}\mathcal{V}(\tau)\mathcal{P}\mathcal{U}(t,\tau)^\dagger \tilde{\rho}(t).$$

However, this came at the cost of reintroducing the dependence on $\mathcal{Q}\rho$. So far we have not made use of the weak coupling assumption. From their definitions we see that both propagators $\mathcal{G}(t,\tau), \mathcal{U}(t,\tau)$ can be set to the identity at lowest order in λ. This significantly simplifies the complexity of the superoperator (using $\mathcal{P}\mathcal{V}(t)\mathcal{P} = 0$ again)

$$\partial_t \mathcal{P}\tilde{\rho}(t) = -\lambda^2 \int_0^t d\tau\, \mathcal{P}\mathcal{V}(t)\mathcal{V}(\tau)\mathcal{P}\tilde{\rho}(t) + \mathcal{O}(\lambda^3),$$

and shows that the dependency on $\mathcal{Q}\rho$ is of higher order in λ only. Finally we are now able to trace out the bath to obtain the equation for the reduced density matrix $\tilde{\rho}_S(t) = \mathrm{Tr}_B \rho(t) = \mathrm{Tr}_B \mathcal{P}\rho(t)$

$$\begin{aligned}
\partial_t \tilde{\rho}_S(t) &= -\lambda^2 \int_0^t d\tau\, \mathrm{Tr}_B \left\{\mathcal{V}(t)\mathcal{V}(\tau)(\tilde{\rho}_S(t) \otimes \rho_B)\right\} + \mathcal{O}(\lambda^3), \\
&= -\lambda^2 \int_0^t d\tau\, \mathrm{Tr}_B \left\{[\tilde{V}(t), [\tilde{V}(\tau), \tilde{\rho}_S(t) \otimes \rho_B]]\right\} + \mathcal{O}(\lambda^3), \\
&= -\lambda^2 \int_0^t d\tau\, \mathrm{Tr}_B \left\{[\tilde{V}(t), [\tilde{V}(t-\tau), \tilde{\rho}_S(t) \otimes \rho_B]]\right\} + \mathcal{O}(\lambda^3).
\end{aligned}$$

Our final task is thus to bring this equation into the Lindblad form (11). To do this we decompose the interaction into a sum of factorizable terms

$$V = \sum_k A_k \otimes \Gamma_k. \tag{16}$$

Since V is Hermitian we can always do this in such a way that A_k, B_k are both Hermitian as well (any operator can be written as the sum of two Hermitian operators $R + iJ$, then any terms proportional to i must vanish due to the hermiticity of V, thus the above form). Furthermore we can introduce a complete set of eigenstates of H_S on both sides of A_k to split it into parts with characteristic frequencies $\omega = E - E'$, such that $(A_k^\dagger(\omega) = A_k(-\omega))$

$$V = \sum_{k,\omega} A_k(\omega) \otimes \Gamma_k \qquad \Rightarrow \qquad \tilde{V}(t) = \sum_{k,\omega} A_k(\omega) e^{-i\omega t} \otimes \tilde{\Gamma}_k(t) = \sum_{k,\omega} A_k^\dagger(\omega) e^{i\omega t} \otimes \tilde{\Gamma}_k(t),$$

which we insert into the differential equation (and replacing $A_k^\dagger(\omega) = A_k(-\omega)$ where needed) to get

$$\partial_t \tilde{\rho}_S(t) = \lambda^2 \sum_{k,\omega} \sum_{k',\omega'} e^{i(\omega'-\omega)t} \Gamma^t_{kk'}(\omega) [A_{k'}(\omega') \tilde{\rho}_S(t), A_k^\dagger(\omega)] + \text{h.c.} \tag{17}$$

where we introduced the integrated bath correlation function

$$\Gamma^t_{kk'}(\omega) = \int_0^t d\tau \, e^{i\omega\tau} \mathrm{Tr}_B \left[\tilde{\Gamma}_k(\tau) \Gamma_{k'} \rho_B \right]. \tag{18}$$

The next step is to realize that most terms in (17) oscillate much faster than the typical time τ_I it takes for $\tilde{\rho}_S(t)$ to change substantially. Thus the effective contribution to the time-evolution of $\tilde{\rho}_S(t)$ is strongly suppressed for all terms with $\omega' \neq \omega$. The weak coupling assumption then allows us to separate the time-scales of the free system $\tau_S \sim \omega^{-1}$, the relaxation of the (free) bath τ_B and the interaction τ_I

$$\tau_S \sim \tau_B \ll \tau_I \sim \tau_S / \lambda^2.$$

We can thus define an intermediate time scale $\bar{\tau} = \tau_S / \lambda$, which is well separated both from τ_S

$$\tilde{\rho}_S(t + \tilde{\tau}) = \tilde{\rho}_S(t) + \mathcal{O}(\bar{\tau}/\tau_S) = \tilde{\rho}_S(t) + \mathcal{O}(\lambda), \tag{19}$$

and also from τ_B. To eliminate the oscillatory terms, we consider the density matrix averaged over a time interval of duration $\bar{\tau}$

$$\bar{\rho}_S(t) = \int_0^1 d\sigma \, \tilde{\rho}_S(t + \sigma\bar{\tau}) = \tilde{\rho}_S(t) + O(\lambda),$$

which we can therefore use interchangeably with the unaveraged quantity (at lowest order in λ). Its evolution is governed by

$$\begin{aligned} \partial_t \bar{\rho}_S(t) &= \lambda^2 \sum_{k,\omega} \sum_{k',\omega'} \int_0^1 d\sigma \, e^{i(\omega'-\omega)(t+\sigma\bar{\tau})} \Gamma^{t+\sigma\bar{\tau}}_{kk'}(\omega) [A_{k'}(\omega') \tilde{\rho}_S(t + \sigma\bar{\tau}), A_k^\dagger(\omega)] + \text{h.c.} \\ &= \lambda^2 \sum_{k,\omega} \sum_{k',\omega'} e^{i(\omega'-\omega)t} \Gamma^\infty_{kk'}(\omega) [A_{k'}(\omega') \bar{\rho}_S(t), A_k^\dagger(\omega)] \int_0^1 d\sigma \, e^{i(\omega'-\omega)\tau_S/\lambda\sigma} + \text{h.c.} \end{aligned}$$

where we also used the fact the bath relaxes much faster than $\tau_B \ll \bar{\tau}$ and thus we can safely extend the integration of (18) to infinity. (To avoid issues with periodical recurrences, one also has to assume that the bath is infinite.) As we have separated the fast oscillations, we can now take the limit $\lambda \to 0$, while keeping ω and τ_S fixed. The integral then vanishes for all $\omega' \neq \omega$ and we are thus left with

$$\partial_t \bar{\rho}_S(t) = \lambda^2 \sum_{\omega} \sum_{k,k'} \Gamma^\infty_{kk'}(\omega) [A_{k'}(\omega) \bar{\rho}_S(t), A_k^\dagger(\omega)] + \text{h.c.}$$

Splitting the bath correlator into a Hermitian and an anti-Hermitian part $\Gamma^\infty_{k'k}(\omega) = \gamma_{k'k}(\omega)/2 + iS_{k'k}(\omega)$ turns this into the Lindblad equation

$$\partial_t \bar{\rho}_S(t) = -i[H_{LS}, \bar{\rho}_S(t)] + \lambda^2 \sum_{\omega} \sum_{k,k'} \gamma_{kk'}(\omega) \left[A_{k'}(\omega) \bar{\rho}_S(t) A_k^\dagger(\omega) - \frac{1}{2} \{ A_k^\dagger(\omega) A_{k'}(\omega), \bar{\rho}_S(t) \} \right],$$

with a Hamiltonian piece H_{LS} that commutes with H_S and thus shifts all energy levels

$$H_{LS} = \lambda^2 \sum_{\omega} \sum_{k,k'} S_{kk'}(\omega) A_k^\dagger(\omega) A_{k'}(\omega).$$

The one thing left to prove is the positive definiteness of the matrices $\gamma_{kk'}(\omega)$. By writing

$$\mathcal{C}_v(\omega) = v^\dagger \gamma(\omega) v = \int_{-\infty}^{\infty} d\tau \, e^{i\omega\tau} \mathrm{Tr}_B \left[e^{iH_B\tau} C_v^\dagger e^{-iH_B\tau} C_v \rho_B \right] = \int_{-\infty}^{\infty} d\tau \, e^{i\omega\tau} \hat{\mathcal{C}}_v(\tau)$$

for any complex vector v_k and $C_v = \sum_k v_k \Gamma_k$, we can translate this into a statement about time correlation functions $\hat{\mathcal{C}}_v(\tau)$ and their Fourier transform $\mathcal{C}_v(\omega)$. By Bochner's theorem [55] we conclude that $\mathcal{C}_v(\omega) \geq 0$ if and only if $\hat{\mathcal{C}}_v(\tau)$ is positive definite, which implies that for any set of times τ_x and complex weights w_i we have

$$\sum_{i,j} w_i^* \hat{\mathcal{C}}_v(\tau_x - \tau_j) w_j \geq 0.$$

We can decompose $\hat{\mathcal{C}}_v(\tau)$ by introducing complete sets of eigenstates of H_B inside the trace to obtain

$$\hat{\mathcal{C}}_v(\tau) = \sum_{\epsilon,\epsilon'} |\langle \epsilon' | C_v | \epsilon \rangle|^2 \langle \epsilon | \rho_B | \epsilon \rangle e^{i(\epsilon - \epsilon')\tau}.$$

From $\sum_{i,j} w_i^* e^{i(\epsilon-\epsilon')(\tau_x - \tau_j)} w_j = |\sum_i e^{-i(\epsilon-\epsilon')\tau_x} w_i|^2$ it follows that $e^{i(\epsilon-\epsilon')\tau}$ is positive definite. Since ρ_B is also positive definite, the proof is complete by linearity. Thus we can diagonalize $\gamma_{kk'}(\omega)$ into positive eigenvalues γ_ω^α with eigenvectors (operators) E_ω^α. Writing $L_\omega^\alpha = \lambda \sqrt{\gamma_\omega^\alpha} E_\omega^\alpha$ and returning from the interaction picture we obtain the final form of the Lindblad equation

$$\partial_t \rho_S(t) = -i[H_S + \lambda^2 H_{LS}, \rho_S(t)] + \sum_{\omega,\alpha} \left[L_\omega^\alpha \rho_S(t) L_\omega^{\alpha\dagger} - \frac{1}{2} \{ L_\omega^{\alpha\dagger} L_\omega^\alpha, \rho_S(t) \} \right].$$

3 Closed Hierarchies

In complete analogy to unitary dynamics, the dissipative Lindblad equation can be reinterpreted as an equation of motion of the observables, rather than the density matrix. This corresponds to adopting Heisenberg's point of view on quantum dynamics. The density matrix then represents an initial condition, while operators change in time according to an equation dual to the Lindblad equation. Unitary dynamics is completely reversible, which means that all information about the initial state could, in principle, be recovered from the final state. In practice, however, this is usually not feasible, since local information (in form of the value of some low-order n-point function) gets distributed to increasingly higher-order n-point functions, thus constructing a hierarchy of correlation functions. The number of n-point functions grows exponentially in the order n and polynomially in the volume. The number of dependent observables in the full hierarchy then typically scales with the size of the Hilbert space and thus exponentially in the volume. Each interaction with the Hamiltonian creates multiple new dependencies, which therefore grow exponentially with time. This (practical) intractability of information represents the currently still insurmountable hurdle in quantum real-time dynamics. Statistical or equilibrium quantum physics (where the evolution occurs in imaginary time) does not suffer from this problem. The thermal average reduces the information content to a few characteristics at a given energy scale. These can be measured using a set of low n-points functions, whose size only scales polynomially with the volume. The dissipative nature of the Lindblad equation provides a similar effect. Due to the inherent information loss, the system should approach a set of fixed states or a limiting cycle. In either case one only needs a limited number of observables to describe its current state after a sufficiently long adjustment period. One can then hope that these observables are part of a closed set (under application of the dual Lindblad equation), such that the late-time behavior can be predicted exactly from the initial expectation values of the full set. If the size of this closed set only scales polynomially with the volume, one has significantly reduced the complexity of the problem and has thus constructed a practical path for its simulation. The goal of this section is to derive conditions for the existence of such closed sets and to discuss some concrete examples.

3.1 Lindblad Equation in the Heisenberg Picture

Any solution of the time-evolution superoperator $\mathcal{A}(t)$ of density matrices ρ can be reinterpreted as a dual map $\tilde{\mathcal{A}}(t)$ acting on observables using its Kraus form

$$\begin{aligned}\mathcal{O}(t) = \langle O\rangle(t) &= \mathrm{Tr}\left[O\mathcal{A}(t)\rho\right] = \sum_\alpha \mathrm{Tr}\left[OM^\alpha(t)\rho M^{\alpha\dagger}(t)\right] \\ &= \sum_\alpha \mathrm{Tr}\left[M^{\alpha\dagger}(t)OM^\alpha(t)\rho\right] = \mathrm{Tr}\left[\tilde{\mathcal{A}}(t)O\rho\right] = \langle O(t)\rangle.\end{aligned}$$

The equation of motion for the observable can then be written in terms of the dual map and the dual Lindblad superoperator $\tilde{\mathcal{L}}$

$$\partial_t O(t) = \tilde{\mathcal{A}}(t)\,\tilde{\mathcal{L}}\,O, \tag{20}$$

and the form of the dual Lindblad superoperator $\tilde{\mathcal{L}}$ is given by

$$\begin{aligned}\tilde{\mathcal{L}}O &= i[H,O] + \sum_\alpha \left[L^{\alpha\dagger}OL^\alpha - \frac{1}{2}\{L^{\alpha\dagger}L^\alpha, O\}\right] \\ &= i[H,O] + \frac{1}{2}\sum_\alpha \left[L^{\alpha\dagger}[O,L^\alpha] + [L^{\alpha\dagger},O]L^\alpha\right],\end{aligned} \tag{21}$$

By formally defining an inverse $\tilde{\mathcal{A}}(t)^{-1}$ (which is not a positive map) we bring (20) into the form of the Heisenberg equation (1)

$$\partial_t O(t) = \tilde{\mathcal{A}}(t)\,\tilde{\mathcal{L}}\,\tilde{\mathcal{A}}(t)^{-1}\,O(t) = \tilde{\mathcal{L}}_H(t)\,O(t),$$

We derive this equation simply in order to make the analogy to unitary dynamics. In practice, it is, however, much simpler to use (20) and express the derivative of $O(t)$ by the evolved value

of the observable $\tilde{\mathcal{L}}\,O$. The constraints leading to the Kraus form and the Lindblad equation can be reformulated in the Heisenberg picture. The trace constraint results from the invariance of the identity operator $\mathbb{1}(t) = \mathbb{1}$ ($\tilde{\mathcal{L}}\mathbb{1} = 0$) as the total probability measure. Hermiticity guarantees that observables will always be mapped to observables. Finally, complete positivity ensures that any observable that can be written as a reduced projection operator $O_S = \mathrm{Tr}_B[P_{SB}\rho_B]$ will never acquire negative eigenvalues. (It does, however, not mean that projection operators are mapped onto themselves, only the range of their expectation values $0 \leq \langle P(t)\rangle \leq 1$ is preserved, which makes them indistinguishable from actual projection operators in terms of measurements).

3.2 Linear Differential Operator

The equation of motion for observables (20) can be recast as an equation of motion for their expectation values

$$\partial_t \mathcal{O}(t) = \langle \partial_t O(t)\rangle = \langle \tilde{\mathcal{A}}(t)\,\tilde{\mathcal{L}}\,O\rangle = \langle \tilde{\mathcal{L}}\,O\rangle(t),$$

where $\tilde{\mathcal{L}}\,O$ is just another observable by the Hermiticity constraint. In this way the dissipator $\tilde{L}$ can be viewed as a linear differential operator which for every expectation value $\langle O\rangle$ returns its time derivative $\langle \tilde{\mathcal{L}}O\rangle$. Given a basis $\{O\}$ for all observables we can write the dual Lindblad superoperator in matrix form to obtain a set of coupled linear differential equations for their expectation values

$$\partial_t \mathcal{O}(t) = \langle \tilde{\mathcal{L}}O\rangle(t) = \sum_{\{O'\}} \mathcal{M}_{O,O'}\,\langle O'\rangle(t) = \sum_{\{O'\}} \mathcal{M}_{O,O'}\,\mathcal{O}'(t).$$

In practice this does not yield a feasible method to calculate the real-time evolution of observables. As we will show in section 3.3 the number of observables in our basis $\{O\}$, and therefore the complexity of the differential equations, grows exponentially with the volume. The dependencies among the observables, however, show a hierarchical structure among n-point functions. For approximate solutions one could just truncate this hierarchy, but for the Lindblad superoperators $\mathcal{L}$ we were are able to derive closure conditions (see section 3.4), such that n-point functions decouple exactly from all higher than n-point functions. The time evolution of their expectation values can thus be calculated by solving the coupled differential equations for this smaller set and the physical properties of the full dissipator $\mathcal{L}$ can be studied on this decoupled set.

3.3 The Hierarchy of Correlation Functions

We can construct a basis for all observables of a lattice system of N-sites with a local Hilbert space of size M as repeated tensor products of the set of M^2 local Hermitian matrices

$$\tau_x^a, \qquad a \in 0,\ldots,M^2-1,\; x \in 1,\ldots,N.$$

The space of observables is thus M^{2N}-dimensional and it is spanned by the elements

$$\Omega(a) = \bigotimes_x \tau_x^{a_x}.$$

An orthogonal basis with respect to the trace can be constructed locally and it automatically yields an orthogonal basis for the full space

$$\mathrm{Tr}_x[\tau_x^a\tau_x^b] = \delta^{ab} \qquad \Rightarrow \qquad \mathrm{Tr}[\Omega(a)\Omega(b)] = \prod_i \mathrm{Tr}_x[\tau_x^{a_x}\tau_x^{b_x}] = \prod_x \delta^{a_x b_x} = \delta^{ab}.$$

Any observable can be written as a linear combination of $\Omega(a)$'s. This follows directly from the repeated use of the following identity on factorizable Hilbert spaces

$$A\otimes B + A^\dagger \otimes B^\dagger = (A+A^\dagger)\otimes(B+B^\dagger) - i(A-A^\dagger)\otimes i(B-B^\dagger).$$

As a convention we take $\tau^0 = \mathbb{1}_M/M$ and τ^a (for $a > 0$) to be the (orthogonal and properly normalized) generators of $SU(M)$ in the fundamental representation. This allows us to subdivide

our basis elements into sets of n-point functions $\Omega_n \in \mathrm{C}_n$, where the degree n is defined as the number of non-identity operator insertions

$$n(\Omega) = n(a) = |\{a_x > 0\}|.$$

The size of each set is given by

$$|\mathrm{C}_n| = \binom{N}{n}(M^2-1)^n.$$

The algebra of all Hermitian operators can be written as

$$[\Omega(a), \Omega(b)] = i\Omega(a,b) = i\sum_c f^{abc}\Omega(c),$$

with real structure constants $f^{abc} = -i\,\mathrm{Tr}[[\Omega(a),\Omega(b)]\Omega(c)]$. To investigate the structure of the hierarchy, we write the Hamiltonian and the Lindblad operators as linear combinations of the basis elements (with real coefficients for the Hermitian Hamiltonian, and complex coefficients for the jump operators). The effect of any n-point piece $\Omega(a)$ in the Hamiltonian on an m-point observable $\Omega(b)$ can be studied individually

$$i[H_n, O_m] = i[\Omega(a),\Omega(b)] = -\Omega(a,b) = -\sum_{c|\,|n-m|<n(c)<n+m} f^{abc}\Omega(c) = \sum_{p=|n-m|+1}^{n+m-1} O_p$$

The lower and upper bounds on the degree of the observables on the right-hand side can be understood as follows. In order to have a non-vanishing commutator, they must share a non-zero index $a_i \neq 0 \neq b_i$ on at least one site. Thus the maximally obtainable rank is $n+m-1$. The lowest possible rank is given by $|n-m|+1$, which happens when the non-zero indices of one operator form a subset of the other operators non-zero indices. The resulting operator is then given by an operator with degree $|n-m|$ times a commutator on a disjoint set of $\min(n,m)$ sites. However, this commutator either vanishes or has support on at least one site. This is due to the fact that the identity operator is the only operator with degree zero and non-vanishing trace. Since the commutator is always traceless it does not produce a term proportional to the identity matrix, and can therefore not have degree zero. Every Hamiltonian that is at least bi-local ($n \geq 2$) thus introduces dependencies of the time-evolution of n-point functions to higher-point functions.

The derivation of a similar statement for dissipative processes is more complicated, due to the non-linearity in the Lindblad operators. However, if we restrict the analysis to Lindblad operators which only act on n sites $I_n = \{x_1, \ldots, x_n\}$

$$L_n = \sum_{a\in S_n} w_a\Omega(a), \qquad\qquad S_n = \{a:\, a_x = 0, \forall\, x \notin I_n\},$$

we can derive the constraint

$$\begin{aligned}
L_n^\dagger[O_m, L_n] + [L_n^\dagger, O_m]L_n &= \sum_{a\in S_n} i(w_a L_n^\dagger i[\Omega(a), O_m] - \bar{w}_a i[\Omega(a), O_m]L_n) \\
&= \sum_{a\in S_n}\sum_{p=|n(a)-m|+1}^{n(a)+m-1} i(w_a L_n^\dagger O_p^a - \bar{w}_a O_p^a L_n) \\
&= \sum_{p=1}^{n+m-1}\left(L_n^\dagger \mathcal{Q}_p + \mathcal{Q}_p^\dagger L_n\right) \\
&= \sum_{p=0}^{n+m-1} O_p.
\end{aligned}$$

We obtain the same upper limit $n+m-1$, but the lower limit decreases first to 1 due to operators of degree lower than n in L_n and finally to zero because multiplication can create the identity

operator of degree 0. It is important to note that the final multiplication $L_n^\dagger \mathcal{Q}_p$ does not raise the upper limit further, since both operators act on the same subset of $n+m-1$ sites. (If we would have chosen L_n differently, for instance more generally as a sum of operators of degree at most n, this step could have raised the maximal degree to $2n+m-1$.) So again the Lindblad equation shows hierarchical behavior with growth of the degree of dependent observables for $n > 2$. However, the multiplicative structure of the Lindblad term allows more flexibility, which already manifests itself as a dependence on the operator of degree zero. As the unit operator is conserved due to the trace constraint, it introduces a constant term into the differential equations for the observables, something we could have never gotten from Hamiltonian dynamics. Furthermore, this hints at the possibility of engineering jump operators which do not exhaust the upper limit of the degree and thus slow the ascent in the hierarchy of n-point functions.

3.4 Closure Conditions

We have shown how the number of co-dependent observables grows hierarchically towards higher n-point functions, and how this inhibits us from tracking their time-dependence, without introducing large errors (due to truncation or slow convergence of statistical methods). In order to have any chance of tracking the time-evolution of an observable, it has to be part of a closed set. A closed set A is defined as a finite subspace of all observables spanned by the basis $\{\Omega(a)\}_a$, which is closed under time-evolution

$$\partial_t A = \mathcal{D}(A) = \{\mathcal{D}(O) : O \in A\} \subset A.$$

As usual, the closure of a set $\bar{A}$ is defined as the smallest closed subspace, which contains A. Thus the closure of the set of one operator $\overline{\{O\}}$ is the minimal set needed to calculate the full time-evolution of that operator. The simplest example is that of a conserved quantity since $\mathcal{D}(O) = 0$ implies that its closure is the one-dimensional subspace of multiples of O. Since the full set $\{\Omega(a)\}_a$ is closed, the closure of any set always exists. For practical purposes, however, we need a set of manageable size, which means that the dimensionality of the closure of an operator should grow only polynomially with the system size. Furthermore, it would be preferable if the closed set of interest could be analytically determined, without an iterative procedure of either enlarging or reducing the set. It is thus natural to first define the sets one would like to be closed, and use them to restrict the form of the dissipator $\mathcal{D}$. The growth of the hierarchy seemed to be fueled mainly by an addition of $n-1$ legs to m-point functions with each application of the dissipator $\mathcal{D}$. A good starting point is thus to demand closure of the set of degree at most m

$$A_m = \{\Omega(a) : n(a) \leq m\} = \bigcup_{n=0}^{m} \mathrm{C}_n, \qquad \mathcal{D}(A_m) \subset A_m, \quad \forall m. \tag{22}$$

These sets only grow polynomially in the system size (typically $A_m \sim N^m$) and are expected to carry most of the information about the system (similar to thermal equilibrium). If we interpret the m-point functions C_m as m-particle operators, the dissipator should then describe three basic kind of scatterings (i) spatial $\mathrm{C}_m \to \mathrm{C}_m$, exchanging $a_x \leftrightarrow a_y$, (ii) flavor change $\mathrm{C}_m \to \mathrm{C}_m$, switching $a_x \to b_x$ and (iii) particle destruction $\mathrm{C}_m \to \mathrm{C}_{m-1}$, sending a flavor to zero $a_x \to 0$. Any scattering can be an arbitrary combination of these three. Particle creation $\mathrm{C}_m \to \mathrm{C}_{m+k}$ however is strictly forbidden by (22).

To simplify the analysis we now restrict ourselves to spins 1/2 ($M = 2$, qubits) living on a periodic hyper-cubic lattice in d dimensions. The interaction Hamiltonian and Lindblad operators are all given by uniform, bi-local interactions of nearest neighbors. The dissipator can then at most create one new particle at a time. This can only happen when one of its bi-local operators overlaps with one of the observables particles τ_x^a, while also acting on an unoccupied site τ_y^0. As this process is completely independent of the number and flavor of particles in the rest of the system, it is sufficient to prove the absence of particle production for one point functions C_1, described by the operators τ_x^a. To derive the necessary conditions, we proceed in three steps. First we prove that the Hamiltonian must be ultra-local. Then we proceed to look at symmetric and anti-symmetric Lindblad operators $L_{xy} = \pm L_{yx}$ separately, in order to derive their respective closure conditions.

3.4.1 Hamiltonian

Let us consider the Hamiltonian

$$H = \sum_{x,a} h^a s_x^a + \sum_{\langle x,y\rangle} \sum_{a,b} J^{ab} s_x^a s_y^b,$$

where $s^a = \sigma^a/2$, $a = 1, 2, 3$ are the spin operators and $\langle x, y\rangle$ denotes all pairs of nearest neighbors. The interaction should be symmetric $J^{ab} = J^{ba}$. The closure conditions follow from acting with the Hamiltonian on a single operator

$$i[H, s_x^a] = \sum_b \epsilon^{abc} s_x^c \bigg(h^b + \sum_{y|\langle x,y\rangle} \sum_d J^{bd} s_y^b \bigg).$$

The closure condition ensuring $\mathcal{D}(s_x^a) \subset A_1$ is thus given by $J^{ab} = 0$, and only ultra-local interactions with a magnetic field h^a are allowed.

3.4.2 Even Lindblad Operators

Even Lindblad operators act on nearest neighbors $\langle x, y\rangle$ and are symmetric under the exchange of the two sites $L_{xy} = L_{yx}$. We can parametrize the set of symmetric operators as

$$L_{xy} = l^0 \mathbb{1} + i \sum_a l^a (s_x^a + s_y^a) + \sum_{a,b} l^{ab} s_x^a s_y^b$$

with coefficients $l^0 \in \mathbb{R}$ and l^a, $l^{ab} = l^{ba} \in \mathbb{C}$. The Lindblad equation is invariant under individual phase rotations of the jump operators $L^\alpha \to e^{i\phi^\alpha} L^\alpha$, thus we can always eliminate the phase of one coefficient, in this case we have chosen l^0. The closure condition $\mathcal{D}(s_x^a) \subset A_1$ yields 27 equations ($\widetilde{\mathcal{L}}_{xy}(\,\cdot\,) = (L_{xy}^\dagger[\,\cdot\,, L_{xy}] + [L_{xy}^\dagger, \,\cdot\,]L_{xy})/2$)

$$m^{abc} = \mathrm{Tr}[s_x^a s_y^b \, \widetilde{\mathcal{L}}_{xy}(s_x^c)] = 0.$$

They can be summarized in seven equations

$$\begin{aligned}
\Im[\bar{l}^a g^a] &= -\frac{1}{2}\left(\Im[\bar{l}^a g^b] + \Im[\bar{l}^a g^c] + \Im[\bar{l}^b h^c] + \Im[\bar{l}^c h^b]\right) \ , \quad a \neq b \neq c \ , \\
\Im[\bar{l}^a l^b] &= \frac{1}{4} \sum_c \epsilon^{abc} \left(\Im[\bar{l}^c g^a] + \Im[\bar{l}^c g^b] - \Im[\bar{l}^a h^b] - \Im[\bar{l}^b h^a]\right) \ , \\
\Im[\bar{g}^a g^b] &= 2 \sum_c \epsilon^{abc} \left(\Im[\bar{l}^a h^a] + \Im[\bar{l}^b h^b]\right) \ , \\
\Im[\bar{g}^a h^b] &= -2 \sum_c \epsilon^{abc} \Im[\bar{l}^a h^c] - \delta^{ab} \sum_{c,d} \epsilon^{acd} \left(\Im[\bar{l}^a g^c] + \Im[\bar{l}^c h^d]\right) \ , \\
\Im[\bar{h}^a h^b] &= \sum_c \epsilon^{abc} \left(\Im[\bar{l}^c g^a] + \Im[\bar{l}^c g^b] + \Im[\bar{l}^a h^b] + \Im[\bar{l}^b h^a]\right) \ , \\
l^0 \Im[g^a] &= -\frac{1}{2} \sum_{b,c} \epsilon^{abc} \Im[\bar{l}^b h^b] \ , \\
l^0 \Im[h^a] &= -\frac{1}{4} \sum_{b,c} \epsilon^{abc} \left(\Im[\bar{l}^a g^b] - \Im[\bar{l}^b h^c]\right) \ ,
\end{aligned}$$

where we have split the matrix l^{ab} into diagonal $g^a = l^{aa}$ and off-diagonal parts $h^1 = l^{23}, h^2 = l^{31}, h^3 = l^{12}$. These equations can readily be solved when all parameters are real, yielding a 10-parameter family $l^0, l^a, g^a, h^a \in \mathbb{R}$. Among them are the projection operators on spin singlet and triplet

$$P_{xy}^s = \frac{1}{4}\mathbb{1} - \sum_a s_x^a s_y^a, \qquad\qquad P_{xy}^t = \frac{3}{4}\mathbb{1} + \sum_a s_x^a s_y^a.$$

A purely dissipative process driven by these operators has been investigated previously with Monte Carlo methods [56–58]. The closure of the hierarchy allows a direct confirmation of their results with our semi-analytical method.

3.4.3 Odd Lindblad Operators

The odd Lindblad operators are antisymmetric under the exchange of the two sites $L_{xy} = -L_{yx}$. Their parametrization is given by

$$L_{xy} = i \sum_a l^a (s_x^a - s_y^a) + \sum_{a,b,c} \epsilon^{abc} h^a s_x^b s_y^c$$

with coefficients $l^a, h^a \in \mathbb{C}$. Again there is one overall complex phase which is irrelevant. Their closure conditions are much simpler

$$\Im[\bar{l}^a h^b] = \Im[\bar{l}^a l^b] = \Im[\bar{h}^a h^b] = 0,$$

thus giving another family with six real parameters l^a, h^a. One candidate, which will be at the center of our in depth analysis in section 4, is given by the symmetrizer ($s^\pm = s^1 \pm i s^2$)

$$Q_{xy} = \frac{1}{2}(s_x^+ + s_y^+)(s_x^- - s_y^-), \tag{23}$$

which converts singlets of a pair of spins at x and y into triplets, while conserving the total spin $s_x^3 + s_y^3 = 0$. It has been proposed as a process for dissipative cooling into a Bose-Einstein condensate (BEC) [34, 39, 40, 51, 52].

4 Dissipative Bose-Einstein Condensation

In this section we focus on a system that is driven by the symmetrizer Lindblad operator Q_{xy} (23). We will show that the final state (or limiting cycle) is among the completely symmetric states. By mapping the spin system to hardcore bosons, we thus see that we can dissipatively drive our system into a Bose-Einstein condensate. We will then discuss some dynamical aspects of how this final state is approached, before we introduce competing unitary and thermal dynamics, to investigate the stability of this process in a noisy environment.

4.1 Non-Equilibrium Steady States

The non-equilibrium steady states ρ_{NESS} are defined as fixed points of the dynamical map, they are thus the kernel of the dissipator

$$\mathcal{L}(\rho_{\text{NESS}}) = \sum_{\langle x,y\rangle} \mathcal{L}_{xy}(\rho_{\text{NESS}}) = 0.$$

It is straightforward to show that totally symmetric superposition states $|S = N/2, S^3 = n\rangle$, which are characterized by the total spin $\vec{S} = \sum_x \vec{s}_x$

$$\vec{S}^2|N/2,n\rangle = \frac{N(N+2)}{4}|N/2,n\rangle, \qquad S^3|N/2,n\rangle = n|N/2,n\rangle, \tag{24}$$

are the only states that fulfill the above condition. Thus the final state is fully characterized by a positive $(N+1)\times(N+1)$-matrix F_{mn} with unit trace $\sum_n F_{nn} = 1$, which defines the final state

$$\rho_{\text{NESS}} = \sum_{mn} F_{mn}|N/2,m\rangle\langle N/2,n|.$$

Since the total spin is conserved $\widetilde{\mathcal{L}}(S^3) = 0$, no entanglement between different S^3-sectors is built up during the evolution. Block-diagonal (in S^3) density matrices are thus always mapped to block-diagonal density matrices, such that the final state can be described by a diagonal matrix $F_{mn} = p_n\delta_{mn}$ and density matrix

$$\rho_{\text{NESS}} = \sum_n p_n|N/2,n\rangle\langle N/2,n|.$$

The weights p_n are completely determined by the initial weight distribution among the different spin sectors. In our numerical analysis we will always start from the completely disordered state $\rho = \mathbb{1}/2^N$, for which the final state is given by

$$\rho_{\text{NESS}} = \frac{1}{2^N}\sum_{n=-N/2}^{N/2}\binom{N}{n+N/2}|N/2,n\rangle\langle N/2,n|. \tag{25}$$

Adding a local but homogenous Hamiltonian will change the final matrix F_{mn}, while introducing thermal spin flips will force the system out of the totally symmetric sector.

4.2 Purely Dissipative Evolution

To study the approach to the NESS-state (25) it is sufficient to know the two-point functions which contribute to the total spin $\vec{S}^2$. Furthermore it is sufficient to consider spin conserving operators, as the density matrices are always block-diagonal. This only leaves three classes of operators ($C_{xx} = 4D_{xx} = \mathbb{1}$)

$$s^3_x, \qquad C_{xy} = s^+_x s^-_y + s^+_y s^-_x, \qquad D_{xy} = s^3_x s^3_y,$$

and their expectation values

$$\mathcal{s}^3_x = \langle s^3_x\rangle, \qquad \mathcal{C}_{xy} = \langle C_{xy}\rangle, \qquad \mathcal{D}_{xy} = \langle D_{xy}\rangle.$$

The local dissipator acts on a local spin operator as

$$\widetilde{\mathcal{L}}_{xy}(s_x^a) = \frac{1}{4}\left(s_y^a - s_x^a\right),$$

thus they obey the diffusion equation

$$\partial_t \mathcal{s}_x^3 = \langle \widetilde{\mathcal{L}}(s_x^3)\rangle = \frac{1}{4}\Delta_x \mathcal{s}_x^3,$$

with the discrete Laplacian given by $\Delta_x f_x = \sum_{y|\langle x,y\rangle}(f_y - f_x)$. As we are already starting from a spatially homogenous initial state their expectation value will not change over time. Since our initial state is also symmetric under reversal of all spins their expectation value will always vanish $\mathcal{s}_x^3 = 0$. To calculate the evolution equation for the two point functions we can reuse the above result, but need to calculate the additional action of the dissipator on nearest-neighbor correlation functions

$$\widetilde{\mathcal{L}}_{xy}(C_{xy}) = \frac{1}{2}(C_{xx} - 2C_{xy} - 4D_{xy}), \qquad \widetilde{\mathcal{L}}_{xy}(D_{xy}) = 0, \tag{26}$$

in order to calculate the full time-evolution of the expectation values

$$\partial_t \mathcal{C}_{xy} = \langle \widetilde{\mathcal{L}}(C_{xy})\rangle = \frac{1}{4}(\Delta_x + \Delta_y)\mathcal{C}_{xy} - \frac{1}{2}\delta_{\langle x,y\rangle}(\mathcal{C}_{xy} + 4\mathcal{D}_{xy}), \tag{27}$$

$$\partial_t \mathcal{D}_{xy} = \langle \widetilde{\mathcal{L}}(D_{xy})\rangle = \frac{1}{4}(\Delta_x + \Delta_y)\mathcal{D}_{xy} + \frac{1}{2}\delta_{\langle x,y\rangle}(\mathcal{D}_{xy} - \mathcal{D}_{xx}), \tag{28}$$

while the equal-site correlators are trivially constant $\mathcal{C}_{xx} = 4\mathcal{D}_{xx} = 1$ by the trace constraint. From the completely disordered state $\rho = \mathbb{1}/2^N$ we determine the initial conditions for these 2-point functions

$$\mathcal{C}_{xy}(0) = 4\mathcal{D}_{xy}(0) = \delta_{xy}.$$

Similarly we use the steady state (25) to calculate their asymptotic values

$$\begin{aligned} \mathcal{C}_{xy}(\infty) &= \frac{1}{2}\left(1 + \delta_{xy}\right), \\ \mathcal{D}_{xy}(\infty) &= \frac{1}{4}\delta_{xy}. \end{aligned} \tag{29}$$

While $\mathcal{C}_{xy}$ has accumulated long-range correlations, $\mathcal{D}_{xy}$ has returned to its initial uncorrelated value. In fact, it never changed at all. Equation 26 highlights the key difference between $\mathcal{C}_{xy}$ and $\mathcal{D}_{xy}$. The nearest-neighbor correlation function $\mathcal{C}_{xy}$ couples to the constant 0-point function $\mathcal{C}_{xx} = \mathbb{1}$, $\mathcal{D}_{xy}$, on the other hand, does not (the appearance of $\mathcal{D}_{xx}$ in its evolution equation is misleading, it cancels exactly with terms from the discrete Laplacian). Thus $\mathcal{D}_{xy} = 0\,(x \neq y)$ is a solution for the time-evolution. In fact, any constant function $\mathcal{D}_{xy} = D\,(x \neq y)$, is formally a solution of (28), but only those with $-\frac{1}{4(N-1)} \leq D \leq \frac{1}{4}$ are compatible with the underlying spin system. A non-zero constant D would also influence the asymptotic value of $\mathcal{C}_{xy} = C\,(x \neq y)$. Inserting both into (27) we obtain the condition

$$\frac{1}{2}(1 - C) - \frac{1}{2}(C + 4D) = 0 \qquad \Rightarrow \qquad 0 \leq C = \frac{1 - 4D}{2} \leq \frac{N}{2(N-1)}.$$

which says nothing else than that the nearest-neighbor terms in (26) have to cancel. The relationship of C and D can also be understood in terms of the linear combination $\vec{s}_x \cdot \vec{s}_y = D_{xy} + \frac{1}{2}C_{xy}$ which always approaches the asymptotic expectation value

$$\langle \vec{s}_x \cdot \vec{s}_y\rangle(\infty) = D + \frac{1}{2}C = \frac{1}{4}, \qquad (x \neq y),$$

confirming that the final state is given in terms of the totally symmetric states (24), which only contain the triplet states of any two spins (not only nearest neighbors). The values of the asymptotic constant C then just reflects how often that triplet state lies in the $1,2$-plane ($s_x^3 + s_y^3 = 0$).

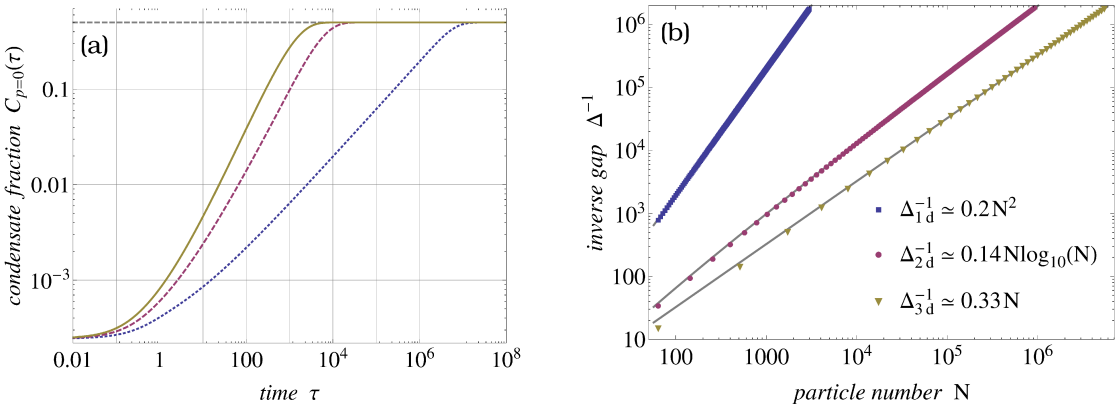

Figure 1: The condensate fraction $\mathcal{C}_{p=0}$ as a function of time τ for a fixed system size $N = 4096$ on a $d = 1$ (*dotted*), $d = 2$ square (*dashed*), and $d = 3$ primitive cubic (*solid*) lattice. The exact asymptotic value $\mathcal{C}_{p=0}(\infty) = (N+1)/(2N)$ is indicated by the dashed horizontal line (a). Numerical results for the inverse dissipative gap Δ^{-1}, the longest time scale in the system, as a function of the number of sites (particles) N, confirming the analytical prediction (31) for hypercubic lattices in dimensions $d = 1$ (*squares*), $d = 2$ (*dots*) and $d = 3$ (*triangles*) (b).

The physical limits of the value of C are therefore completely understood in terms of its expectation value in each of the completely symmetric superposition states with $S^3 = n$ $(x \neq y)$

$$\langle N/2, n|C_{xy}|N/2, n\rangle = 2\binom{N-2}{n+N/2-1}\Big/\binom{N}{n+N/2} = \frac{2(n+N/2)(N/2-n)}{N(N-1)} = \frac{(N^2-4n^2)}{2N(N-1)}.$$

For an infinite temperature ensemble within each sector of S^3 the 2-point function $\mathcal{D}_{xy} = D + (\frac{1}{4} - D)\delta_{xy}$ will always remain homogenous and constant, and thus enters the evolution equation of $\mathcal{C}_{xy}(t)$ as another constant term (in fact, it appears only in one particular linear combination with $\mathcal{C}_{xx}$ (26); thus we can just redefine $\mathcal{C}_{xx} \to 1 - 4D = 2C$ and forget about $\mathcal{D}_{xy}$ altogether). The growth of entanglement between spins at x and y is then completely measurable in terms of the evolution equation of $\mathcal{C}_{xy}$ (27). The general solution is given by linear combinations of exponentially decaying functions (plus the constant term C). The various decay rates are given by the eigenvalues of the operator $\mathcal{M}_{xy,zw}$ (with $\mathcal{C}_{xx} = 2C$)

$$\partial_t \mathcal{C}_{xy} = \sum_{z,w} \mathcal{M}_{xy,zw}\mathcal{C}_{zw}.$$

The speed of the final approach to the steady state is governed by the largest real part in the spectrum of $\mathcal{M}$

$$\Delta = -\max_{\lambda \in \mathrm{Spec}\mathcal{M}} \Re\lambda > 0,$$

which is known as the dissipative gap. Its dependence on the system size can be estimated by mapping the correlation function $C_{xy} \to C(r)$ to a continuum diffusion equation for $r = |x-y| \gg 1$ [59]. This yields a valid approximation since C_{xy} is both translation invariant and isotropic (by virtue of the chosen initial conditions) and varies only slowly at large distances. The difference between the discrete Laplacian Δ_x and the continuum diffusion equation in d-dimensions

$$\partial_t C(r,t) = \partial_r^2 C(r,t) + (d-1)r^{-1}\partial_r C(r,t) \tag{30}$$

is then negligible. The short-range behavior (26) then enters the continuum equation as a boundary condition $C(\epsilon, t) = C$ at some small scale ϵ and guarantees the correct asymptotic limit for the correlation function $C(r, \infty) = C$. Solutions of (30) have been derived in the context of statistical

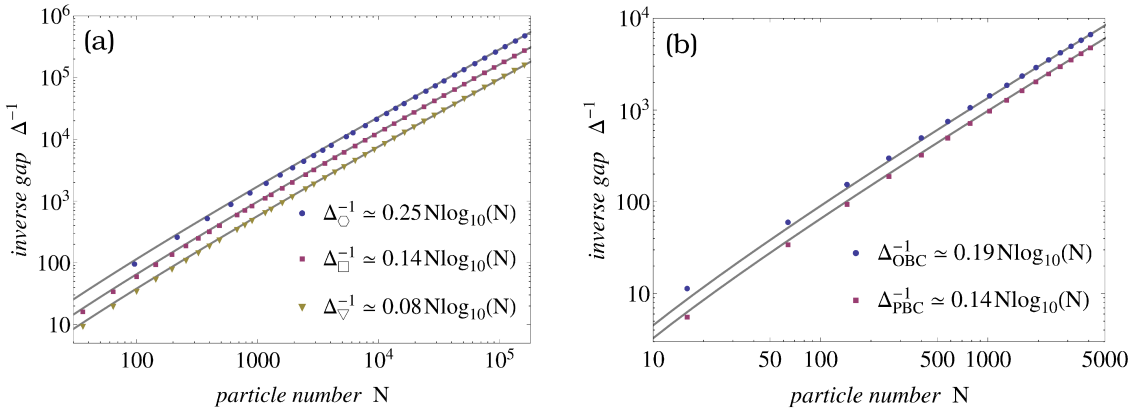

Figure 2: The inverse gap Δ^{-1} for the square ($\square$), triangular ($\triangledown$) and honeycomb ($\hexagon$) lattice geometries in two dimensions with fixed (periodic) boundary conditions (a). Comparison of the inverse gap Δ^{-1} of the square lattice with open (*dots*) and periodic (*squares*) boundary conditions. All systems exhibit the analytically predicted scaling with the system size N (31).

physics [60], and their late time behavior is given by ($\xi(t) \sim t^{1/2}$)

$$\frac{C(\epsilon < r < \xi(t))}{C} \sim \begin{cases} 1 - r/\xi(t), & d = 1, \\ 1 - \ln(r/\epsilon)/\ln(\xi(t)/\epsilon), & d = 2, \\ (\epsilon/r)^{d-2}, & d \geq 3. \end{cases}$$

The boundary condition eventually enforces long-range correlations in all systems, however, with a power-law decay for $d \geq 3$. To estimate the spectral gap $\Delta \sim t_\Delta^{-1}$ in dependence on the system size N, we set the criterion for reaching long-range correlation to be

$$N \sim \frac{1}{N}\sum_{x,y} C_{xy} \sim \lim_{\epsilon\to 0}\int_\epsilon^{\xi(t)} dr\, r^{d-1} C(r,t) \sim \begin{cases} \xi(t), & d = 1, \\ \xi(t)^2/\ln(\xi(t)), & d = 2, \\ \xi(t)^2, & d \geq 3. \end{cases}$$

Thus we obtain the following predictions for the scaling of the dissipative gap with the system size N

$$\Delta^{-1} \sim t_\Delta \sim \begin{cases} N^2, & d = 1, \\ N \ln N, & d = 2, \\ N, & d \geq 3. \end{cases} \tag{31}$$

In all cases the dissipative gap vanishes in the infinite volume limit. In figure 1 we have fitted these predictions to the values of the numerically extracted gap, and were able to confirm all three scaling laws. Furthermore, we have checked the independence of the scaling against different lattice geometries and boundary conditions (see figure 2).

To understand the full time-evolution from the initial state all the way to the final state it is illuminating to consider the Fourier modes

$$\mathcal{C}_p(t) = \frac{1}{N^2}\sum_{x,y} e^{ip_\mu(x-y)_\mu}\mathcal{C}_{xy}(t).$$

Their asymptotic values can be derived from (29) or directly from the final density matrix (25)

$$\mathcal{C}_p(\infty) = \frac{1}{2}\delta_{p,0} + \frac{1}{2N}.$$

In the final state all correlations have been transferred to the zero mode $p = 0$ which we call the condensate fraction, with all others decaying to a minimal value $1/2N$ (which is due to the

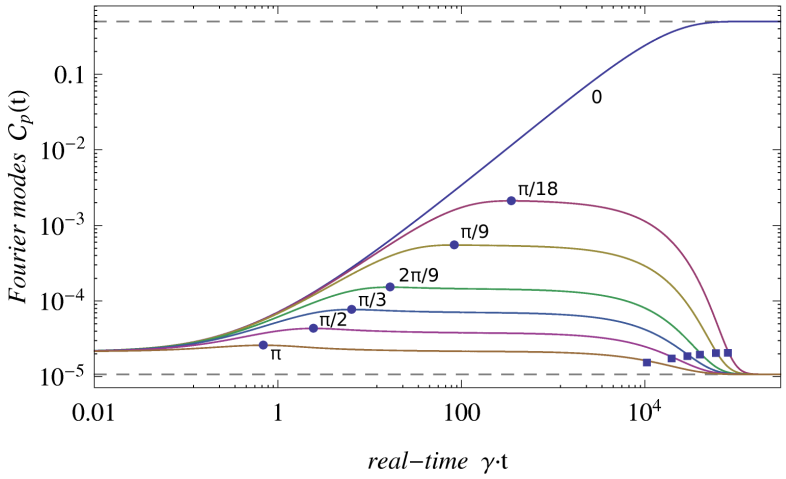

Figure 3: Time evolution of selected Fourier modes $\mathcal{C}_p(t)$ in a three dimensional system with $N = 36^3$ sites. All momenta p point along a lattice axis. The three regimes are clearly visible: Initial growth, transition and the final decay. They are separated by the time scales $t_1 \sim |p|^{-2}$ (*dots*) and $t_2 \sim |p|^{-1/3}$ (*squares*). The two asymptotic values $\mathcal{C}_p(\infty)$ are indicated by the two dashed horizontal lines.

constant 0-point function $\mathcal{C}_{xx} = 1$). Figure 3 shows the full time-evolution of a subset of Fourier modes in three dimensions. The evolution roughly splits into three regimes. First we observe an initial growth of all Fourier modes up to a time-scale $t_1 \sim p^{-2}$. After $t \sim L^2$ we enter a transient regime where only the zero-mode continues to grow at an exponential rate, while the remaining modes exhibit a long-lived plateau. After a time-scale t_2 these modes start to feel the slowed growth of the zero-mode, due to the asymptotic decay towards its maximum value $\mathcal{C}_p(t) \sim \mathcal{C}_p(\infty)[1-\exp(-\Delta t)]$, and thus start to decay exponentially towards their final value $1/2N$. By fitting the single exponential decay to the late-time data, we define t_2 as the intersection of this fit with the transient value of the Fourier mode. We observe a non-trivial momentum scaling $t_2 \sim p^{-1/3}$ for low momentum modes.

4.2.1 Competing Unitary Dynamics

In section 3.4.1 we have shown that coupling the total spin to a magnetic field $H = \vec{h} \cdot \vec{S}$ is allowed by the closure conditions. As S_3 is conserved under evolution by Q_{xy} we choose the magnetic field in a perpendicular direction

$$H_1 = hS^1 = h \sum_x s_x^1.$$

The total spin S_3 is now no longer conserved, which couples C_{xy}, D_{xy} to the additional operators $E_{xy} = s_x^2 s_y^3 + s_x^3 s_y^2$ and $F_{xy} = s_x^2 s_y^2$,

$$[H, C_{xy}] = -2\,[H, D_{xy}] = 2\,[H, F_{xy}] = 2ihE_{xy}\ , \qquad [H, E_{xy}] = 2ih(D_{xy} - F_{xy}).$$

The additional nearest-neighbor dissipator term of the new operators is given by

$$\tilde{\mathcal{L}}_{xy}(E_{xy}) = 0, \qquad \tilde{\mathcal{L}}_{xy}(F_{xy}) = \frac{1}{2}\left(F_{xx} - D_{xy} - \frac{1}{2}C_{xy}\right),$$

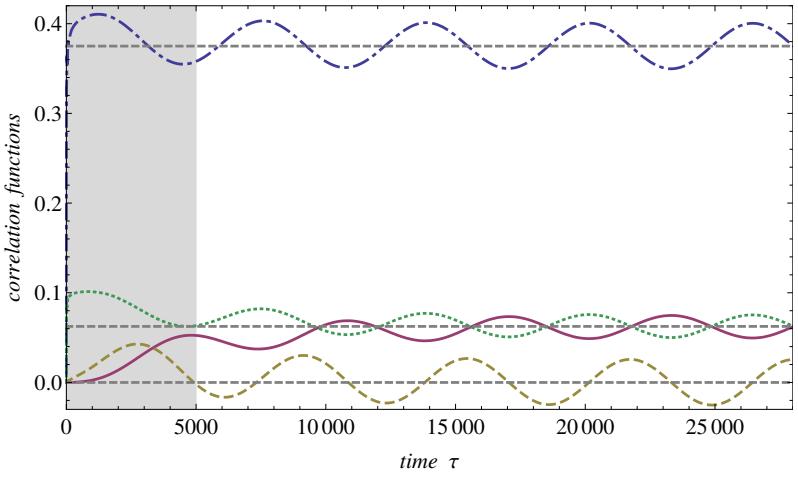

Figure 4: Nearest-neighbor ($\langle x, y\rangle$) correlation functions $\mathcal{C}_{xy}(\tau)$ (*dot-dashed*), $\mathcal{D}_{xy}(\tau)$ (*solid*), $\mathcal{E}_{xy}(\tau)$ (*dashed*), $\mathcal{F}_{xy}(\tau)$ (*dotted*) as functions of time. Results were obtained on a 2-dimensional square lattice with $N = 4096$ sites and magnetic field $h = 10^{-3}$. Late-time averages are indicated by dashed lines. The time scale set by the dissipative gap is indicated by the gray region ($\tau < 1/\Delta$).

which proves closure of the enlarged set of observables ($E_{xx} = 0, F_{xx} = \mathbb{1}/4$). The evolution equations under the full unitary and dissipative evolution $\widetilde{\mathcal{L}}(\,\cdot\,) = i[H, \cdot\,] + \sum_{\langle x,y\rangle} \widetilde{\mathcal{L}}_{xy}(\,\cdot\,)$ are

$$\begin{aligned}
\partial_t \mathcal{C}_{xy} &= \langle \widetilde{\mathcal{L}}(C_{xy})\rangle = \frac{1}{4}(\Delta_x + \Delta_y)\mathcal{C}_{xy} - \frac{1}{2}\delta_{\langle x,y\rangle}(\mathcal{C}_{xy} + 4\mathcal{D}_{xy}) - 2h\,\mathcal{E}_{xy},\\
\partial_t \mathcal{D}_{xy} &= \langle \widetilde{\mathcal{L}}(D_{xy})\rangle = \frac{1}{4}(\Delta_x + \Delta_y)\mathcal{D}_{xy} + \frac{1}{2}\delta_{\langle x,y\rangle}(\mathcal{D}_{xy} - \mathcal{D}_{xx}) + h\,\mathcal{E}_{xy},\\
\partial_t \mathcal{E}_{xy} &= \langle \widetilde{\mathcal{L}}(E_{xy})\rangle = \frac{1}{4}(\Delta_x + \Delta_y)\,\mathcal{E}_{xy} + \frac{1}{2}\delta_{\langle x,y\rangle}\,\mathcal{E}_{xy} + 2h\,(\mathcal{F}_{xy} - \mathcal{D}_{xy}),\\
\partial_t \mathcal{F}_{xy} &= \langle \widetilde{\mathcal{L}}(F_{xy})\rangle = \frac{1}{4}(\Delta_x + \Delta_y)\,\mathcal{F}_{xy} + \frac{1}{4}\delta_{\langle x,y\rangle}\,(2\mathcal{F}_{xy} - 2\mathcal{D}_{xy} - \mathcal{C}_{xy}) - h\,\mathcal{E}_{xy}.
\end{aligned}$$

From the completely disordered initial state we determine the initial conditions for all observables $\mathcal{C}_{xy}(0) = 4\mathcal{D}_{xy}(0) = 4\mathcal{F}_{xy}(0) = \delta_{xy}$ and $\mathcal{E}_{xy}(0) = 0$. The time-evolution can again be solved by diagonalizing the corresponding linear operator $\mathcal{M}_h$ (as none of the sets decouples anymore, the operator $\mathcal{M}_h$ now acts in the space spanned by all four sets). At vanishing magnetic field $h = 0$, the linear operator $\mathcal{M}_h$ has three vanishing eigenvalues, associated with the constant solutions $C = (1 - 4D)/2$, E and G, which is the constant value of the difference $G_{xy} = C_{xy} - 4F_{xy} = s^+_x s^+_y + s^-_x s^-_y$ with evolution equation ($G_{xx} = 0$)

$$\partial_t \mathcal{G}_{xy} = \langle \widetilde{\mathcal{L}}(G_{xy})\rangle = \frac{1}{4}(\Delta_x + \Delta_y)\mathcal{G}_{xy} + \frac{1}{2}\delta_{\langle x,y\rangle}\mathcal{G}_{xy} + 2h\,\mathcal{E}_{xy}.$$

The eigenvalue with the largest non-zero real part is again given by the dissipative gap $-\Delta$. At non-zero magnetic field only one zero eigenvalue remains, while the other two obtain an imaginary part $\pm 2ih$. The dissipative gap remains unchanged. As a consequences of the two purely imaginary eigenvalues only one particular combination of constant solutions remains, while the other two describe a non-decaying oscillatory mode with frequency $2h$. This behavior of the observables is completely comprehensible from the underlying quantum system. Since the Hamiltonian $H = hS^1 = h(S^+ + S^-)/2$ can be written in terms of the raising and lowering operators $S^\pm$ of the total spin S^3, the final state $t \gg \Delta^{-1}$ of the density matrix can still be written in terms of the fully symmetric states (24). They are no longer affected by the dissipative part of the evolution equations. The magnetic Hamiltonian, however, rotates these states into each other. Thus we can go into the basis where S^1 is diagonal and immediately read off the eigenvalues of the Hamiltonian $H \in -hN/2, -h(N/2-1), \ldots, hN/2$. All energy differences are multiples of h and therefore all

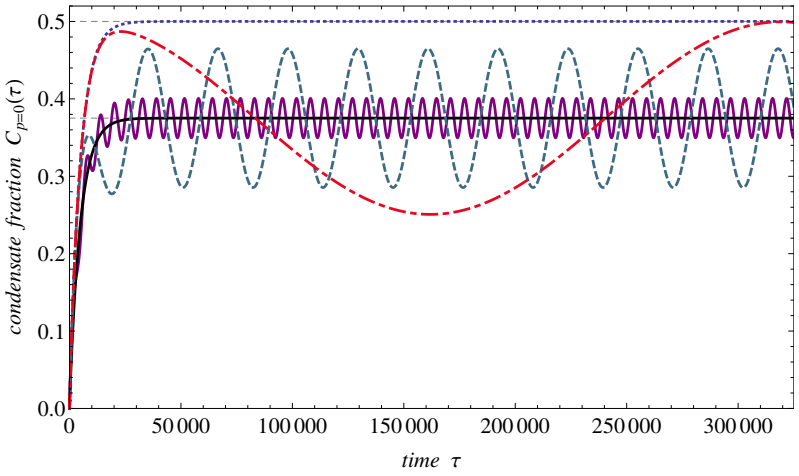

Figure 5: The time-evolution of the condensate fraction $\mathcal{C}_{p=0}(\tau)$ on a 2-dimensional square lattice with $N = 64^2$ sites. The magnetic field takes values $\eta = 0$ (*dotted*), $\eta = 10^{-5}$ (*dot-dashed*), $\eta = 10^{-4}$ (*dashed*), $\eta = 5 \cdot 10^{-4}$ (*solid, purple*) and $\eta = 1$ (*solid, black*). The dashed horizontal lines indicate the asymptotic value $\mathcal{C}^{\infty}_{p=0} = (N+1)/(2N)$ as well as the late-time average $\overline{\mathcal{C}}^{\infty}_{p=0} = (3N+5)/(8N)$.

observable frequencies at late times have to be as well. The reason why $\mathcal{M}_h$ only knows about the frequencies $0, \pm 2h$ lies in our particular choice of observables. Neither of them contains a product of s^1 with either of $s^{2,3}$. Thus all observables are either quadratic in the raising/lowering operators $\hat{s}^{\pm} = s^2 \pm i s^3$, or diagonal in the s^1 basis. In the interaction picture of H their components thus only transform with frequencies $\pm 2h$ and 0. This means that our set of observables is at most capable to extract information about those $3N - 2$ entries in the final density matrix (of a total of $N(N+2) = (N+1)^2 - 1$) which transform under these frequencies. However, this is a limitation of low-point functions in any system, and to obtain information about every entry of the density matrix would require to measure up to N-point functions. The nature of the achievement of our derivation lies somewhere else, namely in the fact that we can make exact predictions about that limited subspace of observables (entries in the density matrix) with only polynomial knowledge about the initial state, something which would be completely unfeasible with unitary dynamics. The three non-decaying modes describe the limit cycle of the system and a self-consistent parametrization of all observables at late times is given by ($x \neq y$)

$$\begin{aligned}
\mathcal{C}_{xy}(t \gg \Delta^{-1}) &= \frac{3}{8} + 2\, g(h,N) \cos(2ht - \varphi), \\
\mathcal{D}_{xy}(t \gg \Delta^{-1}) &= \frac{1}{16} - g(h,N) \cos(2ht - \varphi), \\
\mathcal{E}_{xy}(t \gg \Delta^{-1}) &= 2\, g(h,N) \sin(2ht - \varphi), \\
\mathcal{F}_{xy}(t \gg \Delta^{-1}) &= \frac{1}{16} + g(h,N) \cos(2ht - \varphi),
\end{aligned}$$

where the phase offset φ and the amplitude $g(h,N)$ of the oscillation have to be determined numerically. Figure 4 shows the behavior of the nearest-neighbor correlation functions. After a phase of initial approach $t < \Delta^{-1}$ the synchronized oscillation of the limit cycle are clearly visible. The condensate fraction only reaches its maximal value $\mathcal{C}^{\infty}_{p=0} = (N+1)/(2N)$ in the limit of vanishing magnetic field $h \to 0$. The effect of non-zero magnetic field can be seen in Figure 5. The condensate fraction now oscillates around a reduced value $\overline{\mathcal{C}}^{\infty}_{p=0} = (3N+5)/(8N)$ and the numerically determined amplitude shows a decrease with the strength of the oscillation $g(h,N) \sim h^{-1}$.

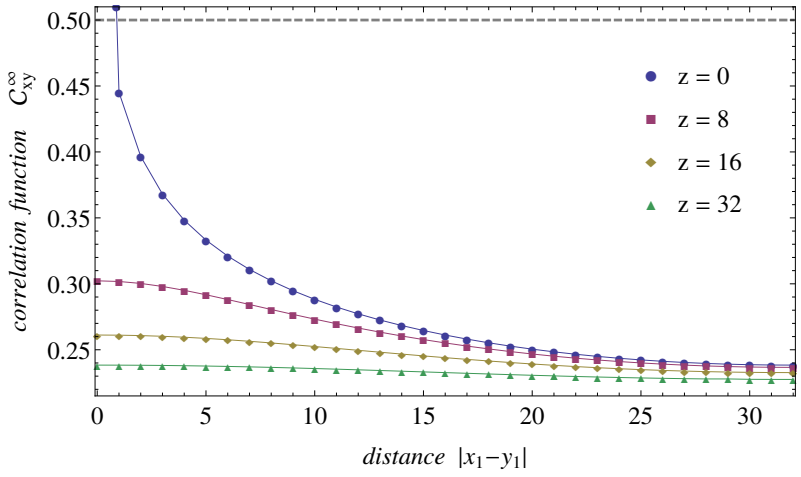

Figure 6: Exponential decay of the steady state ($t \to \infty$) correlation function $\mathcal{C}_{xy}$ on a 2-dimensional square lattice with $N = 64^2$ sites due to thermal noise ($\kappa/\gamma = 10^{-5}$, $T/h \approx 21$). The constant correlation function $\mathcal{C}_{xy} = 1/2$ of pure Bose-Einstein condensation is indicated by the dashed horizontal line. The correlation function is shown for slices with constant separation in one direction $z = |x_2 - y_2|$. The estimated correlation length (38) is $\xi \approx 69$, and thus of the order of the linear extent of the system $L = 64$.

4.2.2 Competing Thermal Noise

We continue the investigation of dissipative processes by adding thermal noise to the evolution equation. Here we model the noise as spin flips, induced by the local raising and lowering Lindblad operators $L^{\pm}_x = s^{\pm}_x$ ($\widetilde{\mathcal{L}}^{\pm}_x(\,\cdot\,) = (L^{\pm\dagger}_x[\,\cdot\,, L^{\pm}_x] + [L^{\pm\dagger}_x, \cdot\,]L^{\pm}_x)/2$) [47, 50, 61, 62]. Unlike the unitary process studied in the previous section, these operators do not enlarge the closed set

$$\widetilde{\mathcal{L}}^{\pm}_x(s^3_x) = -s^3_x \pm \frac{\mathbb{1}}{2}, \qquad \widetilde{\mathcal{L}}^{\pm}_x(C_{xy}) = -\frac{1}{2}C_{xy}, \qquad \widetilde{\mathcal{L}}^{\pm}_x(D_{xy}) = -D_{xy} \pm \frac{1}{2}s^3_y, \tag{32}$$

and the evolution equations under the dissipator $\widetilde{\mathcal{L}} = \sum_{\langle x,y\rangle} \gamma \widetilde{\mathcal{L}}_{xy} + \sum_x (\gamma^+ \widetilde{\mathcal{L}}^+_x + \gamma^- \widetilde{\mathcal{L}}^-_x)$ become

$$\begin{aligned}
\partial_t s^3_x &= \frac{\gamma}{4}\Delta_x s^3_x - (\gamma^+ + \gamma^-)s^3_x + \frac{1}{2}(\gamma^+ - \gamma^-), \\
\partial_t \mathcal{C}_{xy} &= \frac{\gamma}{4}(\Delta_x + \Delta_y)\mathcal{C}_{xy} - \frac{\gamma}{2}\delta_{\langle x,y\rangle}(\mathcal{C}_{xy} + 4\mathcal{D}_{xy}) - (\gamma^+ + \gamma^-)\mathcal{C}_{xy}, \\
\partial_t \mathcal{D}_{xy} &= \frac{\gamma}{4}(\Delta_x + \Delta_y)\mathcal{D}_{xy} + \frac{\gamma}{2}\delta_{\langle x,y\rangle}(\mathcal{D}_{xy} - \mathcal{D}_{xx}) - 2(\gamma^+ + \gamma^-)\mathcal{D}_{xy} + \frac{1}{2}(\gamma^+ - \gamma^-)(s^3_x + s^3_y).
\end{aligned} \tag{33}$$

To investigate the asymptotic late-time behavior, we first consider the pure noise limit $\gamma = 0$. From the above equations it is clear that the asymptotic state acquires a constant net magnetization

$$s^3_x(\infty) = m = \frac{1}{2}\frac{\gamma^+ - \gamma^-}{\gamma^+ + \gamma^-}, \qquad \mathcal{D}_{xy}(\infty) = m^2 \quad (x \neq y), \tag{34}$$

while the off-diagonal correlations $\mathcal{C}_{xy}$ decay exponentially with rate $(\gamma^+ + \gamma^-)$. The final state is thus a thermal state of the Hamiltonian

$$H = h\sum_x s^3_x,$$

where the temperature is set by the ratio of the spin flip rates

$$\frac{\gamma^+}{\gamma^-} = \exp\left(-\frac{2h}{T}\right) \qquad \Leftrightarrow \qquad m = \frac{1}{2}\tanh\left(-\frac{h}{T}\right). \tag{35}$$

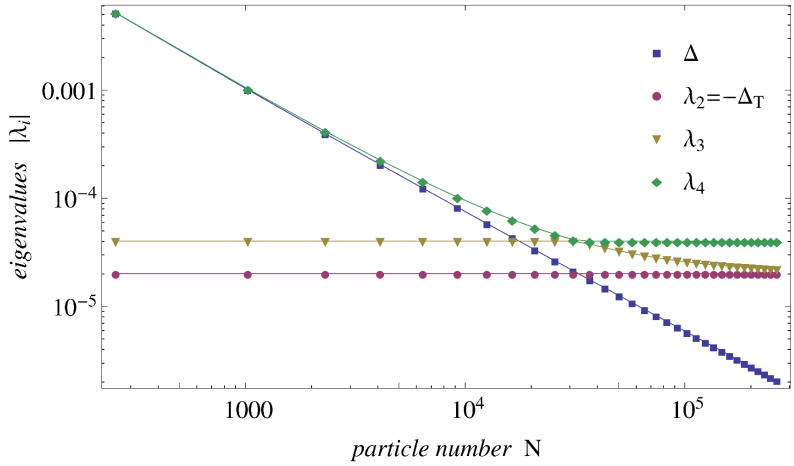

Figure 7: Spectrum of the linear differential operator $\mathcal{M}_T$ on a 2-dimensional square lattice ($\gamma = 1$, $\kappa = 10^{-7}$, $T/h = 2 \cdot 10^2$). The three smallest non-vanishing eigenvalues $\lambda_2 = -\Delta_T$, λ_3 and λ_4 are compared with the dissipative gap Δ of pure dissipative Bose-Einstein condensation. The constant thermal gap $\Delta_T \approx 2 \cdot 10^{-5}$ places a lower bound on the absolute value of all eigenvalues of $\mathcal{M}_T$.

The Hamiltonian H could be added to the dissipator without changing the evolution equations (33), and can thus be viewed as the true Hamiltonian of the system in the limit where it decouples from its environment. The temperature only characterizes the asymptotic state (35), but not the absolute rate $\kappa = \gamma^- - \gamma^+$ at which this state is approached. The full evolution equation

$$\begin{aligned}
\partial_t s_x^3 &= \frac{\gamma}{4}\Delta_x s_x^3 + \frac{\kappa}{2m}(s_x^3 - m), \\
\partial_t \mathcal{C}_{xy} &= \frac{\gamma}{4}(\Delta_x + \Delta_y)\mathcal{C}_{xy} - \frac{\gamma}{2}\delta_{\langle x,y\rangle}(\mathcal{C}_{xy} + 4\mathcal{D}_{xy}) + \frac{\kappa}{2m}\mathcal{C}_{xy}, \\
\partial_t \mathcal{D}_{xy} &= \frac{\gamma}{4}(\Delta_x + \Delta_y)\mathcal{D}_{xy} + \frac{\gamma}{2}\delta_{\langle x,y\rangle}(\mathcal{D}_{xy} - \mathcal{D}_{xx}) + \frac{\kappa}{m}\left(\mathcal{D}_{xy} - m\frac{s_x^3 + s_y^3}{2}\right),
\end{aligned} \tag{36}$$

is then characterized by the dimensionless ratios of the couplings κ/γ and the effective temperature T/h (which sets the magnetization m). When both couplings $\gamma, \kappa > 0$ are turned on, the asymptotic values of s_x^3 and $\mathcal{D}_{xy}$ remain unchanged at their thermal values (34). However, the presence of the Lindblad operator Q_{xy} still forces a buildup of off-diagonal correlations $\mathcal{C}_{xy}$, thus driving the system away from the thermal state. However, with $\kappa > 0$, these correlations can no longer be calculated analytically. We can, however, get an impression of the shape of the asymptotic correlation function in figure 6, by solving for the steady state of the corresponding continuum correlation function (30)

$$\partial_t C(r,t) = \gamma\partial_r^2 C(r,t) + \gamma(d-1)r^{-1}\partial_r C(r,t) + \frac{\kappa}{2m}C(r,t) = 0. \tag{37}$$

This equation can be solved in closed form in terms of a modified Bessel-function

$$C(r) \propto r^{-\frac{d-2}{2}} K_{\frac{d-2}{2}}(r/\xi) \sim r^{\frac{1-d}{2}} \exp(-r/\xi)(1 + O(r^{-1})), \quad \xi = \sqrt{-\frac{2m\gamma}{\kappa}} = \sqrt{\frac{\gamma}{\gamma^+ + \gamma^-}}. \tag{38}$$

The long-range order is thus destroyed by the thermal noise and in its place we find short-ranged correlations governed by a finite correlation length. The linear operator $\mathcal{M}_T$ corresponding to the differential equations (36) has only real eigenvalues, thus the asymptotic behavior is dominated by the thermal dissipative gap (see figure 7)

$$\Delta_T = \gamma^+ + \gamma^- = -\frac{\kappa}{2m} \geq 0.$$

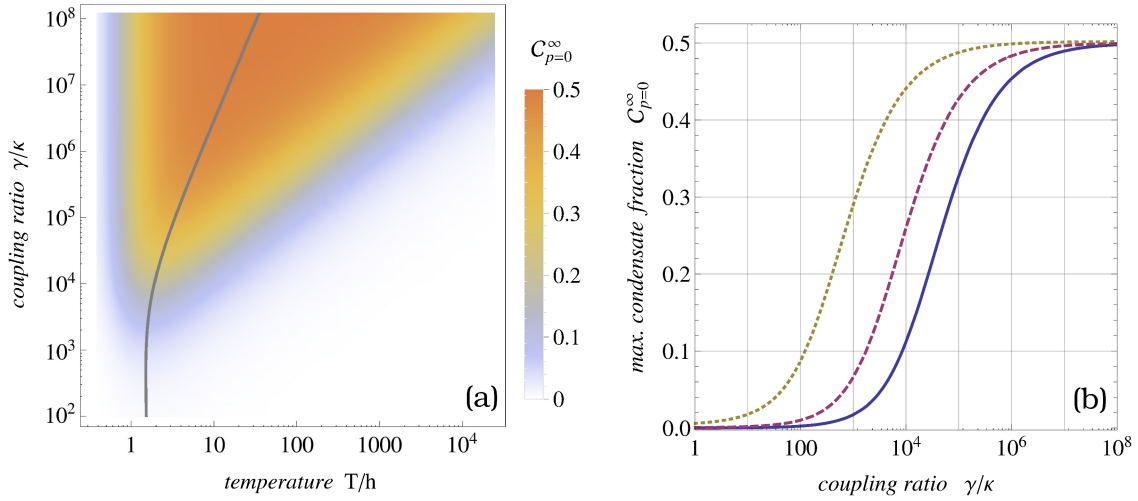

Figure 8: The dependence of the asymptotic condensate fraction $\mathcal{C}_{p=0}(\infty)$ for $N = 64^2$ particles on the square lattice on the coupling ratio γ/κ and the temperature T/h. Indicate by the gray line is the location of the maximum for a given ratio γ/κ (a). The maximal obtainable condensate fraction on lattices of different sizes $N = 16^2$ (*dotted*), $N = 48^2$ (*dashed*) and $N = 96^2$ (*solid*) as a function of the ratio γ/κ. Since the correlations are short-ranged, the condensate fraction drops with increasing volume (b).

This is in complete agreement with the correlation length derived above. The physical picture is that Q_{xy} induces a random walk of the spins, while also correlating them along its path. The number of steps it takes, before the correlation is destroyed by $L_x^{\pm}$ is proportional to $\gamma\Delta_T^{-1}$, which thus sets the correlation length $\xi^2 \sim \gamma\Delta_T^{-1}$. Since the asymptotic correlations are short-ranged, the time needed to build up these correlations is finite and independent of the system size.

In figure 8a we investigate the steady state phase diagram on a square lattice of $N = 64^2$ spins. The condensate fraction of the steady state is measured as a function of the coupling ratio γ/κ and the effective temperature T/h. Condensation only occurs for large dissipative coupling ratio $\gamma/\kappa \geq \mathcal{O}(10^3)$ at intermediate temperatures. At low temperatures $T \to 0$ the spin-lowering operators dominate $\gamma^- \gg \gamma, \gamma^+$, therefore the total spin is minimized $S^3 \to -N/2$. Therefore no long-range order in the transverse plane, as measured by $\mathcal{C}_{p=0}$, can occur. At high temperatures $T \to \infty$ both thermal couplings diverge $\gamma^+ \sim \gamma^- \gg \gamma$ such that the spin flips completely dominate the dynamics ($\xi \to 0$). Figure 8b shows that the ratio γ/κ has to be drastically increased in order to maintain the same condensate fraction in larger systems. This is evident from the estimate of the correlation length (38), which states that in order to have a correlation length of the order of the linear extent of the system $\xi \sim L$, the coupling ratio has to scale as $\gamma/\kappa \sim L^2 = N^{2/d}$. Once again this shows that a condensate is much easier to obtain in higher dimensions d.

5 Worm Algorithm

Before we discovered the closed hierarchy of observables described in section 3, we tried to tackle the Lindblad equation with quantum Monte Carlo methods. Previous work already described a sign-problem-free loop cluster algorithm for purely measurement-driven processes [56–58]. Our goal was then to extend this to non-Hermitian Lindblad operators $L \neq L^\dagger$. We worked out a sign-problem-free directed loop algorithm for a process closely related to the symmetrization process described in section 3. However, approaching the final state, which is maximally correlated at all scales, proved to be numerically much harder, than approaching a disordered state via measurement operations. Nevertheless, we want to provide a description of our algorithm, as it might be useful as a guidance for systems which do not have closed hierarchies. How the class of models with closed hierarchies and the class which allow for sign-problem-free Monte Carlo algorithms overlap is still an open question at this point. We were able to find more examples of the former class, since the closure conditions are very simple to check for any model, while the following example lies in both classes.

5.1 Model

We are considering a purely dissipative process with $H = 0$. Each Lindblad operator acts on two spins $\frac{1}{2}$ at neighboring sites of the lattice. For each pair of neighboring sites x, y there are two different Lindblad operators given in terms of the individual raising and lowering operators $s^+ = s^{-\dagger}$

$$L^1 = \frac{1}{2}(s_x^+ + s_y^+)(s_x^- - s_y^-) = -\frac{1}{2}(s_x^- + s_y^-)(s_x^+ - s_y^+), \qquad L^2 = \mathbb{1} - L^{1\dagger}L^1. \tag{39}$$

One can show that $L^{1\dagger}L^1$ is the projection operator on the spin singlet state

$$L^{1\dagger}L^1 = \mathbb{1} - \frac{(\vec{s}_x + \vec{s}_y)^2}{2},$$

thus $L^2 = (\vec{s}_x + \vec{s}_y)^2/2$ is the triplet projection operator and we have

$$L^{1\dagger}L^1 + L^{2\dagger}L^2 = \mathbb{1} - L^2 + L^2 = \mathbb{1}.$$

The Lindblad equation then takes the simplified form

$$\partial_t \rho(t) = \mathcal{L}\rho(t) = \sum_{\langle x,y\rangle} \left[\sum_{\alpha=1,2} L_{xy}^\alpha \rho(t) L_{xy}^{\alpha\dagger} - \rho(t) \right]. \tag{40}$$

Since it will become useful later, we solve the full time-evolution map for a 2-spin system. Using the identities

$$L^2L^1 = L^1, \qquad L^1L^2 = 0 = L^1L^1, \qquad L^2L^2 = L^2, \qquad L^0 = \mathbb{1},$$

it is straightforward to make the ansatz

$$\rho(t) = \sum_{\alpha=0}^{2} w_\alpha(t) L^\alpha \rho L^{\alpha\dagger}, \tag{41}$$

for the time-evolution of the 2-spin density matrix. The Lindblad equation then yields

$$\partial_t \rho(t) = \sum_{\alpha=0}^{2} \partial_t w_\alpha(t) L^\alpha \rho L^{\alpha\dagger} = w_0(t) \left[L^1 \rho L^{1\dagger} + L^2 \rho L^{2\dagger} - L^0 \rho L^{0\dagger} \right].$$

The contribution of the identity map is clearly exponentially decaying, $w_0(t) = e^{-t}$, from its initial value $w_0(0) = 1$. The other two functions in the ansatz are then given by the integral

$$w_{1,2}(t) = \int_0^t d\tau\, w_0(\tau) = 1 - e^{-t},$$

such that the full map obeys the trace condition at all times

$$\sum_{\alpha=0}^{2} w_\alpha(t) L^{\alpha\dagger} L^\alpha = \mathbb{1} e^{-t} + (1-e^{-t})(L^{1\dagger}L^1 + L^{2\dagger}L^2) = \mathbb{1}.$$

5.2 Setup

To describe the algorithm, a few preliminary remarks are in order. First of all it is important to realize that the dissipation superoperator $\mathcal{L}$ (40) can be described as a regular operator (matrix) acting on the vector space of density matrices ρ. Two copies of an orthonormal basis $|\psi_i\rangle$ of the underlying Hilbert space provide a basis for this vector space

$$\begin{aligned}
\partial_t \rho_{ij}(t) &= \langle\psi_i|\mathcal{L}\rho(t)|\psi_j\rangle \\
&= \sum_{\langle x,y\rangle} \langle\psi_i| \sum_{kl} \left[\sum_{\alpha=1,2} L^\alpha_{xy}|\psi_k\rangle\langle\psi_k|\rho(t)|\psi_l\rangle\langle\psi_l|L^{\alpha\dagger}_{xy} - |\psi_k\rangle\langle\psi_k|\rho(t)|\psi_l\rangle\langle\psi_l| \right] |\psi_j\rangle \\
&= \sum_{\langle x,y\rangle} \sum_{kl} \left[\sum_{\alpha=1,2} \langle\psi_i|L^\alpha_{xy}|\psi_k\rangle\langle\psi_l|L^{\alpha\dagger}_{xy}|\psi_j\rangle - \delta_{ik}\delta_{lj} \right] \rho_{kl} \\
&= \sum_{kl} \mathcal{L}_{ij,kl}\, \rho_{kl}.
\end{aligned}$$

Since this is exactly the action of an operator in the doubled Hilbert space we can immediately write down its solution

$$\rho(t) = \Theta(t)\rho(0) = e^{t\mathcal{L}}\rho(0).$$

A simulation scheme of the exponentiated superoperator can now be constructed in complete analogy to simulations in statistical quantum mechanics (where one is interested in the thermal density matrix $\rho \sim \exp(-\beta H)$ in terms of the exponentiated Hamiltonian). First we split the full time-evolution into N time steps of duration $\epsilon = t/N$. Each of these time step can then be approximated by a series of M partial evolution operators

$$\Theta(t) = \Theta(\epsilon)^N = \prod_{i=1}^{N} \left[\prod_{j=1}^{M} \Theta_j(\epsilon) \right] + \mathcal{O}(\epsilon^2). \tag{42}$$

On a hypercubic lattice in d dimensions with an even number of sites in all directions the number of partial evolutions can be taken to the be the number of nearest neighbors of a site $M = 2d$. The set of all nearest neighbors $\langle x,y\rangle$ can then be split into $2d$ disjoint sets $\{\langle x,y\rangle_j\}_{j=1}^{2d}$, such that no site appears twice in a given set. Accordingly, the full dissipator can be split as well

$$\mathcal{L} = \sum_{j=1}^{2d} \mathcal{L}_j, \qquad\qquad \mathcal{L}_j = \sum_{\langle x,y\rangle_j} \left[\sum_{\alpha=1,2} L^\alpha_{xy}\rho(t)L^{\alpha\dagger}_{xy} - \rho(t) \right]. \tag{43}$$

The partial dissipators $\mathcal{L}_j$ now define the partial evolution operators $\Theta_j(\epsilon) = \exp(\epsilon\mathcal{L}_j)$. Although different partial operators do not commute $[\Theta_j, \Theta_k] \neq 0$ (thus the error of order ϵ^2 in (42)), the individual nearest-neighbor contributions from each partial operator do, such that we can express them as

$$\Theta_j(\epsilon) = \prod_{\langle x,y\rangle_j} \Theta_{xy}(\epsilon),$$

where $\Theta_{xy}(\epsilon)$ is the exact 2-site solution derived earlier (41). Each of the evolution operators Θ is a valid map of density matrices, Θ_{xy} is a solution of a Lindblad equation (and is readily given in Kraus form (41)) and compositions of maps are again maps. By choosing an orthonormal basis for the Hilbert space $|\psi_k\rangle$, and introducing a complete set of doubled states $\sum_{kl}|\Psi_{kl}\rangle\langle\Psi_{kl}|$

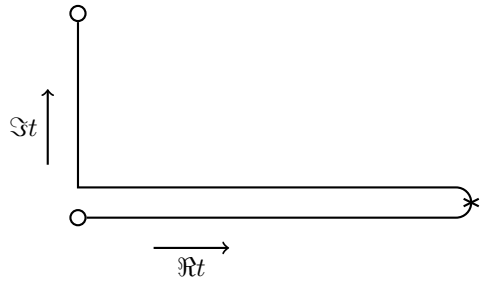

Figure 9: The Keldysh contour for the real-time-evolution of a thermal initial state. The imaginary time separation of forward and backward propagation along the real-time axis is only to guide the eye. After the imaginary time-evolution of duration β the contour is periodically identified with the other real-time contour ($\circ$). The infinite temperature initial condition $\rho \sim \mathbb{1}$ corresponds to $\beta = 0$, such that the two real-time contours can be identified directly at $t = 0$. Measurement operators can be inserted in between forward and backward propagation ($\times$).

($|\Psi_{kl}\rangle = |\psi_k\rangle\langle\psi_l|$) between all Θ_j's we turn the transition amplitudes of the evolution operator (42) into a statistical ensemble in $(d+1)$-dimensions

$$\begin{aligned}\langle\Psi_{(kl)_0}|\Theta(t)|\Psi_{(kl)_{MN}}\rangle &= \sum_{(kl)_j}\langle\Psi_{(kl)_1}|\Theta_1(\epsilon)|\Psi_{(kl)_1}\rangle\langle\Psi_{(kl)_1}|\Theta_2(\epsilon)|\Psi_{(kl)_2}\rangle \\ &\quad \ldots\langle\Psi_{(kl)_{MN-2}}|\Theta_{MN-1}(\epsilon)|\Psi_{(kl)_{MN-1}}\rangle\langle\Psi_{(kl)_{MN-1}}|\Theta_{MN}(\epsilon)|\Psi_{(kl)_{MN}}\rangle \\ &= \sum_S \Theta^{(kl)_{MN}}_{(kl)_0}(S),\end{aligned}$$

where $S = \{(kl)_i\}_{i=1}^{MN-1}$ is the configuration of the density matrix in all time-slices and $\Theta^{(kl)_{MN}}_{(kl)_0}(S)$ is the weight of that configuration (given by the product of the weights of each time-slice). So far all this has been constructed in complete analogy to statistical quantum mechanics, albeit on a doubled Hilbert space. The crucial difference comes from the boundary condition. While in statistical quantum mechanics one takes the trace (periodic boundary conditions) to define the partition sum, the two ends correspond to different physical times and thus obey independent boundary conditions, namely those of a Keldysh contour (see figure 9). The initial states are weighed by an initial density matrix $\rho_{(kl)_0}$ (thermal, infinite temperature or general density matrix), while the final state is weighed by an observable $O_{(kl)_{MN}}$ (most trivial would be the measurement of total probability $\delta_{(kl)_{MN}}$) to calculate the expectation value (for an illustration of how this works see figure 9)

$$\langle O\rangle(t) = \operatorname{Tr} O\Theta(t)\rho = \sum_{(kl)_0}\sum_{(kl)_{MN}}\sum_S \rho_{(kl)_0}\Theta^{(kl)_{MN}}_{(kl)_0}(S)O_{(kl)_{MN}}.$$

In general, the weights $\Theta^{(kl)_{MN}}_{(kl)_0}(S)$ would be riddled with complex phases, thus eliminating any hope of efficiently sampling the above quantity. However, for the particular combination of Lindblad operators chosen here we can show that in the s^3-basis all configurations have positive weight $\Theta^{(kl)_{MN}}_{(kl)_0}(S) \geq 0$ and thus efficient sampling is possible. It is sufficient to prove that the 2-site solution $\Theta_{xy}(\epsilon)$ has only positive weights. We write

$$\begin{aligned}(\Theta_{xy}(\epsilon))^{mn}_{kl} &= \langle\psi_m|\left[e^{-\epsilon}|\psi_k\rangle\langle\psi_l| + (1-e^{-\epsilon})(L^1|\psi_k\rangle\langle\psi_l|L^{1\dagger} + L^2|\psi_k\rangle\langle\psi_l|L^{2\dagger})\right]|\psi_n\rangle \\ &= e^{-\epsilon}\delta_{km}\delta_{ln} + (1-e^{-\epsilon})(\langle\psi_m|L^1|\psi_k\rangle\langle\psi_l|L^{1\dagger}|\psi_n\rangle + \langle\psi_m|L^2|\psi_k\rangle\langle\psi_l|L^{2\dagger}|\psi_n\rangle) \qquad (44) \\ &= e^{-\epsilon}\delta_{km}\delta_{ln} + \frac{1-e^{-\epsilon}}{2}(\langle\psi_m|L^+|\psi_k\rangle\langle\psi_n|L^+|\psi_l\rangle^* + \langle\psi_m|L^-|\psi_k\rangle\langle\psi_n|L^-|\psi_l\rangle^*),\end{aligned}$$

where $L^\pm = L^2 \pm L^1$ can be rewritten as

$$L^\pm = (s^3_x + s^3_y)^2 + \frac{(1\pm s^3_x)(1\mp s^3_y)}{4} + s^\mp_x s^\pm_y, \qquad (45)$$

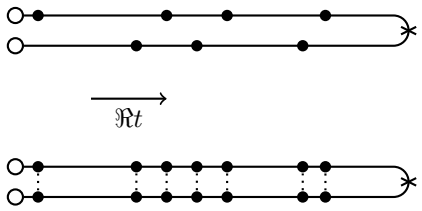

Figure 10: (Top) Insertion times of unitary (Hamiltonian) interactions are uncorrelated on the forward and backward contours. (Bottom) Insertions for dissipative (Lindblad) interactions are correlated, they happen simultaneously on both contours.

making it manifest that all matrix elements are real and positive in the s^3 basis

$$\langle s_x^{3\prime}, s_y^{3\prime}|L^{\pm}|s_x^3, s_y^3\rangle \geq 0 \qquad \Rightarrow \qquad (\Theta_{xy}(\epsilon))_{kl}^{mn} \geq 0 \qquad \Rightarrow \qquad \Theta_{kl}^{mn}(S) \geq 0.$$

5.3 The Algorithm

We have decomposed the full time-evolution operator $\Theta(t)$ into a series of 2-site operators $\Theta_{xy}(\epsilon)$ with only positive weights. To sample efficiently from the full evolution operator we now need to construct an algorithm. Although cluster-rules fulfilling detailed balance can be formulated for the 2-site evolution operator (44), the resulting cluster algorithm becomes inefficient very quickly in the time t. This is due to the fact that the operators $L^{\pm}$ represent specific constraints on the state history S, that can only be represented by clusters which tend to grow very large. A worm algorithm allows more flexibility, since the worm can simply backtrack whenever it faces a constraint that is only fulfilled by the current configuration. As $L^{\pm}$ conserve the total spin $s_x^3 + s_y^3$ in each copy of the doubled Hilbert space, the goal of the worm is to identify the world-line of a spin within one copy and flip it to the opposite spin. This can be done "on the fly" such that the path does not have to be memorized. The worm can intersect itself and flip the same spin several times before a new (globally) valid configuration is found. As the second copy of the Hilbert space is not affected by the movement of the worm it serves solely as a spectator. The rules of the worm in one copy thus depend on the state of the other copy. We adopt the simplified tensor product notation

$$\Theta_{xy}(\epsilon) = e^{-\epsilon}\mathbb{1}\otimes\mathbb{1} + \frac{1-e^{-\epsilon}}{2}(L^+\otimes\bar{L}^+ + L^-\otimes\bar{L}^-),$$

acting on the doubled Hilbert space spanned by the states $|\psi_k\rangle\otimes|\psi_l\rangle^*$. Splitting the evolution operator into pieces with equal configuration on the second copy yields five terms (as we are working in a basis in which $L^{\pm}$ are real, we drop the complex conjugate for simplicity)

$$\begin{aligned}\Theta_{xy}(\epsilon) \quad = \quad & \left[\frac{(1+e^{-\epsilon})}{2}L^{\parallel} + \frac{(1-e^{-\epsilon})}{2}L^{\times}\right]\otimes\frac{(s_x^3+s_y^3)^2}{4} \\ & + \left[e^{-\epsilon}L^{\parallel} + \frac{(1-e^{-\epsilon})}{2}L^{-}\right]\otimes\frac{(1-s_x^3)(1+s_y^3)}{4} \\ & + \left[e^{-\epsilon}L^{\parallel} + \frac{(1-e^{-\epsilon})}{2}L^{+}\right]\otimes\frac{(1+s_x^3)(1-s_y^3)}{4} \\ & + \frac{(1-e^{-\epsilon})}{2}L^{+}\otimes s_y^+ s_x^- \\ & + \frac{(1-e^{-\epsilon})}{2}L^{-}\otimes s_x^+ s_y^-.\end{aligned} \tag{46}$$

The first term corresponds to all spins either up or down, the second and third term correspond to different spins which do not cross, and the last two terms correspond to an exchange of different spins. The operators on the left, acting on the first Hilbert space, now correspond to the set of

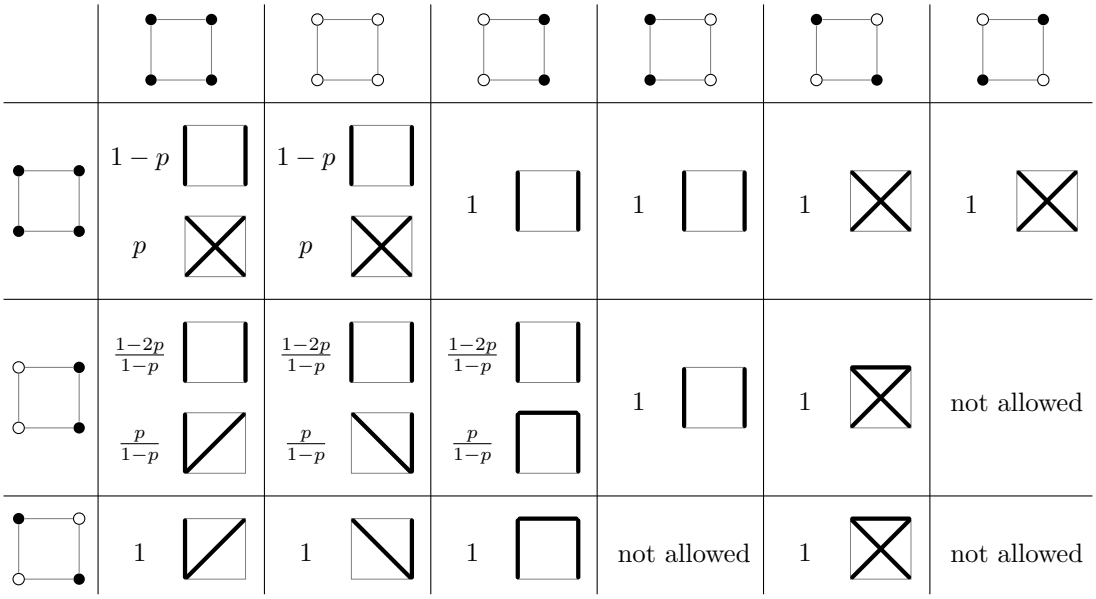

Figure 11: Graphical representation of the worm rules (46). The rules depend on the configurations of both the background (left) and current contour plaquette (top). The circles $\bullet, \circ = \uparrow, \downarrow$ represent either spin up or down (in both contours), with $\bullet \neq \circ$. Real time future is towards the top. Solid lines indicate possible paths. Multiple paths leaving a site are selected with equal probability, while no paths indicate that the worm has to bounce back. The probabilities for choosing between different sets of paths are given as functions of $p = \frac{1-e^{-\epsilon}}{2} \approx \frac{\epsilon}{2}$.

worm-rules in a given background of the second Hilbert space. We have introduced the operators $L^{\parallel} = \mathbb{1}, L^{\times} = 2L^2 - \mathbb{1}$, such that all the operators $L^{\parallel}$, $L^{\times}$, L^{+}, L^{-} have four entries 1 and twelve zeros (in the σ^3 basis). The worm rules then split into three steps. First, determine the background on the other contour. Second, choose one among the allowed operators which support the current state of the plaquette (have an entry 1 for that state), with the relative probabilities given by their prefactors. Third, move the worm according to the rules of the chosen operator and update the plaquette accordingly. For example, if the worm enters a plaquette with all spins pointing up on both contours, it can choose between the operators $L^{\parallel}$ and $L^{\times}$ with probabilities $(1 + e^{-\epsilon})/2 \approx 1 - \epsilon/2$ and $(1 - e^{-\epsilon})/2 \approx \epsilon/2$. The worm rules for $L^{\parallel}, L^{\times}$ are deterministic. They only depend on the point where the worm enters the plaquette. For $L^{\parallel}$ the worm always stays on the same spatial site, but moves to the adjacent time-step, while $L^{\times}$ moves in both time and space. On the other hand, the moves for $L^{\pm}$ are chosen at random. For $L^{\parallel}, L^{\times}$ the worm always has exactly two possibilities to leave a plaquette in a supported configuration, for all entry points. Since one of them would have left the plaquette unchanged, the worm always chooses the other with probability 1. However, for $L^{\pm}$ the number of possible exits depends on the entry point of the worm. In the case that there is only one allowed exit, the worm has to backtrack and leave the plaquette unchanged. The case with two exits is deterministic as above, while in the case of three supported exits, the worm chooses with equal probability from the two non-backtracking options. (The case of no options never occurs, since one can always backtrack, four options are impossible due to spin conservation.) As the number of supported exits is symmetric under reversal of the worm, and all supported configurations have weight 1, the rules obey detailed balance. These rules are not unique, but other choices would either introduce higher backtracking probabilities (which is undesirable in terms of efficiency) or violate detailed balance, thus unnecessarily complicating the proof of convergence to the right distribution. A graphical summary of the worm rules for the evolution (46) is given in figure 11.

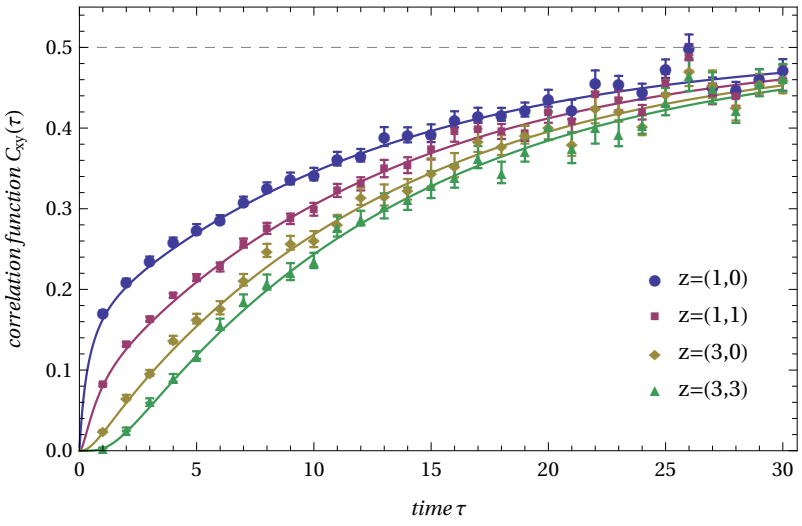

Figure 12: Evolution of correlation functions $\mathcal{C}_{xy}(\tau)$ of $N = 6^2$ particles on the square lattice under the modified dissipator (43). Monte Carlo results for selected correlation functions at spatial separations $z = x-y$ along a lattice axis (*circles, diamonds*) and on the diagonal (*squares, triangles*) were obtained with the worm algorithm. Each time point represents an independent simulation and error bars are Monte Carlo error estimates. The number of samples was increased linearly with τ ($\tau = 1 :\sim 5 \cdot 10^4$, $\tau = 90 :\sim 5 \cdot 10^5$) to obtain a similar level of uncertainty for all data points. The solid lines are the corresponding exact solutions obtained from the differential equations (47). The dashed line indicates the asymptotic value $\mathcal{C}_{xy}(\infty) = \frac{1}{2}$ $(x \neq y)$.

5.4 Implementation and Verification

We have implemented the worm algorithm for a number of system sizes $N \leq 64$ in one dimension and on the square lattice. The measured correlation functions $\mathcal{C}_{xy}, \mathcal{D}_{xy}$ agreed, within the statistical errors, with the exact result obtained from the differential equations derived from the dissipator (43)

$$\partial_t \mathcal{C}_{xy} = \langle \widetilde{\mathcal{L}}(C_{xy}) \rangle = \frac{1}{2}(\Delta_x + \Delta_y)\mathcal{C}_{xy} - \frac{1}{2}\delta_{\langle x,y \rangle}(\mathcal{C}_{xx} + 4\mathcal{D}_{xy}), \tag{47}$$

$$\partial_t \mathcal{D}_{xy} = \langle \widetilde{\mathcal{L}}(D_{xy}) \rangle = \frac{1}{2}(\Delta_x + \Delta_y)\mathcal{D}_{xy} + \delta_{\langle x,y \rangle}(\mathcal{D}_{xy} - \mathcal{D}_{xx}). \tag{48}$$

This is illustrated in figure 12, for selected spatial correlation functions on the $N = 6^2$ square lattice. Sampling at late times τ, when the system is close to its asymptotic state, is quite costly, as the worm has to run through the entire Keldysh contour to switch between different sectors of S_3 to realize a state close to ρ_{NESS} (25). We observed a linear increase with τ in the number of samples needed for a constant target error, with the effort per sample scaling linearly in τ as well. On the other hand, resolving the difference to the asymptotic value would require exponential accuracy $\delta\mathcal{O} \sim \exp(-\tau\Delta_T)$ anyhow, making it unfeasible to extract information about the late time behavior beyond the asymptotic values. The dynamical behavior far from the nonequilibrium steady state seems to be amenable to Monte Carlo studies. This is best exemplified by the evolution of the condensate fraction $\mathcal{C}_{p=0}$ in figure 13, where the initial buildup of correlations is captured to high precision by the Monte Carlo data. The worm algorithm also correctly captures the condensation at late times $\tau > \Delta_T^{-1}$ even though the results become noisier.

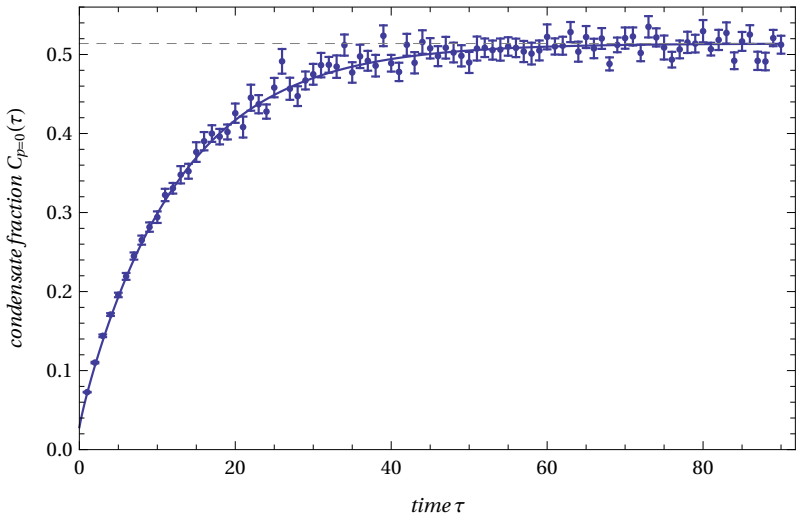

Figure 13: The evolution of the condensate fraction $\mathcal{C}_{p=0}(\tau)$ in the same system as described in figure 12. Simulation results are shown as individual points with Monte Carlo error estimates, while the solid line is the exact result. The dashed line indicates the asymptotic value $\mathcal{C}_{p=0}(\infty) = \frac{1}{2} + \frac{1}{2N}$.

6 Conclusions

6.1 Discussion

We have discussed the Lindblad equation as the Markovian master equation describing evolution of an open quantum system in terms of its density matrix. The Lindblad equation is the most general linear differential equation preserving the trace (total probability) and complete positivity of the density matrix. Its solutions can be brought into the Kraus form, which brings forth a Heisenberg-type interpretation of the dynamics, with evolving observables and a static density matrix. The expectation values of observables then obey a set of linear coupled differential equations and a set of initial values, depending on the initial density matrix. Hamiltonians and jump operators (with the exception of ultra-local operators) usually lead to a hierarchy of observables, coupling any observable acting on finitely many degrees of freedom to observables with an increasing number of degrees of freedom it acts upon. Numerically solving the system of differential equations then quickly becomes unfeasible and a truncation scheme has to be introduced. Here we showed that for open systems obeying the Markovian master equation, conditions can be formulated such that a scheme that is free of truncation errors arises. We have discussed in depth the case of a stronger constraint which strictly forbids the growing of the domain-size of dependent variables in spin $\frac{1}{2}$ systems or hardcore bosons. This enabled us to solve the full time-evolution of sets of 1- and 2-point functions exactly, without having to resort to observables of higher rank.

One might assume that closed hierarchies are an oversimplification such that the quantum nature of the underlying system is lost and the equations merely describe classical physics. However, we were able to show clearly that this is not the case. First of all, the initial state of the system is not restricted at all by the closed hierarchy conditions. Entanglement is thus a naturally built in feature of these systems. Furthermore, we have shown that entanglement can be created and destroyed within this framework and that entanglement is measurable throughout the evolution. The closed hierarchy allows us to follow the evolution for arbitrarily long times and for large system-sizes that are otherwise unreachable.

Among the bi-local jump operators fulfilling the constraint we studied a symmetrizer, which drives the system into a Bose-Einstein condensate. The symmetrization occurs by a dissipative random walk of the spins. This leads to an interesting scaling phenomenon of the longest time-scale (given by the inverse of the dissipative gap) in the system depending on the dimensionality of the underlying lattice. The random walk is stable against the introduction of an arbitrary uniform

magnetic field, but not against randomized spin flips induced by the contact with a thermal bath. The relative strength of the spin flip and random walk rates yield a finite average number of steps a spin takes, before the correlation is lost due to a spin flip. Naturally, the random walk thus only correlates the system on a characteristic length scale, thus destroying the long range correlations of the Bose-Einstein condensate. For finite systems, however, the symmetrization operator still provides an effective protocol for creating many-body entanglement, as long as thermal fluctuations can be sufficiently controlled. Our findings are consistent with small systems ($N = 4$) realized experimentally so far [34], and do not preclude the creation of long-range order in larger systems realizable in the foreseeable future.

6.2 Outlook

Although we have formulated the principle of closed hierarchies in the most general terms, our work has focused solely on the stricter condition of non-growing observables. This made the task of identifying closed sets of observables rather simple, but we were still able to find processes with interesting dynamics. Nevertheless, it would be interesting to find more general examples, in which the closure of 2-point functions would include higher-point functions. Gradually increasing the maximal degree in the closure of 2-point functions would allow for a controlled approach of the complexity of unitary quantum physics.

The closure conditions derived in this work are specific to spin $\frac{1}{2}$. Increasing the number of local degrees of freedom (higher spin representations) would make them even more involved, but also provides the possibility for even more complex behavior.

Another interesting approach would be to classify and study systems for which a sign-problem-free Monte Carlo algorithm can be formulated. Some of these might not be covered by our analysis of closed hierarchies. Our comparison of data obtained with the worm algorithm and the exact results derived from the closed hierarchy provide a proof of concept, that Monte Carlo techniques are able to capture interesting quantum real-time dynamics, albeit for open systems only.

Both homogenous and inhomogeneous systems could be of interest for quantum computation, as a mean to study initial state preparation. Creation of highly entangled initial states might be constrained by similar scaling limitations as we have found here, with and without thermal noise.

The application of linear response theory [63] could provide additional insights into the asymptotic dynamics of dissipative processes near the nonequilibrium steady state. Whether a generalization of the fluctuation-dissipation theorem [64] for open quantum systems exist is an intriguing question for future studies.

Part II

Anyonic Statistics in Doubled-Chern-Simons Theories

7 Introduction

The idea of quantum computing, or universal quantum simulation is nearly four decades old [65–67]. During the first two decades research focused primarily on theoretical aspects of quantum computation, such as a fundamental theoretical framework, necessary requirements [68, 69], possible applications and developing algorithms [70] which harness the resource provided by quantum entanglement. In terms of a physical realization of a quantum computer, the vast progress of the last two decades in the ability to manipulate quantum many-body systems [71, 72] have brought us to the cusp of surpassing classical computation capabilities. However, some of the most fundamental issues in quantum computing remain unsolved. Most prominent among them is the issue of decoherence, whereby the entanglement is destroyed by errors, inevitably occurring in any realistic system. One theoretical resort is to use topological quantum states [73], whose information is stored nonlocally in a many-body system and thus allows for fault-tolerant quantum computation schemes [74–76]. Topological quantum computations are executed by realizing unitary operations [73, 77, 78] through braiding of anyonic quasi-particles with fractional statistics [79–82]. In order to realize a universal set of quantum gates, the anyons have to be non-Abelian and their fractional statistics have to allow for arbitrarily good approximations of the quantum gates.

The prototype for topological field theories are Chern-Simons theories [83]. They have been studied extensively in relation to the fractional quantum Hall effect [84–86] and numerous other condensed matter applications [87–89]. Inspired by the latest progress with gauge theories in atomic quantum simulators, we investigate the possibilities of formulating Chern-Simons theories as doubled lattice gauge theories [90–94] with finite gauge groups [95–98]. The doubling is realized by two gauge fields, one living on the links of the primal lattice, the other on its dual. The theory is described in the Hamiltonian formulation [99–101] where the Chern-Simons term manifests itself through a non-commuting operator algebra for the primal and dual degrees of freedom. Similar theories have been proposed for lattice loop models [87] and spin liquids [102–104], while some constructions avoid the explicit construction of the dual field [105–109].

As the Hamiltonian of a pure Chern-Simons gauge theory vanishes, it is very difficult to create the states with the desired anyonic properties in condensed matter systems, since the physical states are intricately linked to the topology of the manifold on which the theory is formulated [110, 111]. This can be circumvented by starting with a Yang-Mills-like interaction and adding the Chern-Simons term on top of that. The gauge field of the pure Yang-Mills theory then acquires a (topological) mass [112–115]. The topological nature of the Chern-Simons term is still present and reappears in the ground state, when gaping out all higher states (by sending the mass to infinity). To illustrate this procedure we explicitly calculate the spectrum for a series of small finite groups, the cyclic group $\mathbb{Z}(k) \subset U(1)$ as an example of an Abelian group as well as the permutation group $S_3 \subset O(2)$ (real representations) with trivial center, the quaternion group $H \equiv \bar{D}_2 \subset SU(2)$ (pseudo-real) with center $\mathbb{Z}(2)$ and finally $\Delta(27) \subset SU(3)$ [116–119], a 27-element subgroup of $SU(3)$ with irreducible complex representations and center $\mathbb{Z}(3)$.

Many different models have been suggested to investigate anyonic quasi-particles, starting from Kitaev's Abelian toric code [73] and its non-Abelian extensions [120], all the way to a broad classification of topological orders by Levin and Wen [121]. Although these theoretical explorations have deepened our understanding of topological theories, we have been denied a practical realization of these models so far. Thus the question whether topological quantum systems with the desired non-Abelian anyonic quasi-particles can be designed, can still not be answered affirmatively [122, 123]. Our approach has the advantage of directly working in the Hamiltonian language on a locally finite Hilbert space. Thus it immediately lends itself to an implementation in an atomic simulator. Another main obstacle to a practical realization of any model is the stability at non-zero temperature [37, 124–129], which we do not address in this work.

This part of the thesis is structured as follows: First we introduce a few useful concepts of the theory of finite groups. We follow Ref. [130] in deriving the Hamiltonian formulation from the doubled Chern-Simons-Maxwell action of two $U(1)$ gauge fields in the continuum. We use canonical quantization to derive its operator algebra. We derive the same algebra in the lattice formulation, and show how it can be naturally embedded on crosses of the primal lattice and its dual. By compactifying the gauge field we obtain the lattice formulation of Chern-Simons-Maxwell theory for the discrete groups $\mathbb{Z}(k)$. We then extend the formalism to Chern-Simons-Yang-Mills theories for arbitrary discrete groups [131]. In the process we consolidate many features of the doubled Chern-Simons-Maxwell theory as an integral part of the broader framework. The consistency conditions of these theories allow for entire families of Chern-Simons-Yang-Mills-like theories. After introducing a classification scheme for these theories, we discuss the electric spectrum on a single cross. From these states the ground state in the infinite mass limit can be calculated exactly [132]. We show that these models have Abelian anyons, by calculating the fractional statistics of primal and dual charges, and show how they can be interpreted as extensions of the toric code [73].

8 Groups and Representations

8.1 Axiomatic Definition of a Group

A group $(G, \bullet)$ is a set of elements $g \in G$ and a group law

$$\bullet : G \times G \to G.$$

It has to fulfill the following axioms

$$\begin{aligned} \text{Associativity}: &\quad (g \bullet h) \bullet k = g \bullet (h \bullet k), \\ \text{Existence of identity element}: &\quad \exists e \in G : e \bullet g = g = g \bullet e \, \forall g \in G, \\ \text{Existence of inverse}: &\quad \forall g \in G, \exists h \in G : g \bullet h = e = h \bullet g. \end{aligned}$$

In the following we will denote the inverse of an element g as g^{-1}, and use the short-hand notation $gh \equiv g \bullet h$ for the group law, wherever it is implicit and unambiguous from the context.

8.2 Group Homomorphisms and Representations

A group homomorphism is a map $f : G \to H$ from one group $(G, \bullet)$ to another $(H, *)$ which preserves the group law

$$f(g \bullet h) = f(g) * f(h).$$

In particular we have $f(e_G) = e_H$ and $f(g^{-1}) = f(g)^{-1}$. We distinguish Abelian groups for which the group law is commutative

$$g \bullet h = h \bullet g \quad \forall g, h \in G,$$

from non-Abelian groups where the order matters. In the special case where $H = U(n)$, the group of unitary $n \times n$ matrices under matrix multiplication, we call the homomorphism a representation of the group G.

8.3 Abelianization

For every group G we can calculate its derived (commutator) subgroup $G^{(1)} = [G, G]$. It is defined as the smallest subgroup containing all commutators

$$g, h \in G \quad \Leftrightarrow \quad [g, h] = g^{-1} h^{-1} g h \in G^{(1)},$$

or equivalently the subgroup generated by all commutators. Since it contains all commutators, the derived subgroup is a normal subgroup $G^{(1)} \lhd G$ and its quotient

$$G_{ab} = G / G^{(1)},$$

is an Abelian group, which we call the Abelianization of G (or G made Abelian). It is by definition the largest Abelian quotient group of G. For an Abelian group the derived subgroup is trivial $G^{(1)} = e$ and therefore the group is equal to its own Abelianization. The elements of the Abelianization are given by the cosets of $G^{(1)}$

$$G_{ab} = \{g G^{(1)} | g \in G\}.$$

8.4 Group Symmetries

8.4.1 Automorphisms

Automorphisms $\mathrm{Aut}(G)$ are a special set of bijective homomorphisms $\phi : G \leftrightarrow G$, from the group G to itself. Since they are invertible they form a group under composition

$$\circ : \mathrm{Aut}(G) \times \mathrm{Aut}(G) \to \mathrm{Aut}(G), \qquad (\phi \circ \tau)(\cdot) = \phi(\tau(\cdot)).$$

The unit-element is given by the trivial map $g \to g$ and associativity is inherited from the composition of maps. Automorphisms are sometimes called symmetries of the group G, since they just permute the group elements while preserving the group law. For discrete groups (with $|G| < \infty$) they have a representation in $U(|G|)$ acting on the vector space $\mathbb{C}^{|G|} = \text{span}\{|g\rangle\,,\, g \in G\}$, $\langle g|h\rangle = \delta_{gh}$ as

$$U(\phi)\,|g\rangle = |\phi(g)\rangle\,.$$

Automorphisms define equivalence classes of Hermitian operators $\mathcal{H}$ on $\mathbb{C}^{|G|}$ through

$$\mathcal{H} \sim \mathcal{H}' \quad \Leftrightarrow \quad \exists\,\phi \in \text{Aut}(G)\,:\,\mathcal{H}' = U(\phi)\,\mathcal{H}\,U(\phi)^\dagger\,.$$

All operators in the same class share the same spectrum, they differ only in the labeling of the states.

8.4.2 Inner Automorphisms

Conjugations by a group element $g^h = h\,g\,h^{-1}$ define a group homomorphism from the group G to its own automorphism group $\text{Aut}(G)$

$$\text{Inn} : G \to \text{Aut}(G), \qquad\qquad \text{Inn}(h) = (\cdot)^h.$$

The set of all conjugations $\text{Inn}(G) \lhd \text{Aut}(G)$ form a normal subgroup and are called inner automorphisms. The group law is given by the isomorphism

$$\text{Inn}(G) \simeq G/C(G)\,,$$

which is a consequence of the center $z \in C(G)$ being the preimage of the trivial map $g^z = g$. The inner automorphisms form a normal subgroup since they are invariant under conjugation by any $\phi \in \text{Aut}(G)$

$$\phi \circ (\cdot)^h \circ \phi^{-1} = (\cdot)^{\phi(h)}\,.$$

In the theories we are about to define, a global gauge transformation acts as an inner automorphism on all group valued objects. Therefore the inner automorphism group can be viewed as a part of the symmetry group of theses theories.

8.4.3 Outer Automorphisms

Since $\text{Inn}(G)$ is normal in $\text{Aut}(G)$ we can characterize all non-inner automorphisms by the quotient

$$\text{Out}(G) = \text{Aut}(G)/\text{Inn}(G)\,,$$

which is called the outer automorphisms group. By construction the outer automorphism group acts on conjugacy classes $\mathcal{C}(g) \subset G$ (their image as an automorphism is given up to a conjugation). Furthermore for any representation

$$\Gamma\,:\,G \to U(n)\,,$$

it follows that also $\Gamma^\phi(g) = \Gamma(\phi^{-1}(g))$ $(\forall \phi \in \text{Aut}(G))$ is a representation. Since the character is a class function $\chi_\Gamma(g^h) = \chi_\Gamma(g)$, the outer automorphism group also acts on the characters. The outer automorphism group is therefore a subgroup of the symmetry group of the character table

$$\begin{aligned} g \;&\to\; g' = \phi(g)\,, \quad \Gamma \;\to\; \Gamma' = \Gamma^\phi\,, \\ \Gamma(g) \;&\to\; \Gamma'(g') = \Gamma^\phi(\phi(g)) = \Gamma(\phi^{-1}(\phi(g))) = \Gamma(g)\,. \end{aligned}$$

This relation can be used to either construct new representations using outer automorphisms or restrict the outer automorphism group given the character table.

8.5 Theory of Discrete Groups

Discrete Groups can be characterized by their conjugacy classes and irreducible representations. Two group elements are conjugate to each other if

$$g \sim h \quad \Leftrightarrow \quad \exists k \in G : \, g = (h)^k = khk^{-1}.$$

Irreducible representations are realizations of the group law as unitary matrices $\Gamma(G) \subset U(n)$ which cannot be decomposed into a direct sum of lower dimensional representations. Two representations are unitarily equivalent if they are related by a unitary transformation

$$\Gamma \sim \Gamma' \quad \Leftrightarrow \quad \exists U \in U(n) : \, \Gamma(g) = U\Gamma'(g)U^\dagger \quad \forall g \in G.$$

The character of a representation

$$\chi_\Gamma(g) = \mathrm{Tr}\, \Gamma(g)\,,$$

is invariant under unitary transformation of the representation and conjugation of the group element. The characters of all conjugacy classes $\mathcal{C}(g) = g^G$ are thus a unique fingerprint of an irreducible representation. The characters of a reducible representation are given by the sum of its irreducible parts. The decomposition of a product of representations can therefore be inferred solely from its characters

$$\chi_{\Gamma^i}(\mathcal{C}) \times \chi_{\Gamma^j}(\mathcal{C}) = \sum_k m_{ij}^k \chi_{\Gamma^k}(\mathcal{C}),$$

where $m(\Gamma) \in \mathbb{N}_0$ are the multiplicities of all irreducible representations appearing in the sum

$$\Gamma^i \otimes \Gamma^j = \bigoplus_k m_{ij}^k \, \Gamma^k.$$

Since there is an equal number of conjugacy classes and irreducible representations the character table $\chi_{\Gamma^j}(\mathcal{C}_i)$ can be viewed as a transformation matrix from the basis of multiplicities to the basis of characters

$$\begin{pmatrix} \chi_\Gamma(\mathcal{C}_1) \\ \chi_\Gamma(\mathcal{C}_2) \\ \vdots \\ \chi_\Gamma(\mathcal{C}_n) \end{pmatrix} = \begin{pmatrix} \chi_{\Gamma^1}(\mathcal{C}_1) & \chi_{\Gamma^2}(\mathcal{C}_1) & \dots & \chi_{\Gamma^n}(\mathcal{C}_1) \\ \chi_{\Gamma^1}(\mathcal{C}_2) & \chi_{\Gamma^2}(\mathcal{C}_2) & \dots & \chi_{\Gamma^n}(\mathcal{C}_2) \\ \vdots & \vdots & \ddots & \vdots \\ \chi_{\Gamma^1}(\mathcal{C}_n) & \chi_{\Gamma^2}(\mathcal{C}_n) & \dots & \chi_{\Gamma^n}(\mathcal{C}_n) \end{pmatrix} \begin{pmatrix} m(\Gamma^1) \\ m(\Gamma^2) \\ \vdots \\ m(\Gamma^n) \end{pmatrix}.$$

Very useful equations are the orthogonality relation of the characters

$$\sum_{g \in G} \chi_{\Gamma^i}(g)^* \chi_{\Gamma^j}(g) = \sum_{\mathcal{C}} |\mathcal{C}| \chi_{\Gamma^i}(\mathcal{C})^* \chi_{\Gamma^j}(\mathcal{C}) = |G| \, \delta_{ij},$$

as well as the sum rule for the dimensions of irreducible representations

$$\sum_\Gamma d_\Gamma^2 = |G|.$$

Both are corollaries of the more general orthogonality relation

$$\sum_{g \in G} \Gamma^i(g)^*_{ab} \Gamma^j(g)_{cd} = \frac{|G|}{d_{\Gamma^i}} \delta_{ij} \delta_{ac} \delta_{bd},$$

among all matrix entries $\Gamma^i(g)_{ab}\,(a, b \in 1, \dots, d_{\Gamma^i})$ of all irreducible representations.

9 Doubled Chern-Simons-Maxwell Theory

In this section we give a brief introduction to doubled Chern-Simons-Maxwell theory. Naive lattice regularization of the Chern-Simons term suffers from a doubling problem, similar to the one in fermionic systems (both theories have terms with a single derivative in their Lagrangian). Avoiding this subtle issue altogether, we start our investigation directly from a doubled continuum theory and derive its operator algebra (section 9.1). We then show how to implement this algebra on the lattice, first with non-compact gauge fields (section 9.2) and later we compactify them in section 9.3.

9.1 In the Continuum

In the continuum we can write down the Lagrangian density for the doubled Chern-Simons-Maxwell theory

$$\mathcal{L}_{\text{Maxwell}} = -\frac{1}{4e^2}F_{\mu\nu}F^{\mu\nu} - \frac{1}{4\tilde{e}^2}\tilde{F}_{\mu\nu}\tilde{F}^{\mu\nu}, \qquad \mathcal{L}_{CS} = \frac{k}{4\pi}\epsilon^{\mu\nu\rho}(A_\mu\partial_\nu\tilde{A}_\rho + \tilde{A}_\mu\partial_\nu A_\rho),$$

with the usual field strength tensor $F_{\mu\nu} = \partial_\mu A_\nu - \partial_\nu A_\mu$ and metric signature $g_{\mu\nu} \sim (-,+,+)$. Unlike in four dimensions, the charges are dimensionful quantities $[e^2] = [\tilde{e}^2] = [M^{-1}]$. Through a field redefinition one can achieve parity between the primal and dual charges $e = \tilde{e}$, and this will be assumed throughout. The Chern-Simons coupling k on the other hand is dimensionless, and is called the level of the theory. While a standard Chern-Simons term would break parity and time-reversal, this can be remedied in the doubled theory, by declaring the dual field $\tilde{A}$ a pseudo-vector. To illustrate what we mean, we look at the symmetry properties under full space-time inversions $\mathcal{I}x^\mu = -x^\mu$ which are closely related to parity and time-reversal. We define the following transformation properties for the vector and pseudo-vector field

$$\mathcal{I}A_\mu(x) = -A_\mu(-x), \qquad \mathcal{I}\tilde{A}_\mu(x) = \tilde{A}_\mu(-x).$$

It is then straightforward to show that each term in the Lagrangian contains an even number of vectors, and is thus symmetric under inversions. We now proceed to the Hamiltonian formulation, by first fixing the temporal gauge $A_0 = 0 = \tilde{A}_0$. From the gauge-fixed Lagrangian density

$$\mathcal{L} = \frac{1}{4e^2}\left(2\dot{A}_i^2 - (\epsilon_{ij}\partial_i A_j)^2 + 2\dot{\tilde{A}}_i^2 - (\epsilon_{ij}\partial_i\tilde{A}_j)^2\right) + \frac{k}{4\pi}\epsilon_{ij}(\dot{\tilde{A}}_i A_j + \dot{A}_i\tilde{A}_j),$$

we derive the conjugate momenta

$$\Pi_i = \frac{1}{e^2}\dot{A}_i + \frac{k}{4\pi}\epsilon_{ij}\tilde{A}_j, \qquad \tilde{\Pi}_i = \frac{1}{e^2}\dot{\tilde{A}}_i + \frac{k}{4\pi}\epsilon_{ij}A_j.$$

The Legendre transformation yields the Hamiltonian density

$$\mathcal{H} = \Pi_i\dot{A}_i + \tilde{\Pi}_i\dot{\tilde{A}}_i - \mathcal{L} = \frac{e^2}{2}E_i^2 + \frac{1}{2e^2}B^2 + \frac{e^2}{2}\tilde{E}_i^2 + \frac{1}{2e^2}\tilde{B}^2.$$

The Hamiltonian looks like pure doubled Maxwell theory, but the Chern-Simons coupling k reenters through the definition of the electric fields

$$E_i = \Pi_i - \frac{k}{4\pi}\epsilon_{ij}\tilde{A}_j, \qquad B = \epsilon_{ij}\partial_i A_j,$$
$$\tilde{E}_i = \tilde{\Pi}_i - \frac{k}{4\pi}\epsilon_{ij}A_j, \qquad \tilde{B} = \epsilon_{ij}\partial_i\tilde{A}_j.$$

After canonical quantization of the gauge fields and their conjugate momenta

$$[\Pi_i(x), A_j(y)] = [\tilde{\Pi}_i(x), \tilde{A}_j(y)] = -i\delta_{ij}\delta(x-y),$$
$$[\Pi_i(x), \tilde{A}_j(y)] = [\tilde{\Pi}_i(x), A_j(y)] = 0,$$

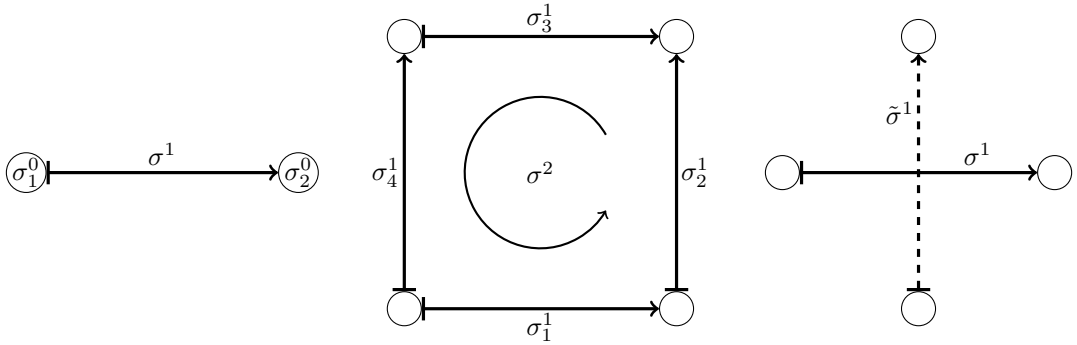

$$\partial\sigma^1 = \sigma_2^0 - \sigma_1^0, \qquad \partial\sigma^2 = \sigma_1^1 + \sigma_2^1 - \sigma_3^1 - \sigma_4^1, \qquad \star\sigma^1 = \tilde{\sigma}^1, \quad \star\tilde{\sigma}^1 = -\sigma^1.$$

Figure 14: The action of the boundary operator ∂ on 1-cells (left) and 2-cells (middle). The Hodge-dual operator $\star$ rotates a cross of primal and dual links counter-clockwise by $\pi/2$ (right).

the Chern-Simons term interlocks the algebras of the two gauge fields

$$[E_i(x), \tilde{E}_j(y)] = -i\frac{k}{2\pi}\epsilon_{ij}\delta(x-y), \tag{49}$$

with all other fields commuting except

$$[E_i(x), B(y)] = [\tilde{E}_i(x), \tilde{B}(y)] = i\epsilon_{ij}\partial_j\delta(x-y), \tag{50}$$

as in pure Maxwell theory. The non-zero commutator of the primal and dual electric fields implies that we have to complement the generators of gauge transformations

$$G = \partial_i E_i + \frac{k}{2\pi}\tilde{B}, \qquad\qquad \tilde{G} = \partial_i \tilde{E}_i + \frac{k}{2\pi}B,$$

to define gauge invariance $[G(x), H] = [\tilde{G}(x), H] = 0$ of the Hamiltonian $H = \int d^2x\,\mathcal{H}$ and a sensible Gauss law $G(x)|\Psi_{\rm phys}\rangle = \tilde{G}(x)|\Psi_{\rm phys}\rangle = 0$ ($[G(x), \tilde{G}(y)] = 0$). The dual magnetic field $\tilde{B}$ has the effect of a charge density for the primal field (and vice versa), a feature we will encounter for all theories of this type. The quantized field operators transform under space-time inversions as

$$\mathcal{I}E_i(x) = E_i(-x) \qquad \mathcal{I}B(x) = B(-x) \qquad \mathcal{I}\tilde{E}_i(x) = -\tilde{E}_i(-x) \qquad \mathcal{I}\tilde{B}(x) = -\tilde{B}(-x).$$

9.2 On the Lattice

Before proceeding to compact gauge fields, it is interesting to see how neatly the non-compact Chern-Simons-Maxwell algebra (49,50) can be realized on a square lattice $X = a(\mathbb{Z}, \mathbb{Z})$ and its dual $\tilde{X} \simeq X$ (the lattice of all plaquettes. Since our gauge theories contains 0-forms (G), 1-forms (A_i, Π_i, E_i) and 2-forms (B) that are associated with vertices, links, and plaquettes of the lattice, we will start by defining the latter in terms of $0, 1, 2$-cells in a cell-complex.

9.2.1 Lattice Conventions

We describe the two-dimensional lattice X in terms of oriented p-cells σ_i^p ($p = 0, 1, 2$), where σ_i^0 are vertices, σ_i^1 are links, and σ_i^2 are plaquettes. We can evaluate any p-form α^p on any linear combination of p-cells (an element of the cell-complex), using the bilinear contraction

$$\alpha^p\left(\sum_i w_i\sigma_i^p\right) = \sum_i w_i\alpha^p(\sigma_i^p) = \sum_i w_i\alpha_i^p,$$

where we used the shorthand notation $\alpha_i^p = \alpha^p(\sigma_i^p)$ for the value of the p-form on a particular p-cell. The geometric relations of the lattice are encoded in the incidence matrices $C_{ij}^p \in \{0 \pm 1\}$, which define the boundary operator ∂ on a $(p+1)$-cell

$$\partial \sigma_i^{p+1} = \sum_j C_{ij}^p \sigma_j^p,$$

as well as a coboundary operator d

$$d\sigma_i^p = \sum_j C_{ji}^p \sigma_j^{p+1}.$$

Using the constraint $\sum_k C_{ik}^{p+1} C_{kj}^p = 0$ (which in 2-d just means that the boundary of an area is a set of closed curves), one can show that $\partial^2 = 0 = d^2$. Furthermore we can define a Hodge-dual operator $\star$, that takes a primal p-cell to a $(2-p)$-cell of the dual lattice and vice versa (as the primal and dual lattice element live at the same physical location, we will use the same index for them)

$$\star\sigma_i^0 = \tilde{\sigma}_i^2, \qquad \star\sigma_i^1 = \pm\tilde{\sigma}_i^1, \qquad \star\tilde{\sigma}_i^1 = \mp\sigma_i^1, \qquad \star\sigma_i^2 = \tilde{\sigma}_i^0.$$

The signs $\pm$ depend on the relative orientation of the primal and dual link, with $\star\sigma_i^1 = \tilde{\sigma}_i^1$ if $\sigma_i^1 \parallel \hat{1}, \tilde{\sigma}_i^1 \parallel \hat{2}$. Applying the Hodge-dual operator twice returns the original cell up to a minus sign for 1-forms $\star\star\,\sigma_i^1 = -\sigma_i^1$. Thus the Hodge dual operator $\star$ naturally realizes the ϵ-tensor on the lattice. In two dimensions the primal and dual incidence matrices are related by

$$\begin{aligned} C_{\star ji}^0 &= \tilde{C}_{ij}^1, & (\star\tilde{\sigma}_j^1 = \pm\sigma_j^1 \;\Rightarrow\; C_{\star ji}^0 = \pm C_{ji}^0), \\ \tilde{C}_{\star ji}^0 &= C_{ij}^1, & (\star\sigma_j^1 = \pm\tilde{\sigma}_j^1 \;\Rightarrow\; \tilde{C}_{\star ji}^0 = \pm\tilde{C}_{ji}^0), \end{aligned}$$

which implies the following operator identity

$$d = \star\partial\star\,.$$

9.2.2 Form Language Lattice Gauge Theory

The (vector-)gauge fields $A_i, \tilde{A}_j$ are naturally 1-forms. Since the Chern-Simons term couples orthogonal components of A_i and $\tilde{A}_j$, it is natural to associate the primal field A with the links of the primal lattice $\sigma_i^1 \in X$, and the dual field $\tilde{A}$ with the links of the dual lattice $\tilde{\sigma}_i^1 \in X$. The Gauss-law G lives on the vertices σ_i^0, while the magnetic fields are exterior derivatives of the gauge field defined by the boundary of a plaquette

$$aB(\sigma_i^2) = dA(\sigma_i^2) = A(\partial\sigma_i^2) = \sum_j C_{ij}^1 A_j$$

Introducing the shorthands

$$G_i = G(\sigma_i^0), \qquad A_i = A(\sigma_i^1), \qquad \tilde{A}_{\star i} = \tilde{A}(\star\sigma_i^1) = \pm\tilde{A}(\tilde{\sigma}_i^1), \qquad B_i = B(\sigma_i^2),$$

allows us to write the the lattice Lagrange function $L \sim \int d^2x\mathcal{L}$ in a very compact way

$$L = \sum_i \left[\frac{a^2}{2e^2}(\dot{A}_i^2 + \dot{\tilde{A}}_i^2) + \frac{ka^2}{4\pi}(\dot{\tilde{A}}_i A_{\star i} + \dot{A}_i \tilde{A}_{\star i})\right] - \sum_i \frac{a^2}{2e^2}\left[B_i^2 + \tilde{B}_i^2\right].$$

The gauge fields transforms under the 0-form $\chi_i = \chi(\sigma_i^0)$ as

$$A_i' = A_i - \frac{1}{a}\chi(\partial\sigma_i^1) = A_i - \frac{1}{a}\sum_j C_{ij}^0 \chi_j,$$

which leaves the magnetic fields unchanged

$$aB'(\sigma_i^2) = A'(\partial\sigma_i^2) = A(\partial\sigma_i^2) - \frac{1}{a}\chi(\partial^2\sigma_i^2) = aB(\sigma_i^2),$$

while the Lagrange function changes by a total time derivative

$$L' = L - \frac{1}{a}\frac{\partial}{\partial t}\left(\sum_i \frac{ka^2}{4\pi}(\tilde{A}_i\chi(\partial\star\tilde{\sigma}_i^1) + A_i\tilde{\chi}(\partial\star\sigma_i^1))\right).$$

Again we derive canonically conjugate momenta

$$\Pi_i = \frac{a^2}{e^2}\dot{A}_i + \frac{ka^2}{4\pi}\tilde{A}_{\star i}, \qquad\qquad \tilde{\Pi}_i = \frac{a^2}{e^2}\dot{\tilde{A}}_i + \frac{ka^2}{4\pi}A_{\star i},$$

and obtain the lattice Hamiltonian through the Legendre transformation

$$H = \sum_i \frac{a^2e^2}{2}(E_i^2 + \tilde{E}_i^2) + \sum_i \frac{a^2}{2e^2}\left[B_i^2 + \tilde{B}_i^2\right],$$

with the electric field 1-forms given by ($E_i = E(\sigma_i^1)$)

$$E_i = \frac{1}{a^2}\Pi_i - \frac{k}{4\pi}\tilde{A}_{\star i}, \qquad\qquad \tilde{E}_i = \frac{1}{a^2}\tilde{\Pi}_i - \frac{k}{4\pi}A_{\star i}.$$

After canonical quantization we find that the electric fields living on dual links do not commute

$$[E_i, \tilde{E}_{\star i}] = [\tilde{E}_i, E_{\star i}] = -i\frac{k}{2\pi a^2}.$$

The remaining non-trivial commutators are given by

$$[E_i, A_i] = [\tilde{E}_i, \tilde{A}_i] = -i\frac{1}{a^2}, \qquad [E_i, B_j] = -i\frac{C_{ji}^1}{a^3}, \qquad [\tilde{E}_i, \tilde{B}_j] = -i\frac{\tilde{C}_{ji}^1}{a^3},$$

and the local gauge transformations are generated by ($B(\star\sigma_i^0) = B(\sigma_i^2) = B_i$)

$$\frac{G_i}{a^2} = -\frac{1}{a}E(d\sigma_i^0) + \frac{k}{2\pi}\tilde{B}_i, \qquad\qquad \frac{\tilde{G}_i}{a^2} = -\frac{1}{a}\tilde{E}(d\tilde{\sigma}_i^0) + \frac{k}{2\pi}B_i, \tag{51}$$

which commute with the electric and magnetic field operators

$$[G_i, \tilde{E}_j] = -\sum_k C_{ki}^0 a[E_k, \tilde{E}_j] + \frac{ka^2}{2\pi}[\tilde{B}_i, \tilde{E}_j] = -i\frac{k}{2\pi a}(C_{\star ji}^0 - \tilde{C}_{ij}^1) = 0,$$
$$[G_i, B_j] = -\sum_k C_{ki}^0 a[E_k, B_j] = i\frac{1}{a^2}\sum_k C_{ki}^0 C_{jk}^1 = 0.$$

and therefore also with the Hamiltonian $[G_i, H] = [\tilde{G}_i, H] = 0$.

9.3 Compact Gauge Theory on the Lattice

We now compactify the gauge fields from $\mathbb{R}$ to $U(1)$ by turning them into the complex phases $\phi_i, \tilde{\phi}_i \in [0, 2\pi[$ of the parallel transporters

$$U_i = \exp(iaA_i) = \exp(i\phi_i), \qquad\qquad \tilde{U}_i = \exp(ia\tilde{A}_i) = \exp(i\tilde{\phi}_i).$$

The magnetic field then becomes a phase as well

$$a^2B_i = a\sum_j C_{ij}^1 A_j = \sum_j C_{ij}^1\phi_j \quad \in [0, 2\pi[\,.$$

We incorporate it by making the magnetic Hamiltonian 2π-periodic (up to a constant shift)

$$H^B = -\sum_i \frac{1}{a^2e^2}\left[\cos(a^2B_i) + \cos(a^2\tilde{B}_i)\right] = -\sum_i \frac{1}{a^2e^2}\mathrm{Re}\left[U_{\square_i} + \tilde{U}_{\square_i}\right], \tag{52}$$

which we can express in terms of the parallel transporters $U_{\square_i} = \prod_j U_j^{C^1_{ij}}$. To simplify the derivation of the electric operator algebra, we are only considering a pair of positively oriented links (the other case is analogous, with primal and dual degrees of freedom interchanged)

$$\star\sigma^1 = \tilde{\sigma}^1, \qquad\qquad \star\tilde{\sigma}^1 = -\sigma^1.$$

The conjugate momenta can then formally be expressed as partial derivatives $\Pi = -i\partial_A, \tilde{\Pi} = -i\partial_{\tilde{A}}$ and we obtain the following electric field operators

$$\begin{aligned} aE &= -i\frac{1}{a}\partial_A - \frac{k}{4\pi}a\tilde{A} = -i\partial_\phi - \frac{k}{4\pi}\tilde{\phi}, \\ a\tilde{E} &= -i\frac{1}{a}\partial_{\tilde{A}} + \frac{k}{4\pi}aA = -i\partial_{\tilde{\phi}} + \frac{k}{4\pi}\phi. \end{aligned}$$

The parallel transporters are now the true degrees of freedom of each cross, and we get the following non-trivial commutation relations on each cross

$$[E, U] = \frac{1}{a}U, \qquad [\tilde{E}, \tilde{U}] = \frac{1}{a}\tilde{U}, \qquad [E, \tilde{E}] = -i\frac{k}{2\pi a^2}.$$

The phases $\phi, \tilde{\phi}$ are not self-adjoint operators. Therefore additional care has to be taken to make the local electric Hamiltonian

$$H^E = \frac{a^2e^2}{2}(E^2 + \tilde{E}^2),$$

self-adjoint. This can be achieved by choosing twisted boundary conditions on the wave function $\Psi(\phi, \tilde{\phi})$ on the local gauge-field torus $[0, 2\pi[^2$

$$\Psi(\phi + 2\pi, \tilde{\phi}) = \exp(-ik\tilde{\phi}/2)\Psi(\phi, \tilde{\phi}), \qquad \Psi(\phi, \tilde{\phi} + 2\pi) = \exp(ik\phi/2)\Psi(\phi, \tilde{\phi}). \tag{53}$$

The simplest way to understand this is by an analogy to a quantum mechanical particle on a torus [133], with mass $m = e^{-2}$, covariant derivative $\vec{D} = a(E, \tilde{E}) = -i\vec{\nabla}_\phi + \vec{a}$ moving in a gauge potential $\vec{a} = \frac{k}{4\pi}(-\tilde{\phi}, \phi)$ corresponding to a constant magnetic field

$$b = \epsilon_{ij}\partial_i a_j = \frac{k}{2\pi}.$$

Since the gauge potential a is only periodic up to a gauge transformation

$$\vec{a}(\phi + 2\pi, \tilde{\phi}) = \vec{a}(\phi, \tilde{\phi}) - \vec{\nabla}_\phi(-\frac{k}{2}\tilde{\phi}), \qquad \vec{a}(\phi, \tilde{\phi} + 2\pi) = \vec{a}(\phi, \tilde{\phi}) - \vec{\nabla}_\phi(\frac{k}{2}\phi), \tag{54}$$

the same gauge transformation must also be applied to the wave function, thus the boundary conditions (53). The effect of this is twofold. First, the Chern-Simons level gets quantized $k \in \mathbb{Z}$, to make the boundary conditions self-consistent

$$\begin{aligned} \Psi(\phi + 2\pi, \tilde{\phi} + 2\pi) &= \exp(-ik(\tilde{\phi} + 2\pi)/2)\Psi(\phi, \tilde{\phi} + 2\pi) \\ &= \exp(-ik(\tilde{\phi} + 2\pi)/2 + ik\phi/2)\Psi(\phi, \tilde{\phi}), \\ &= \exp(-ik\pi + ik\phi/2)\Psi(\phi + 2\pi, \tilde{\phi}), \\ &= \exp(-ik2\pi)\Psi(\phi + 2\pi, \tilde{\phi} + 2\pi). \end{aligned}$$

Second, the primal and dual $U(1)$ gauge symmetry each break down to a $\mathbb{Z}(k)$ symmetry. The generators of gauge transformations (51) can be rewritten as a sum of mutually commuting operators

$$G_i = -\mathcal{G}(d\sigma_i^0), \qquad \mathcal{G}_i = aE_i + \frac{ka}{2\pi}\tilde{A}_{\star i} = \frac{1}{a}\Pi_i + \frac{k}{4\pi}a\tilde{A}_{\star i} = -i\partial_\phi + \frac{k}{4\pi}\tilde{\phi},$$

where $\mathcal{G}_i$ is a local operator on a pair of crossing primal and dual links. The intimate relation with the electric field operators $k \leftrightarrow -k \Rightarrow aE \leftrightarrow \mathcal{G}$ leads to the following algebra on a single cross

$$\begin{aligned} [\mathcal{G}, \tilde{U}] = [\tilde{\mathcal{G}}, U] = 0, \qquad [\mathcal{G}, U] = U, \qquad [\tilde{\mathcal{G}}, \tilde{U}] = \tilde{U}, \\ [E, \mathcal{G}] = [\tilde{E}, \mathcal{G}] = [E, \tilde{\mathcal{G}}] = [\tilde{E}, \tilde{\mathcal{G}}] = 0, \qquad [\mathcal{G}, \tilde{\mathcal{G}}] = i\frac{k}{2\pi}, \qquad [\mathcal{G}, H^E] = [\tilde{\mathcal{G}}, H^E] = 0. \end{aligned} \tag{55}$$

However all these commutators are only valid on a formal level in the compact theory. On further inspection one sees that $\mathcal{G}$ does not preserve the boundary conditions (53)

$$\begin{aligned} \Psi'(\phi, \tilde{\phi} + 2\pi) &= \exp(i\chi\mathcal{G})\Psi(\phi, \tilde{\phi} + 2\pi) \\ &= \exp(i\chi\frac{k}{4\pi}(\tilde{\phi} + 2\pi))\Psi(\phi + \chi, \tilde{\phi} + 2\pi) \\ &= \exp(i\chi\frac{k}{4\pi}(\tilde{\phi} + 2\pi) + ik(\phi + \chi)/2)\Psi(\phi + \chi, \tilde{\phi}) \\ &= \exp(ik\phi/2 + i\chi k)\Psi'(\phi, \tilde{\phi}), \end{aligned}$$

but introduces a self-adjoint extension parameter $\tilde{\theta} = \chi k$ (rotating into a different domain of H), which only vanishes for χ an integer multiple of $\frac{2\pi}{k}$, and thus breaking the $U(1)$ symmetry down to $\mathbb{Z}(k)$ (the same also happens to $\tilde{\mathcal{G}}$, breaking the dual gauge symmetry from $U(1) \to \mathbb{Z}(k)$). As the gauge symmetry is not a fundamental symmetry of the system but rather a redundancy in the description, this breakdown is not further worrisome. It is just a reflection of the fact that all energy levels of the electric Hamiltonian in the compact theory are only k-fold degenerate and not infinitely as in the non-compact theory. Thus the $\mathbb{Z}(k)$ gauge invariance just lifts the k-fold redundancy present in this system. The operators

$$T = \exp(i\frac{2\pi}{k}\mathcal{G}), \qquad \tilde{T} = \exp(i\frac{2\pi}{k}\tilde{\mathcal{G}}),$$

act on the degenerate states, while preserving the domain. Furthermore their k-th power represents the boundary condition

$$\begin{aligned} T^k\Psi(\phi, \tilde{\phi}) &= \exp(i\sigma k/2)\Psi(\phi + 2\pi, \tilde{\phi}) = \Psi(\phi, \tilde{\phi}), \\ \tilde{T}^k\Psi(\phi, \tilde{\phi}) &= \exp(-i\sigma k/2)\Psi(\phi, \tilde{\phi} + 2\pi) = \Psi(\phi, \tilde{\phi}), \end{aligned}$$

thus the physical states are eigenstates of $T, \tilde{T}$ with the eigenvalues being the k-th roots of unity $\xi_k^l = e^{i\frac{2\pi l}{k}}$. However, since the two operators do not commute

$$\begin{aligned} T\tilde{T}\Psi(\phi, \tilde{\phi}) &= \exp(-i\phi/2)T\Psi(\phi, \tilde{\phi} + \frac{2\pi}{k}) \\ &= \exp(i(-\phi + \tilde{\phi} + \frac{2\pi}{k})/2)\Psi(\phi + \frac{2\pi}{k}, \tilde{\phi} + \frac{2\pi}{k}) \\ &= \exp(i(\tilde{\phi} + \frac{4\pi}{k})/2)\tilde{T}\Psi(\phi + \frac{2\pi}{k}, \tilde{\phi}) \\ &= \exp(i\frac{2\pi}{k})\tilde{T}T\Psi(\phi, \tilde{\phi}), \end{aligned} \tag{56}$$

we can label all states by their energy level E_n and unit-root ξ_k^l eigenvalue of T

$$H|n, l\rangle = E_n|n, l\rangle, \qquad T|n, l\rangle = \xi_k^l|n, l\rangle, \qquad \tilde{T}|n, l + 1\rangle.$$

The last equality follows from the commutation relations, and identifies $\tilde{T}$ as a raising operator of l modulo k. The roles of $T, \tilde{T}$ are interchangeable, we could have just as well diagonalized $\tilde{T}$, turning T into the lowering operator.

10 Lattice Gauge Theories with Discrete Gauge Group

In this section we want to generalize the algebra we uncovered in section 9.2.2 for the compact $U(1)/\mathbb{Z}(k)$ gauge theory on the lattice to arbitrary finite discrete groups G. We start by defining field-value and transformation operators in the discrete gauge group G in section 10.1. We then identify the non-abelian charges and their fluxes (section 10.2), before establishing the Gauss law (section 10.3). This enables us to identify gauge invariant quantities to construct electric and magnetic Hamiltonians for the lattice theory (section 10.4).

10.1 Operator Algebra on a Single Link

As we have seen before, the compact gauge field degrees of freedom are parallel transporters U living on the links of the lattice and taking values in the gauge group $U \in G$. They form the $|G|$-dimensional Hilbert space $\mathbb{C}^{|G|}$, with an orthonormal basis $\{|U\rangle, U \in G\}$. As we are no longer dealing with a cyclic group $\mathbb{Z}(k)$ we can no longer faithfully represent the parallel transporter by a unitary operator (we will show in section 11.7.1 how such an operator can be defined for each Abelian representation of the group). However, we can talk about the projection operators $P(u), u \in G$

$$P(u)|U\rangle = \delta_{u,U}|U\rangle, \qquad P(u)P(u') = \delta_{u,u'}P(u), \tag{57}$$

which allow us to define operators from arbitrary complex functions $f : G \to \mathbb{C}$

$$f(U) = \sum_{u\in G} f(u)P(u).$$

For the cyclic groups $\mathbb{Z}(k)$ a single operator T sufficed to describe all possible gauge transformations $T(l) = T^l$. The structure for a general (non-Abelian, non-cyclic) group is more complex. For non-Abelian groups the set of gauge transformation operators acting at one end of the link can no longer be expressed in terms of operators acting on the other end. We will call these two distinct sets left and right gauge transformation operators, as they act on the parallel transporter by left and right multiplication,

$$\begin{aligned} L(g)|U\rangle &= |gU\rangle, & R(g)|U\rangle &= |Ug^{-1}\rangle, \\ L(g)P(u) &= P(gu)L(g), & R(h)P(u) &= P(uh^{-1})R(h). \end{aligned}$$

It follows immediately that L, R are both $|G|$-dimensional representations obeying the group law

$$\begin{aligned} L(g)L(h) &= L(gh), & L(g^{-1}) &= L(g)^\dagger, & L(e) &= \mathbb{1}_{|G|}, \\ R(g)R(h) &= R(gh), & R(g^{-1}) &= R(g)^\dagger, & R(e) &= \mathbb{1}_{|G|}, \end{aligned}$$

and that they commute with each other

$$[L(g), R(h)] = \mathbb{1}_{|G|}.$$

The left transformation operators $L(g)$ of a link σ^1_i are associated with the vertex σ^0_j with $C^0_{ij} = -1$, while the right transformation operators $R(g)$ are associated with the vertex σ^0_j with $C^0_{ij} = +1$.

10.2 Flux Basis

The decomposition of the $|G|$-dimensional representation into irreducible representations yields the flux basis

$$\{|\Gamma^p_{ab}\rangle, \Gamma^p \text{ irreducible representation of } G,\ a, b \in 1, \ldots, d_{\Gamma^p}\}.$$

They are connected to the link states by a unitary transformation

$$|\Gamma^p_{ab}\rangle = \sum_{U\in G} |U\rangle\langle U|\Gamma^p_{ab}\rangle = \sqrt{\frac{d_{\Gamma^p}}{|G|}} \sum_{U\in G} \Gamma^p(U)_{ab}|U\rangle.$$

The prefactors in the matrix elements $\langle U|\Gamma^p_{ab}\rangle = \sqrt{d_{\Gamma^p}/|G|}\Gamma^p(U)_{ab}$ are chosen such that the flux states form an orthonormal basis

$$\langle\Gamma^p_{ab}|\Gamma^q_{cd}\rangle = \sum_{U\in G}\langle\Gamma^p_{ab}|U\rangle\langle U|\Gamma^q_{cd}\rangle = \frac{\sqrt{d_{\Gamma^p}d_{\Gamma^q}}}{|G|}\sum_{U\in G}\Gamma^p(U)^*_{ab}\Gamma^q(U)_{cd} = \delta_{pq}\delta_{ac}\delta_{bd}.$$

As expected the different fluxes Γ^p decouple under gauge transformations, and each transforms according to its irreducible representation

$$\begin{aligned} L(g)R(h)|\Gamma^p_{ab}\rangle &= \sum_{U\in G}|gUh^{-1}\rangle\langle U|\Gamma^p_{ab}\rangle \\ &= \sum_{U\in G}|U\rangle\langle g^{-1}Uh|\Gamma^p_{ab}\rangle \\ &= \sum_{cd}\Gamma^p(g^{-1})_{ac}|\Gamma^p_{cd}\rangle\Gamma^p(h)_{db} \\ &= \sum_{cd}\Gamma^p(g)^*_{ca}|\Gamma^p_{cd}\rangle\Gamma^p(h)_{db}. \end{aligned}$$

10.3 Gauss Law

Local gauge transformations $V_i(g)$ at a single site σ^0_i also form a representation of the group G

$$V_i(g)V_i(h) = V_i(gh).$$

They are a product of transformation operators acting on adjacent links

$$V_i(g) = \bigotimes_{\sigma^1_j} T_{ij}(g), \qquad T_{ij}(g) = \begin{cases} L_j(g), & \text{for } C^0_{ij} = -1 \\ \mathbb{1}_{|G|}, & \text{for } C^0_{ij} = 0 \\ R_j(g), & \text{for } C^0_{ij} = 1 \end{cases}.$$

The Gauss law then restricts the Hilbert space to the physical states which obey

$$V_i(g)|\text{physical}\rangle = |\text{physical}\rangle,$$

which means that the physical states transform under the trivial representation Γ^1 at each site. Alternatively one could choose a representation p (and a component $a \in 1,\dots,d_{\Gamma^p}$) for all sites independently, which would correspond to having static charges in the system, such that the local transformation behavior at site i with charge (p,a) would become

$$V_i(g)|p,a\rangle = \sum_{b=1}^{d_{\Gamma^p}}\Gamma^p(g)_{ab}|p,b\rangle.$$

10.4 Hamiltonian

The magnetic Hamiltonian (52) generalizes to non-Abelian theories. The ordered parallel transporters around a plaquette $U_{\square_i} = \prod_j U_j^{C^1_{ij}}$ are no longer gauge invariant, but they transform as

$$U'_{\square_i} = g_k U_{\square_i} g_k^{-1},$$

where g_k is the gauge transformation applied to an arbitrarily chosen starting and endpoint σ^0_k of the plaquette boundary loop $U_{\square_i}$. This implies that the conjugacy class of the plaquette variable $U_{\square_i}$ is gauge invariant and independent of the choice of the starting point σ^0_k and thus represents a magnetic flux on the plaquette. The irreducible representations Γ^p provide a complete basis for the class-functions of G. Thus we can write the most general magnetic Hamiltonian on a single plaquette as

$$\mathbb{H}_B = \frac{1}{a^2e^2}h_B(U_\square) = \frac{1}{a^2e^2}\sum_{\Gamma^p}h_B(\Gamma^p)\,\mathrm{Re}\chi_{\Gamma^p}(U_\square).$$

We introduce the distance measure between two group elements

$$d(g,h) = 1 - \frac{1}{d_{\Gamma^f}} \mathrm{Re}\chi_{\Gamma^f}(g^{-1}h),$$

where Γ^f is the smallest faithful representation of G. This allows us to write a magnetic Hamiltonian that favors flat connections $U_\Box = e$

$$h_B(U_\Box) = d_{\Gamma^f} d(U_\Box, e) = d_{\Gamma^f} - \mathrm{Re}\chi_{\Gamma^f} U_\Box,$$

with the constant term chosen such that $h_B(e) = 0$. The electric Hamiltonian should act separately on the individual links. The gauge invariant quantities on the link are the fluxes (the irreducible representations). Assigning different energies to different flux states is exactly the role of the electric part of the Hamiltonian

$$\mathbb{H}_E = \frac{e^2}{2} \sum_{\Gamma^p_{ab}} h_E(\Gamma^p) |\Gamma^p_{ab}\rangle\langle\Gamma^p_{ab}| = \frac{e^2}{2} \sum_{\Gamma^p} h_E(\Gamma^p)\, P_{\Gamma^p}.$$

For continuous groups the electric Hamiltonian is usually a Laplacian in group space. We can mimic that for discrete groups by a discrete Laplacian in terms of hopping operators $h(g)$

$$\mathbb{H}_E = \frac{e^2}{2} \sum_{\langle g,e\rangle} (1 - h(g)).$$

Here the sum goes over all nearest neighbors of the unit-element e, defined by the distance measure $d(g,e)$. Since all elements in the same conjugacy class have the same distance to the unit element $d(e,g^h) = d(e,g)$, this discrete Laplacian is gauge invariant and the hopping can be realized with either all left or all right transformation operators $h(g) = L(g), R(g)$. The manifestly gauge invariant coefficients $h_E(\Gamma^p)$ can be obtained by calculating

$$h_E(\Gamma^p) = \frac{2}{e^2} \langle \Gamma^p_{ab} | \mathbb{H}_E | \Gamma^p_{ab} \rangle,$$

especially $h_E(\Gamma^1) = 0$ for the trivial representation (flux) Γ^1.

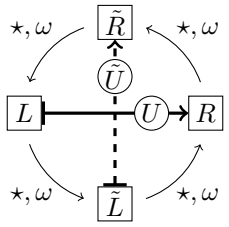

Figure 15: The cross-based operator algebra. The parallel transporter U ($\tilde{U}$) is associated with an oriented link of the primal (dual) lattice. The parallel transporter transforms under left and right multiplications L, R ($\tilde{L}, \tilde{R}$), which are part of gauge transformation operators at opposite ends of the primal (dual) links. The thin arrows indicate the action of the Hodge-dual operators $\star$ on the links and their transformation operators $T = L, R, \tilde{L}, \tilde{R}$ as well as the convention for the twisted commutator $[T, \star T] = \omega$. The algebra is the same on the other type of crosses with the roles of the primal and dual lattice interchanged, while keeping the orientation of $\star$ and ω.

11 Doubled Lattice Chern-Simons-Yang-Mills Theories

In this section we use the basic building blocks derived in the previous section 10 and generalize the algebra on crosses of links on the doubled lattice. The commutator of operators from different copies of the lattice are not completely fixed by the Gauss law constraints we derive in section 11.1, and classes of different theories can be identified (see section 11.4). In section 11.2 we demonstrate how charge fluxes are no longer well-defined on both lattices simultaneously, if the theory has a non-trivial commutator and as a consequence thereof the Hamiltonians on the two lattices no longer commute (see section 11.3). For some small groups we derive the classes of possible theories in section 11.5 and derive the spectrum of their electric Hamiltonians (section 11.6). In the strong coupling limit (in the absence of a magnetic Hamiltonian) these theories feature excitations with Abelian anyonic statistics, as we demonstrate in section 11.7.

11.1 Operator Algebra on a cross of links

The algebra of a cross of links is given by two copies of the single link algebra presented in section 10.1, one acting on the primal lattice P, L, R and one on the dual $\tilde{P}, \tilde{L}, \tilde{R}$. All projection operators commute with each other, as well as with the transformation operators of the other sublattice. This is a necessary property of the parallel transporters $U, \tilde{U}$. For simplicity, we derive all relations for a positively oriented cross only and indicate how to convert this to the other crosses. Inspired by the non-commutativity of transformation operators $T, \tilde{T}$ of the cyclic group $\mathbb{Z}(k)$ (56) we implement the Chern-Simons like interaction through a twist of the commutator of the transformations of the primal and the dual link

$$[L(g), \tilde{L}(h)] = \omega(g, h), \tag{58}$$

where ω is a unitary operator since both $L, \tilde{L}$ are. The need for a sensible Gauss law on all sites heavily constrains the possible commutators $\omega(g, h)$. Since any pair of one primal and one dual site share operators from either zero or two crosses we get the following constraint

$$[V(g), \tilde{V}(h)] = [L_1(g), \tilde{L}_1(h)][R_2(g), \tilde{R}_2(h)] = \omega_1(g, h)\, \omega_2(g, h) = \mathbb{1}. \tag{59}$$

Since $\omega_{1,2}(g, h)$ act on the Hilbert space of different crosses, they are restricted to $U(1)$ phases in order to be able to fulfill the constraint, and we have

$$\omega_2(g, h) = \omega_1(g, h)^{-1} = \bar{\omega}_1(g, h), \tag{60}$$

for any two neighboring crosses. Furthermore the commutator $\omega(g, h) \in U(1)$ itself commutes with all other operators in the algebra, which implies that it has to fulfill the group law

$$\omega(gg', h) = [L(gg'), \tilde{L}(h)] = L(g')^{-1}[L(g), \tilde{L}(h)]\tilde{L}(h)^{-1}L(g')\tilde{L}(h) = \omega(g, h)\, \omega(g', h),$$

and is therefore a homomorphism $\omega(\cdot, h) : G \to U(1)$, for all $h \in G$ (the same is also true with the roles of the two arguments exchanged). We will show in section 11.4 how we can use this to characterize all sensible twists $\omega(g, h)$ by homomorphisms from the group G to its Abelianization G_{ab}. The other commutators on the same cross are related to this one if we demand invariance under 90° rotations of the cross

$$[L(g), \tilde{L}(h)] = [\tilde{L}(h), R(g)] = [R(g), \tilde{R}(h)] = [\tilde{R}(h), L(g)] = \omega(g, h). \tag{61}$$

From (59) and (60) we see that we have to replace $\omega \to \bar{\omega}$ for all crosses where the orientation of the links is reversed (the two interacting crosses in (59) have different relative orientation of their links). This also provides a symmetry which interchanges the two types of crosses and the primal and dual fields. All this is reminiscent of the cyclic case $\mathbb{Z}(k)$, where $L \sim T$, $R \sim T^{-1}$ and

$$[T, \tilde{T}] = [\tilde{T}, T^{-1}] = [T^{-1}, \tilde{T}^{-1}] = [\tilde{T}^{-1}, T] = \exp(i\frac{2\pi}{k}), \tag{62}$$

are trivial identities following from (56). In fact we can rewrite (61,62) as

$$[T(g), \star T(h)] = \omega(g, h), \tag{63}$$

for both crosses and all $T = L, \tilde{L}, R, \tilde{R}$, if we define $\star T$ as in figure 15. The twisted algebra of a single cross lives on the doubled Hilbert space $\mathbb{C}^{2|G|}$, with an orthonormal basis

$$\{|U, \tilde{U}\rangle,\, U, \tilde{U} \in G\}, \qquad \langle U, \tilde{U}|U', \tilde{U}'\rangle = \delta_{UU'}\delta_{\tilde{U}\tilde{U}'}.$$

The twist can be realized by an insertion of appropriate phase factors on the primal transformation operators

$$\begin{aligned} L(g)|U, \tilde{U}\rangle &= \omega(g, \tilde{U})|gU, \tilde{U}\rangle, & R(g)|U, \tilde{U}\rangle &= \bar{\omega}(g, \tilde{U})|Ug^{-1}, \tilde{U}\rangle, \\ \tilde{L}(h)|U, \tilde{U}\rangle &= |U, h\tilde{U}\rangle, & \tilde{R}(h)|U, \tilde{U}\rangle &= |U, \tilde{U}h^{-1}\rangle. \end{aligned} \tag{64}$$

It is straightforward to verify the commutation relations

$$\begin{aligned} [L(g), \tilde{L}(h)]\,|U, \tilde{U}\rangle &= L(g)^{-1}\tilde{L}(h)^{-1}\omega(g, h\tilde{U})|gU, h\tilde{U}\rangle \\ &= \omega(g^{-1}, \tilde{U})\,\omega(g, h\tilde{U})|U, \tilde{U}\rangle \\ &= \omega(g^{-1}g, \tilde{U})\,\omega(g, h)|U, \tilde{U}\rangle \\ &= \omega(g, h)|U, \tilde{U}\rangle. \end{aligned}$$

This is just one realization. By a change of basis we could move the phases to the dual operators, or distribute them among both. Of special interest are unitary transformations which are diagonal in the link basis and therefore commute with the projection operators $P(u), \tilde{P}(u)$

$$|U, \tilde{U}\rangle' = \exp(i\varphi(U, \tilde{U}))|U, \tilde{U}\rangle,$$

which correspond to gauge transformations of the abstract gauge field a in (54). The transformed realization is then given by

$$\begin{aligned} L(g)'|U, \tilde{U}\rangle' &= \exp(i\varphi(gU, \tilde{U}) - i\varphi(U, \tilde{U}))\,\omega(g, \tilde{U})\,|gU, \tilde{U}\rangle', \\ R(g)'|U, \tilde{U}\rangle' &= \exp(i\varphi(Ug^{-1}, \tilde{U}) - i\varphi(U, \tilde{U}))\,\bar{\omega}(g, \tilde{U})\,|Ug^{-1}, \tilde{U}\rangle', \\ \tilde{L}(h)'|U, \tilde{U}\rangle' &= \exp(i\varphi(U, h\tilde{U}) - i\varphi(U, \tilde{U}))\,|U, h\tilde{U}\rangle', \\ \tilde{R}(h)'|U, \tilde{U}\rangle' &= \exp(i\varphi(U, \tilde{U}h^{-1}) - i\varphi(U, \tilde{U}))\,|U, \tilde{U}h^{-1}\rangle'. \end{aligned} \tag{65}$$

By setting $e^{i\varphi(U,\tilde{U})} = \bar{\omega}(U, \tilde{U})$, for instance, one can move the twist to the dual operators

$$\begin{aligned} L(g)'|U, \tilde{U}\rangle' &= |gU, \tilde{U}\rangle', & R(g)'|U, \tilde{U}\rangle' &= |Ug^{-1}, \tilde{U}\rangle', \\ \tilde{L}(h)'|U, \tilde{U}\rangle' &= \bar{\omega}(U, h)|U, h\tilde{U}\rangle', & \tilde{R}(h)'|U, \tilde{U}\rangle' &= \omega(U, h)|U, \tilde{U}h^{-1}\rangle'. \end{aligned}$$

This small exercise illustrates how the twisted commutator (58) subject to the Gauss law constraint (59) reduces to the operators in (64), and even though (65) looks like a more general construction, it is, in fact, unitarily equivalent.

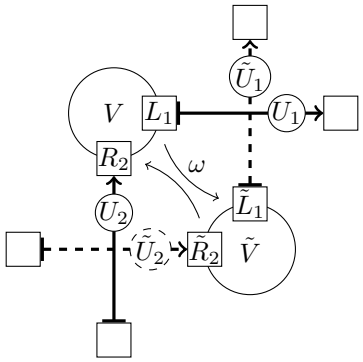

Figure 16: The commutator of neighboring primal and dual gauge transformations $V, \tilde{V}$ vanishes through a non-trivial interplay of the twists ω of the operators on the positively oriented cross $L_1, \tilde{L}_1$ and the negatively oriented cross $R_2, \tilde{R}_2$ (see eq. 59).

11.2 Link-Flux Basis

One important effect of the twist ω is that fluxes are non longer simultaneously well-defined on both sublattices. One simple way to see this is by going to a partial flux basis, with definite flux on the dual lattice

$$|U, \Gamma^p_{ab}\rangle = |U\rangle \otimes \sum_{\tilde{U}\in G} |\tilde{U}\rangle\langle\tilde{U}|\Gamma^p_{ab}\rangle = \sqrt{\frac{d_{\Gamma^p}}{|G|}} \sum_{\tilde{U}\in G} \Gamma^p(\tilde{U})_{ab}|U, \tilde{U}\rangle.$$

Dual transformations do not mix dual fluxes

$$\tilde{L}(g)\tilde{R}(h)|U, \Gamma^p_{ab}\rangle = \sum_{cd} \Gamma^p(g)^*_{ca}|U, \Gamma^p_{cd}\rangle\Gamma^p(h)_{db},$$

but the primal transformations do

$$\begin{aligned}
L(g)R(h)|U, \Gamma^p_{ab}\rangle &= \sqrt{\frac{d_{\Gamma^p}}{|G|}} \sum_{\tilde{U}\in G} \Gamma^p(\tilde{U})_{ab}\omega(g, \tilde{U})\bar{\omega}(h, \tilde{U})|gUh^{-1}, \tilde{U}\rangle \\
&= \sqrt{\frac{d_{\Gamma^p}}{|G|}} \sum_{\tilde{U}\in G} \Gamma^p(\tilde{U})_{ab}\Gamma^{\tilde{p}(g)}(\tilde{U})\bar{\Gamma}^{\tilde{p}(h)}(\tilde{U})|gUh^{-1}, \tilde{U}\rangle \\
&= \sqrt{\frac{d_{\Gamma^p}}{|G|}} \sum_{\tilde{U}\in G} \Gamma^{p\star\tilde{p}(g)\star\tilde{p}(h)^{-1}}(\tilde{U})_{ab}|gUh^{-1}, \tilde{U}\rangle \\
&= |gUh^{-1}, \Gamma^{p\star\tilde{p}(g)\star\tilde{p}(h)^{-1}}_{ab}\rangle.
\end{aligned}$$

The flux states on the primal lattice need to compensate the twist ω, but are also easy to define

$$|\Gamma^p_{ab}, \tilde{U}\rangle = \sqrt{\frac{d_{\Gamma^p}}{|G|}} \sum_{U\in G} \Gamma^p(U)_{ab}\,\omega(U, \tilde{U})|U, \tilde{U}\rangle.$$

Primal transformations do not mix primal fluxes

$$\begin{aligned}
L(g)R(h)|\Gamma^p_{ab}, U\rangle &= \sqrt{\frac{d_{\Gamma^p}}{|G|}} \sum_{U\in G} \Gamma^p(U)_{ab}\,\omega(gUh^{-1}, \tilde{U})|gUh^{-1}, \tilde{U}\rangle \\
&= \sum_{cd} \Gamma^p(g)^*_{ca}|\Gamma^p_{cd}, \tilde{U}\rangle\Gamma^p(h)_{db},
\end{aligned}$$

but the dual transformations do

$$\begin{aligned}\tilde{L}(g)\tilde{R}(h)|\Gamma^p_{ab},\tilde{U}\rangle &= \sqrt{\frac{d_{\Gamma^p}}{|G|}}\sum_{U\in G}\Gamma^p(U)_{ab}\,\omega(U,\tilde{U})|U,g\tilde{U}h^{-1}\rangle \\ &= \sqrt{\frac{d_{\Gamma^p}}{|G|}}\sum_{U\in G}\Gamma^p(U)_{ab}\,\Gamma^{p(g)}(U)\bar{\Gamma}^{p(h)}(U)\,\omega(U,g\tilde{U}h^{-1})|U,g\tilde{U}h^{-1}\rangle \\ &= |\Gamma^{p\star p(g)\star p(h)^{-1}}_{ab},g\tilde{U}h^{-1}\rangle.\end{aligned}$$

11.3 Hamiltonian

We use the same principles to build the Hamiltonian as before when the algebra was link-based. In particular, we use the same magnetic Hamiltonian

$$h_B(U_\square) = d_{\Gamma^f} - \mathrm{Re}\chi_{\Gamma^f}U_\square$$

for both sublattices, as conjugacy classes of plaquette fields $U_\square, \tilde{U}_\square$ are still invariant under all gauge transformations. The electric part needs to be adapted, because the hopping operators $h(g) = L(g), R(g)$ no longer commute with the dual gauge transformation operators $\tilde{L}(g), \tilde{R}(g)$. This can be cured easily by redistributing the twist ω among the hopping operators

$$\begin{aligned}h(g)|U,\tilde{U}\rangle &= |gU,\tilde{U}\rangle, \\ \tilde{h}(g)|U,\tilde{U}\rangle &= \omega(U,g)|U,g\tilde{U}\rangle.\end{aligned}$$

We then obtain the following commutation relations

$$\begin{aligned}L(h)h(g)L(h)^{-1} &= h(g^h), & \tilde{L}(h)h(g)\tilde{L}(h)^{-1} &= h(g), \\ L(h)\tilde{h}(g)L(h)^{-1} &= h(g), & \tilde{L}(h)\tilde{h}(g)\tilde{L}(h)^{-1} &= h(g^h),\end{aligned}$$

which shows the gauge invariance of the electric Hamiltonian

$$\mathbb{H}_E = \sum_{\langle g,e\rangle}(2 - h(g) - \tilde{h}(g)). \tag{66}$$

The key observation is now that the hopping operators do not commute

$$[h(g),\tilde{h}(k)] = \bar{\omega}(g,k). \tag{67}$$

This means that the eigenstates will not be product states, which mirrors what we have seen for the flux states. The commutator of the hopping operators (67) comes with the inverse twist $\bar{\omega}$ with respect to the transformation operators (58). This generalizes the similarity between the commutation relations for the gauge transformation $\mathcal{G}$ and electric field operator E in the $\mathbb{Z}(k)$ gauge theory (55), up to an inversion $k \to -k$. This relation also manifests itself by the fact that we can rewrite the gauge transformation operators in terms of hopping operators

$$V_i(g) = \omega(g,\hat{\tilde{U}}_{\square,i})\bigotimes_{\sigma^1_j} h_{ij}(g) = \omega(g,\hat{\tilde{U}}_{\square,i})H_i(g), \qquad h_{ij}(g) = \begin{cases} h^L_j(g), & \text{for } C^0_{ij} = -1 \\ \mathbb{1}_{|G|}, & \text{for } C^0_{ij} = 0 \\ h^R_j(g), & \text{for } C^0_{ij} = 1 \end{cases}, \tag{68}$$

where $h^L_i(g)$ are the hopping operators defined above and $h^R_i(g)$ are their right-multiplication counterparts. But this is exactly the discrete group analogue of (51), which separates the gauge transformations into an electric part on the outgoing links (h, E) plus a part depending on the dual magnetic flux $(\tilde{U}_\square, \tilde{B})$.

11.4 Characterization of the Twisted Algebras

We will discuss two equivalent characterization schemes for the twists ω. The first identifies the twist by two maps $p, \tilde{p} : G \to G_{ab}$ and their kernels $N_p, N_{\tilde{p}}$, which are normal subgroups of G. This classification makes it very simple to identify conjugacy classes of twists defined by

$$\omega \sim \omega' \qquad \Leftrightarrow \qquad \exists \phi, \tilde{\phi} \in \mathrm{Aut}(G) : \omega'(g,h) = \omega(\phi(g), \tilde{\phi}(h)),\ \forall g, h \in G.$$

The second method classifies twists from the Abelianization G_{ab} in terms of a twist matrix K_{ij} which provides a simple method for counting all possible twists.

11.4.1 Normal Subgroups

We have shown that the twists $\omega(g,h)$ are homomorphisms in both arguments

$$\omega : G \times G \to U(1) \qquad \omega(gg', h) = \omega(g,h)\,\omega(g',h), \qquad \omega(g, hh') = \omega(g,h)\,\omega(g,hh').$$

This implies maps $p, \tilde{p} : G \to \{\Gamma : d_\Gamma = 1\}$ from the group on one lattice to the set of one-dimensional irreducible representations on the other

$$\Gamma^{p(h)}(g) = \omega(g,h) = \Gamma^{\tilde{p}(g)}(h).$$

Each notation only makes the group law apparent in one argument. In order to reveal both we have to define a group structure

$$\Gamma^p \otimes \Gamma^q = \Gamma^{p*q},$$

on the set of one-dimensional representations. The group axioms are straightforward fulfilled, with the trivial representation $\Gamma^1 = 1$ being the unit-element, while complex conjugation yields the inverse $\Gamma^{-1} = \bar{\Gamma}$. By definition the one-dimensional representations are the Abelian subset of all irreducible representations. Being Abelian means they are constant on all cosets of the commutator subgroup $G^{(1)}$, which makes them identical to the set of all irreducible representations of the Abelianization $G_{ab} = G/G^{(1)}$ and therefore also isomorphic to the Abelianization itself. We can thus think of $p, \tilde{p}$ as group homomorphisms from G to its Abelianization G_{ab}. They are characterized by normal subgroups $G^{(1)} \subseteq N_p, N_{\tilde{p}} \subseteq G$, which form the kernel of their maps

$$N_p = p^{-1}(e), \qquad\qquad N_{\tilde{p}} = \tilde{p}^{-1}(e).$$

A theory which is symmetric under the exchange of the two sublattices should obey

$$N_p = \phi(N_{\tilde{p}}) = N_\omega, \tag{69}$$

for some automorphism $\phi \in \mathrm{Aut}(G)$. They are therefore characterized by a single normal subgroup N_ω. For non-symmetric theories the two subgroups are not related by an automorphism, but they have the same size $|N_p| = |N_{\tilde{p}}|$ and their quotient groups are isomorphic $G/N_p \simeq G/N_{\tilde{p}}$.

11.4.2 Abelianization

Without loss of generality we can write the homomorphic twist as a map in terms of the Abelianization $G_{ab} = G/G^{(1)}$

$$\omega :\ G_{ab} \times G_{ab} \to U(1).$$

Any finite Abelian group G_{ab} can be written unambiguously as the product of cyclic groups $G_{ab} = \bigotimes_{i=1}^{u} \mathbb{Z}(n_i)$, where the order of each cyclic group is a divisor of all subsequent orders $n_i | n_j, \forall i \leq j$. The twist can then be factorized into twists among pairs of cyclic groups $\omega_{ij} :\ \mathbb{Z}(n_i) \times \mathbb{Z}(n_j) \to U(1)$

$$\omega(g,h) = \prod_{i,j=1}^{u} \omega_{ij}(g_i, h_j).$$

Since we know that the group G_{ab} is finitely generated, it is sufficient to specify the twist on the generating set $\{\hat{g}_i\}_{i=1}^u$, where $\hat{g}_i$ has order n_i and generates the i-th factor in G_{ab}. We can the identify

$$\omega_{ij}(\hat{g}_i, \hat{g}_j) \equiv \omega(\hat{g}_i, \hat{g}_j),$$

and the product structure is inherited from the group. Classification of homomorphisms from a cyclic group $\mathbb{Z}(n_j)$ to the dual (the representations) of the cyclic group $\mathbb{Z}(n_j)$ (which is again the cyclic group $\mathbb{Z}(n_j)$) is then given by simple number theory. Writing the group law additively, with generators $\hat{g}_i = 1 = \hat{g}_j$ the twist is characterized by the single phase $\omega_{ij} = \omega_{ij}(1,1)$, which has to fulfill the consistency conditions

$$\omega_{ij}(n_i, 1) = \omega_{ij}^{n_i} = 1 = \omega_{ij}^{n_j} = \omega_{ij}(1, n_j).$$

So ω_{ij} has to be a n_i-th and n_j-th root of unity simultaneously. By construction, one order has to be a divisor of the other, so we get ($n_{ij} = \min(n_i, n_j)$)

$$\omega_{ij} = \exp(i\frac{2\pi k_{ij}}{n_{ij}}), \quad k_{ij} \in \mathbb{Z}(n_{ij}).$$

The full twist ω is therefore unambiguously characterized by a $u \times u$-matrix k_{ij}. Writing $g = (g_1, g_2, \ldots, g_u)^t$ and $K_{ij} = 2\pi k_{ij}/n_{ij}$ we get

$$\omega(g, h) = \exp(ig^t \cdot K \cdot h).$$

It is straightforward to calculate the total number of possible twists

$$|\{\omega\}| = \prod_{i,j=1}^{u} n_{ij}.$$

11.5 Finite Group Examples

We continue the discussion by choosing $\mathbb{Z}(k), S_3, \bar{D}_2, \Delta(27)$ as examples of small discrete finite groups to illustrate some of the key features of the doubled Chern-Simons-Yang-Mills theories constructed so far.

11.5.1 The Abelian Groups $\mathbb{Z}(n)$

We start with the simple example of the cyclic groups $G = \mathbb{Z}(n)$. Their twists are characterized by a single number $k \in \mathbb{Z}(n)$

$$\omega_k(g, h) = \exp(i2\pi gkh/n).$$

Equivalence classes are formed by numbers with the same order

$$k \sim k' \qquad \Leftrightarrow \qquad \mathrm{ord}(k) = \mathrm{ord}(k'),$$

therefore we have a different theory for every divisor $k|n$ of the group order. Special cases are $k = 1, n$ (they are the only ones if n is prime) with twists

$$\omega_1(g, h) = \exp(i2\pi gh/n), \qquad \omega_n(g, h) = 1,$$

which we call the maximal and the trivial twist, respectively.

11.5.2 The Permutation Group S_3

The Abelianization of the permutation group $G = S_3$ is $G_{ab} = \mathbb{Z}(2)$ (odd and even permutations). As its order is prime, we only get the trivial $\omega = 1$ and the maximal theory ($g, h \in \mathbb{Z}(2)$)

$$\omega(g, h) = (-1)^{gh}.$$

11.5.3 The Quaternion Group $H \equiv \bar{D}_2$

The commutator subgroup of the quaternion group is equal to its center $\pm e$, therefore its Abelianization is $G_{ab} = \mathbb{Z}(2) \times \mathbb{Z}(2)$, a group of order 4 (the Abelianization identifies $i \sim -i$, therefore it has no elements of order 4 anymore). This group is generated by two elements, so $k_{ij} \in \mathbb{Z}(2)$ has four elements. This gives a total of $2^4 = 16$ theories, which we can split into three conjugacy classes. The trivial class has only one element with $k = 0$, an intermediate class with those nine elements $k \neq 0$ with linearly dependent columns (modulo 2) and finally the 6 maximal theories with linearly independent columns. The dependencies of the columns tells us something about the image of the homomorphism defined by $k : G_{ab} \to G_{ab}$, which is the trivial group $\{e\}$, $\mathbb{Z}(2)$, and $\mathbb{Z}(2) \times \mathbb{Z}(2)$ for the three different theories respectively. All of them have a manifestly symmetric representation, for instance

$$k \quad \in \quad \left\{ \begin{pmatrix} 0 & 0 \\ 0 & 0 \end{pmatrix}, \begin{pmatrix} 1 & 0 \\ 0 & 0 \end{pmatrix}, \begin{pmatrix} 1 & 0 \\ 0 & 1 \end{pmatrix} \right\}. \tag{70}$$

11.5.4 The Group $\Delta(27)$

The group $G = \Delta(27)$ is the $SU(3)$ analogue to the quaternion group. Its elements are given by ($\xi_3 = e^{i\frac{2\pi}{3}}$)

$$G = \{T^a Q^b R^c,\ a, b, c = 0, 1, 2\},$$
$$T = \begin{pmatrix} 0 & 0 & 1 \\ 1 & 0 & 0 \\ 0 & 1 & 0 \end{pmatrix}, \qquad Q = \begin{pmatrix} 1 & 0 & 0 \\ 0 & \xi_3 & 0 \\ 0 & 0 & \xi_3^{-1} \end{pmatrix}, \qquad R = \begin{pmatrix} \xi_3 & 0 & 0 \\ 0 & \xi_3 & 0 \\ 0 & 0 & \xi_3 \end{pmatrix}.$$

Its commutator subgroup is also equal to its center $C(G) = G^{(1)} \cong \mathbb{Z}(3)$, therefore its Abelianization is $G_{ab} = \mathbb{Z}(3) \times \mathbb{Z}(3)$ a group of order 9 ($\Delta(27)$ has only elements of order 1, 3, therefore its Abelianization cannot have an element of order 9). This group is generated by two elements, so $k_{ij} \in \mathbb{Z}(3)$ has again four elements. This gives a total of $3^4 = 81$ theories, which we can split into three conjugacy classes. The trivial class has only one element with $k = 0$, an intermediate class with those 32 elements $k \neq 0$ with linearly dependent columns (modulo 3) and finally the 48 maximal theories with linearly independent columns. The image of the homomorphism k is either the trivial group $\{e\}$, $\mathbb{Z}(3)$, or $\mathbb{Z}(3) \times \mathbb{Z}(3)$ for the three conjugacy classes. The matrices (70) are again examples of manifestly symmetric class representatives.

11.6 Spectrum of the Electric Hamiltonian

11.6.1 Projection Operators

The spectrum of the electric Hamiltonian on a single cross (71) can be understood in terms of the three normal subgroups

$$N_1 = G^{(1)} \quad \subseteq \quad N_\omega = \{g \in G : \omega(g, h) = 1, \forall h \in G\} \quad \subseteq \quad N_0 = G,$$

and the projection operators associated with them

$$P_i = \frac{1}{|N_i|} \sum_{g \in N_i} h(g), \qquad \tilde{P}_i = \frac{1}{|N_i|} \sum_{g \in N_i} \tilde{h}(g).$$

All of them commute except

$$P_0 \tilde{P}_0 \neq \tilde{P}_0 P_0,$$

for any non-trivial twist with $N_\omega \neq G$. Coincidentally, the non-Abelian groups $S_3, \bar{D}_2, \Delta(27)$ all share the property that the set of nearest neighbors spans the whole group except for their commutator subgroups

$$H = \{g \in G : \langle e, g \rangle\} = G \setminus G^{(1)}.$$

i	$(n,\tilde{n})$	$2E_i/(e^2\lvert G\rvert)$	d_i
0	$(2,2)^+$	$1-\lvert G_\omega\rvert^{-1/2}$	$\lvert G_\omega\rvert$
1	$(0,3),(3,0)$	$1-\lvert G_{ab}\rvert^{-1}$	$2(\lvert G\rvert-\lvert G_{ab}\rvert)$
2	$(1,3),(3,1)$	1	$2(\lvert G_{ab}\rvert-\lvert G_\omega\rvert)$
3	$(2,2)^-$	$1+\lvert G_\omega\rvert^{-1/2}$	$\lvert G_\omega\rvert$
4	$(0,0)$	$2-2\lvert G_{ab}\rvert^{-1}$	$(\lvert G\rvert-\lvert G_{ab}\rvert)^2$
5	$(0,1),(0,2),(1,0),(2,0)$	$2-\lvert G_{ab}\rvert^{-1}$	$2(\lvert G\rvert-\lvert G_{ab}\rvert)(\lvert G_{ab}\rvert-1)$
6	$(1,1),(1,2),(2,1),(2,2)^0$	2	$\lvert G_{ab}\rvert(\lvert G_{ab}\rvert-2)$

Figure 17: The full spectrum of the electric Hamiltonian for the non-Abelian groups $G = S_3, \bar{D}_2, \Delta(27)$. As $|G_\omega|$ divides both $|G_{ab}|$ and $|G|$ all degeneracies d_i are multiples of $|G_\omega|$. In some special cases the degeneracy of some level vanishes, $d_6 = 0$ for S_3 ($|G_{ab}| = 2$) and $d_2 = 0$ for maximally twisted theories ($G_\omega = G_{ab}$). By accident some of these levels may have the same energy, $E_4 = E_2$ for S_3 and $E_3 = E_6$ for the trivial theory ($|G_\omega| = 1$). The order of the levels $i = 3, 4, 5$ may change in some theories. The ground state is always given by $(2,2)^+$ (72) and is $|G_\omega|$-fold degenerate. States with $n, \tilde{n} = 0$ carry non-Abelian flux, the first excited states $i = 1$ always carry non-Abelian flux on one link.

This implies that H is a union of cosets of $N_1 = G^{(1)}$ and we can thus factor the Abelian projectors $P_1, \tilde{P}_1$ from the hopping terms

$$\begin{aligned}\frac{2}{e^2}\mathbb{H}_E &= 2|H| - \sum_{g\in H}(h(g)P_1 + \tilde{h}(g)\tilde{P}_1)\\ &= 2|H| - (\sum_{g\in G} h(g) - |N_1|)P_1 - (\sum_{g\in G}\tilde{h}(g) - |N_1|)\tilde{P}_1\\ &= 2|H| - (|N_0|P_0 - |N_1|)P_1 - (|N_0|\tilde{P}_0 - |N_1|)\tilde{P}_1\\ &= 2|H| + |N_1|(P_1+\tilde{P}_1) - |N_0|(P_0+\tilde{P}_0). \end{aligned} \tag{71}$$

Although the projectors $P_\omega, \tilde{P}_\omega$ do not appear in the Hamiltonian, they are key to identifying the subspace, where $[P_0, \tilde{P}_0] \neq 0$, since

$$[P_0, \tilde{P}_0] = [P_0P_\omega, \tilde{P}_0\tilde{P}_\omega] = [P_0, \tilde{P}_0]P_\omega\tilde{P}_\omega.$$

Thus only for the states $P_\omega\tilde{P}_\omega|\psi\rangle = |\psi\rangle$ is the Hamiltonian (71) not a sum of mutually commuting operators. For all other states the energy can be read off immediately. If we define the two quantum numbers

$$n = P_1 + P_\omega + P_0(1-\tilde{P}_\omega), \qquad \tilde{n} = \tilde{P}_1 + \tilde{P}_\omega + \tilde{P}_0(1-P_\omega),$$

then all states with the same quantum numbers $(n, \tilde{n})$ are degenerate, except for the sector $n = \tilde{n} = 2$ (for the full spectrum see figure 17).

11.6.2 The Twisted Sector $(n, \tilde{n}) = (2, 2)$

The states with $n = \tilde{n} = 2$ ($P_\omega\tilde{P}_\omega|\psi\rangle = |\psi\rangle$) form the only sector where $P_0 \neq 0 \neq \tilde{P}_0$, such that the Hamiltonian contains non-commuting terms. The cosets $C, \tilde{C}$ of N_ω provide an orthonormal basis for this sector

$$|C, \tilde{C}\rangle = \frac{1}{|N_\omega|}\sum_{g\in C}\sum_{h\in\tilde{C}}|g,h\rangle.$$

Since all the transformation and hopping operators commute with $P_\omega, \tilde{P}_\omega$, they form a representation of the algebra within this sector and we write

$$L(C)|C', \tilde{C}\rangle = \omega(C, \tilde{C})|C' + C, \tilde{C}\rangle, \ldots,$$

where $L(C) = P_\omega L(g \in C)$ and we use the additive notation for the quotient group $C \in G_\omega = G/N_\omega$ (which is an Abelian group since $G^{(1)} \subset N_\omega$). On these cosets the twist obeys the completeness relations

$$\sum_{\tilde{C}} \omega(C,\tilde{C})\bar{\omega}(C',\tilde{C}) = |G_\omega|\delta_{C,C'}, \qquad \sum_{C} \omega(C,\tilde{C})\bar{\omega}(C,\tilde{C}') = |G_\omega|\delta_{\tilde{C},\tilde{C}'},$$

which define a discrete Fourier transformation on G_ω. We leverage this to define a new set of basis states

$$\begin{aligned}
|C,Q\rangle &= L(Q)\frac{1}{\sqrt{|G_\omega|}}\sum_{\tilde{C}}|C,\tilde{C}\rangle = \frac{1}{\sqrt{|G_\omega|}}\sum_{\tilde{C}}\omega(Q,\tilde{C})|C+Q,\tilde{C}\rangle,\\
\langle C',Q'|C,Q\rangle &= \frac{1}{|G_\omega|}\sum_{\tilde{C},\tilde{C}'}\bar{\omega}(Q',\tilde{C}')\omega(Q,\tilde{C})\langle C'+Q',\tilde{C}'|C+Q,\tilde{C}\rangle\\
&= \delta_{C'+Q',C+Q}\frac{1}{|G_\omega|}\sum_{\tilde{C},\tilde{C}'}\bar{\omega}(Q',\tilde{C})\omega(Q,\tilde{C})\\
&= \delta_{C',C}\,\delta_{Q',Q},
\end{aligned}$$

which have the advantage that they separate the action of the transformations

$$L(C')|C,Q\rangle = |C,Q+C'\rangle, \qquad \tilde{L}(C')|C,Q\rangle = \bar{\omega}(Q,C')|C,Q\rangle,$$

from that of the hopping terms

$$h(C')|C,Q\rangle = |C+C',Q\rangle, \qquad \tilde{h}(C')|C,Q\rangle = \omega(C,C')|C,Q\rangle.$$

In this basis it is manifest how the twist ω ensures a minimal degeneracy $|G_\omega|$ (labeled by Q) in this sector. The electric Hamiltonian (71) now acts solely on the states $|C\rangle$ and is given by

$$\frac{2}{e^2}\mathbb{H}_E = |G|(2 - P_0 - \tilde{P}_0), \qquad P_0 = |\Theta\rangle\langle\Theta|, \qquad \tilde{P}_0 = |\tilde{\Theta}\rangle\langle\tilde{\Theta}|,$$

where the two projector eigenstates are given by

$$|\Theta\rangle = \frac{1}{\sqrt{|G_\omega|}}\sum_{C}|C\rangle, \qquad |\tilde{\Theta}\rangle = |G_\omega\rangle, \qquad \langle\Theta|\tilde{\Theta}\rangle = \frac{1}{\sqrt{|G_\omega|}}.$$

The states $|\Theta\rangle, |\tilde{\Theta}\rangle$ provide the two eigenstates

$$|\pm\rangle = \frac{1}{\sqrt{2+2|G_\omega|^{-1/2}}}(|\Theta\rangle \pm |\tilde{\Theta}\rangle), \qquad \frac{2}{e^2}\mathbb{H}_E|\pm\rangle = |G|\left(1 \mp |G_\omega|^{-1/2}\right) \tag{72}$$

We will label these states with $(2,2)^\pm$ respectively, while the remaining $|G_\omega|(|G_\omega|-2)$ states of energy $e^2|G|$ will be labeled as $(2,2)^0$ (compare with figure 17).

11.7 Abelian Anyons

We conclude the analysis of the doubled Chern-Simons-Yang-Mills theory, by showing that in the strong coupling limit $e^2 \to \infty$, where the electric Hamiltonian dominates, the primal and dual Abelian charges exhibit mutual Abelian anyonic statistics.

11.7.1 Parallel Charge Transporters

The parallel charge transporters for an Abelian charge Γ^p are defined as

$$\mathcal{U}(\Gamma^p)|U,\tilde{U}\rangle = \Gamma^p(U)|U,\tilde{U}\rangle, \qquad \tilde{\mathcal{U}}(\Gamma^p)|U,\tilde{U}\rangle = \Gamma^p(\tilde{U})|U,\tilde{U}\rangle. \tag{73}$$

The commutation relations with the transformation operators

$$\begin{aligned}
L(g)R(h)\mathcal{U}(\Gamma^p)|U,\tilde{U}\rangle &= \Gamma^p(U)\omega(gh^{-1},\tilde{U})|gUh^{-1},\tilde{U}\rangle,\\
&= \bar{\Gamma}^p(g)\Gamma^p(h)\mathcal{U}(\Gamma^p)L(g)R(h)|U,\tilde{U}\rangle,\\
\tilde{L}(g)\tilde{R}(h)\tilde{\mathcal{U}}(\Gamma^p)|U,\tilde{U}\rangle &= \bar{\Gamma}^p(g)\Gamma^p(h)\tilde{\mathcal{U}}(\Gamma^p)\tilde{L}(g)\tilde{R}(h)|U,\tilde{U}\rangle,
\end{aligned}$$

show that they remove a charge Γ^p on the left and add one on the right end of the link.

11.7.2 Anyonic Statistics

The proof of mutual Abelian anyonic statistics between primal and dual charges is very simple. Imagine a plaquette of the primal lattice consisting of four crosses. We assume that each cross is in one of the ground states of its electric Hamiltonian $|\psi\rangle = \otimes|0\rangle$. Additionally we put an Abelian charge Γ^p on the dual site at the center of the plaquette, thus $\tilde{V}(g)|\psi\rangle = \Gamma^p(g)|\psi\rangle$. Now we move a primal charge Γ^k counter-clockwise around the plaquette using the parallel charge transporters (73) thus returning to a state $|\psi'\rangle$ in the same charge sector as $|\psi\rangle$ and we can formally write

$$|\psi'\rangle = \Gamma^k(\hat{U}_\square)|\psi\rangle = \omega(\hat{U}_\square, g)|\psi\rangle,$$

where we assume that $\Gamma^k = \tilde{p}(g)$ for some $g \in G$ (only those charges $\Gamma^k \subset \tilde{p}(G)$ which are part of the twist show anyonic statistics, the others are even confining as their fluxes are gapped from the ground state). Using (68) we can rewrite the final state as

$$|\psi'\rangle = \tilde{H}(g)^{-1}\tilde{V}(g)|\psi\rangle.$$

We are now interested in the phase accumulated with respect to the initial state $|\psi\rangle$

$$\begin{aligned}\langle\psi|\psi'\rangle &= \langle\psi|\tilde{H}(g)^{-1}\tilde{V}(g)|\psi\rangle \\ &= \langle\psi|\tilde{H}(g)^{-1}|\psi\rangle\Gamma^p(g).\end{aligned}$$

The form of the ground-state of the individual crosses guarantees that the prefactor

$$1 \geq \langle\psi|\tilde{H}(g)^{-1}|\psi\rangle = (\langle 0|\tilde{h}(g)^{-1}|0\rangle)^4 > 0$$

is real and positive. Thus the braiding of a primal charge $\Gamma^k = \tilde{p}(g)$ and a dual charge Γ^p generates an Abelian phase $\Gamma^p(g)$. The prefactor is generally not equal to 1 since the charge transporter does not commute with the electric Hamiltonian, thus it excites the links. This is irrelevant for the discussion here, but could in principle be overcome by an adiabatic charge-transport procedure. It is not at all surprising to find Abelian anyons in the strong coupling limit. After projecting all links to the ground state, we are left with implementing the Gauss-law on the primal and dual lattice. The degeneracy of a single link is characterized by the quotient group $G_\omega = G/N_\omega$. The states can be characterized by the eigenvalues of the dual transformation operators $\tilde{L}$, while the primal transformation operators act as raising/lowering operators in G_ω. Since the gauge transformation operators $V, \tilde{V}$ all commute, they can be interpreted as stabilizer operators in a toric code with the $\mathbb{Z}(2)$-spins replaced by G_ω-spins. Defects are constructed by simply assigning non-trivial Abelian charges to the primal and dual lattice.

12 Conclusions

We have derived doubled Chern-Simons-Yang-Mills gauge theories on the lattice for arbitrary discrete gauge groups G. These theories are characterized by a finite Hilbert space of dimension $|G|^2$ on each cross of primal and dual lattice links. The Chern-Simons character is introduced by a non-trivial commutator of the primal and dual electric field components (and transformation operators) on each cross. We have characterized all such twisted algebras in terms of subgroups of the Abelianization of the gauge group G_{ab}. Furthermore we have calculated the spectrum of the electric Hamiltonian on a single cross for the non-Abelian groups $S_3, \bar{D}_2, \Delta(27)$ and have shown that the state degeneracy is related to a quotient-group of the Abelianization. In the infinite mass limit $e \to \infty$ we can calculate the (global) ground state exactly for any charge sector, from the degenerate ground states of the single cross. The dual nature of primal and dual transformation operators on the degenerate states allows us to reinterpret the Gauss law as stabilizer operators in a generalized toric code and we show explicitly the presence of mutual fractional statistics among primal and dual charges.

However the anyons are only Abelian, although we explicitly investigated non-Abelian gauge groups. The reason for this shortcoming is easily found. Our doubled lattice construction allows us to create interactions between dual quantities, by twisting their commutators. The twisting is induced by maps from the gauge-group to the representations $p, \tilde{p} : G \to \Gamma^G$. In our derivation we show that these maps have to be group-homomorphism. The set of representations, however, is associated with fusion rules, which generally form a semi-group (fusion with a non-Abelian representation is non-reversible, the Abelian representations form a subgroup). Thus the image of our maps lies within the Abelian representations only. The dual magnetic flux around a primal site can thus only act as an effective Abelian primal charge. The infinite mass limit then effectively projects the theory to a generalized toric code with gauge group G_{ab}, because the non-Abelian flux states are not protected by any symmetry.

Despite its obvious limitations, our theory is well-defined and incorporates the fundamental features we have encountered studying the compact $U(1)$ doubled gauge theories with Chern-Simons term. We can construct a self-consistent, mutually non-commutative operator-algebra on crossing links of the primal and dual lattice. The non-commuting transformation operators of the two crossing links generate a symmetry of the electric Hamiltonian and thus lead to degenerate eigenstates. The magnetic fluxes on plaquettes mimic electric charges on their dual site. This generates the Abelian anyonic statistics that can be observed by braiding primal and dual charges.

Acknowledgments

Support comes in many forms and I would like to seize this opportunity to express my gratitude for all of them.

First of all I would like to thank Uwe-Jens Wiese for the opportunity to complete my PhD as a part of his research team. He provided an inspiring work environment and I am grateful for every bit of knowledge he passed on to me. Especially his propensity for precise language and his style of teaching have been an inspiration and will accompany me in my future career.

Further I am very grateful to my collaborators and co-authors Therkel Olesen, Nadiia Vlasii, Florian Hebenstreit and David Mesterhazy who contributed a lot to the work presented in this thesis. Thank you all for sharing your insights and knowledge as well as pushing the progress on these subjects.

I would also like to thank my fellow students Sascha Schwarz, Jason Aebischer, Carla Gross, Adrian Oeftiger, Anina Steinlin, Simon Dürr and especially Manuel Meyer, with whom I also had the pleasure of sharing an office for a couple of years. All the discussions we have had over the years have elevated my curiosity about physics to the point where I had to pursue a PhD.

Last but not least I want to extend my gratitude and thankfulness to my family and friends, for all the support, patience and understanding that allowed me to accomplish each of my degrees including this one.

Mads and Miriam, there has not been a single hard day in completing this thesis, as each day started and ended with you two.

References

[1] S. R. White, "Density matrix formulation for quantum renormalization groups," *Phys. Rev. Lett.* **69** (Nov, 1992) 2863–2866. https://link.aps.org/doi/10.1103/PhysRevLett.69.2863.

[2] U. Schollwöck, "The density-matrix renormalization group," *Rev. Mod. Phys.* **77** (Apr, 2005) 259–315. https://link.aps.org/doi/10.1103/RevModPhys.77.259.

[3] M. A. Cazalilla and J. B. Marston, "Time-dependent density-matrix renormalization group: A systematic method for the study of quantum many-body out-of-equilibrium systems," *Phys. Rev. Lett.* **88** (Jun, 2002) 256403. https://link.aps.org/doi/10.1103/PhysRevLett.88.256403.

[4] G. Vidal, "Efficient simulation of one-dimensional quantum many-body systems," *Phys. Rev. Lett.* **93** (Jul, 2004) 040502. https://link.aps.org/doi/10.1103/PhysRevLett.93.040502.

[5] F. Verstraete, J. J. García-Ripoll, and J. I. Cirac, "Matrix product density operators: Simulation of finite-temperature and dissipative systems," *Phys. Rev. Lett.* **93** (Nov, 2004) 207204. https://link.aps.org/doi/10.1103/PhysRevLett.93.207204.

[6] S. R. White and A. E. Feiguin, "Real-time evolution using the density matrix renormalization group," *Phys. Rev. Lett.* **93** (Aug, 2004) 076401. https://link.aps.org/doi/10.1103/PhysRevLett.93.076401.

[7] G. Lindblad, "On the generators of quantum dynamical semigroups," *Communications in Mathematical Physics* **48** no. 2, (1976) 119–130.

[8] J. Poyatos, J. Cirac, and P. Zoller, "Quantum reservoir engineering with laser cooled trapped ions," *Phys. Rev. Lett.* **77** no. 23, (1996) 4728.

[9] F. Verstraete, M. M. Wolf, and J. I. Cirac, "Quantum computation and quantum-state engineering driven by dissipation," *Nature physics* **5** no. 9, (2009) 633.

[10] M. J. Kastoryano, F. Reiter, and A. S. Sørensen, "Dissipative preparation of entanglement in optical cavities," *Phys. Rev. Lett.* **106** no. 9, (2011) 090502.

[11] R. Sweke, I. Sinayskiy, and F. Petruccione, "Dissipative preparation of large w states in optical cavities," *Phys. Rev. A* **87** no. 4, (2013) 042323.

[12] E. G. Dalla Torre, J. Otterbach, E. Demler, V. Vuletic, and M. D. Lukin, "Dissipative preparation of spin squeezed atomic ensembles in a steady state," *Phys. Rev. Lett.* **110** no. 12, (2013) 120402.

[13] R. C. F. Caballar, S. Diehl, H. Mäkelä, M. Oberthaler, and G. Watanabe, "Dissipative preparation of phase- and number-squeezed states with ultracold atoms," *Phys. Rev. A* **89** no. 1, (2014) 013620.

[14] R. Sweke, I. Sinayskiy, and F. Petruccione, "Simulation of single-qubit open quantum systems," *Phys. Rev. A* **90** no. 2, (2014) 022331.

[15] R. Sweke, I. Sinayskiy, D. Bernard, and F. Petruccione, "Universal simulation of Markovian open quantum systems," *Phys. Rev. A* **91** no. 6, (2015) 062308.

[16] P. Zanardi, J. Marshall, and L. C. Venuti, "Dissipative universal Lindbladian simulation," *Phys. Rev. A* **93** no. 2, (2016) 022312.

[17] M. Kliesch, T. Barthel, C. Gogolin, M. Kastoryano, and J. Eisert, "Dissipative quantum Church-Turing theorem," *Phys. Rev. Lett.* **107** no. 12, (2011) 120501.

[18] F. Pastawski, L. Clemente, and J. I. Cirac, "Quantum memories based on engineered dissipation," *Phys. Rev. A* **83** no. 1, (2011) 012304.

[19] I. Sinayskiy and F. Petruccione, "Dissipative quantum computing with open quantum walks," in *AIP Conference Proceedings*, vol. 1633, pp. 186–188, AIP. 2014.

[20] E. Jané, G. Vidal, W. Dür, P. Zoller, and J. I. Cirac, "Simulation of quantum dynamics with quantum optical systems," *Quantum Info. Comput.* **3** no. 1, (Jan., 2003) 15–37. `http://dl.acm.org/citation.cfm?id=2011508.2011510`.

[21] I. Bloch, J. Dalibard, and S. Nascimbène, "Quantum simulations with ultracold quantum gases," *Nature Physics* **8** (2012) 267. `http://dx.doi.org/10.1038/nphys2259`.

[22] R. Blatt and C. F. Roos, "Quantum simulations with trapped ions," *Nature Physics* **8** (2012) 277. `http://dx.doi.org/10.1038/nphys2252`.

[23] I. Buluta and F. Nori, "Quantum simulators," *Science* **326** no. 5949, (2009) 108–111. `http://science.sciencemag.org/content/326/5949/108`.

[24] I. M. Georgescu, S. Ashhab, and F. Nori, "Quantum simulation," *Rev. Mod. Phys.* **86** (Mar, 2014) 153–185. `https://link.aps.org/doi/10.1103/RevModPhys.86.153`.

[25] H.-P. Breuer and F. Petruccione, *The theory of open quantum systems*. Oxford University Press on Demand, 2007.

[26] M. Esposito and P. Gaspard, "Exactly solvable model of quantum diffusion," *Journal of statistical physics* **121** no. 3-4, (2005) 463–496.

[27] M. Esposito and P. Gaspard, "Emergence of diffusion in finite quantum systems," *Phys. Rev. B* **71** no. 21, (2005) 214302.

[28] V. Eisler, "Crossover between ballistic and diffusive transport: the quantum exclusion process," *Journal of Statistical Mechanics: Theory and Experiment* **2011** no. 06, (2011) P06007.

[29] B. Horstmann, J. I. Cirac, and G. Giedke, "Noise-driven dynamics and phase transitions in fermionic systems," *Phys. Rev. A* **87** no. 1, (2013) 012108.

[30] M. Žnidarič, "Relaxation times of dissipative many-body quantum systems," *Phys. Rev. E* **92** no. 4, (2015) 042143.

[31] E. Huffman, D. Banerjee, S. Chandrasekharan, and U.-J. Wiese, "Real-time evolution of strongly coupled fermions driven by dissipation," *Annals of physics* **372** (2016) 309–319.

[32] B. Žunkovič, "Closed hierarchy of correlations in Markovian open quantum systems," *New Journal of Physics* **16** no. 1, (2014) 013042.

[33] J. T. Barreiro, M. Müller, P. Schindler, D. Nigg, T. Monz, M. Chwalla, M. Hennrich, C. F. Roos, P. Zoller, and R. Blatt, "An open-system quantum simulator with trapped ions," *Nature* **470** no. 7335, (2011) 486.

[34] P. Schindler, M. Müller, D. Nigg, J. T. Barreiro, E. A. Martinez, M. Hennrich, T. Monz, S. Diehl, P. Zoller, and R. Blatt, "Quantum simulation of dynamical maps with trapped ions," *Nature Physics* **9** no. 6, (2013) 361.

[35] H. Weimer, M. Müller, I. Lesanovsky, P. Zoller, and H. P. Büchler, "A rydberg quantum simulator," *Nature Physics* **6** no. 5, (2010) 382.

[36] C.-E. Bardyn, M. Baranov, E. Rico, A. İmamoğlu, P. Zoller, and S. Diehl, "Majorana modes in driven-dissipative atomic superfluids with a zero Chern number," *Phys. Rev. Lett.* **109** no. 13, (2012) 130402.

[37] C. D. Freeman, C. M. Herdman, D. J. Gorman, and K. B. Whaley, "Relaxation Dynamics of the Toric Code in Contact with a Thermal Reservoir: Finite-Size Scaling in a Low-Temperature Regime," *Phys. Rev.* **B90** (2014) 134302, `arXiv:1405.2315 [cond-mat.stat-mech]`.

[38] N. Lang and H. P. Büchler, "Exploring quantum phases by driven dissipation," *Phys. Rev. A* **92** no. 1, (2015) 012128.

[39] S. Diehl, A. Micheli, A. Kantian, B. Kraus, H. Büchler, and P. Zoller, "Quantum states and phases in driven open quantum systems with cold atoms," *Nature Physics* **4** no. 11, (2008) 878.

[40] B. Kraus, H. P. Büchler, S. Diehl, A. Kantian, A. Micheli, and P. Zoller, "Preparation of entangled states by quantum Markov processes," *Phys. Rev. A* **78** no. 4, (2008) 042307.

[41] M. Roncaglia, M. Rizzi, and J. I. Cirac, "Pfaffian state generation by strong three-body dissipation," *Phys. Rev. Lett.* **104** no. 9, (2010) 096803.

[42] S. Diehl, E. Rico, M. A. Baranov, and P. Zoller, "Topology by dissipation in atomic quantum wires," *Nature Physics* **7** no. 12, (2011) 971.

[43] C. Bardyn, M. Baranov, C. Kraus, E. Rico, A. İmamoğlu, P. Zoller, and S. Diehl, "Topology by dissipation," *New Journal of Physics* **15** no. 8, (2013) 085001.

[44] J. C. Budich, P. Zoller, and S. Diehl, "Dissipative preparation of Chern insulators," *Phys. Rev. A* **91** no. 4, (2015) 042117.

[45] S. Diehl, W. Yi, A. Daley, and P. Zoller, "Dissipation-induced d-wave pairing of fermionic atoms in an optical lattice," *Phys. Rev. Lett.* **105** no. 22, (2010) 227001.

[46] W. Yi, S. Diehl, A. Daley, and P. Zoller, "Driven-dissipative many-body pairing states for cold fermionic atoms in an optical lattice," *New Journal of Physics* **14** no. 5, (2012) 055002.

[47] T. Prosen and I. Pižorn, "Quantum phase transition in a far-from-equilibrium steady state of an x y spin chain," *Phys. Rev. Lett.* **101** no. 10, (2008) 105701.

[48] M. Žnidarič, "Solvable quantum nonequilibrium model exhibiting a phase transition and a matrix product representation," *Phys. Rev. E* **83** no. 1, (2011) 011108.

[49] Z. Cai and T. Barthel, "Algebraic versus exponential decoherence in dissipative many-particle systems," *Phys. Rev. Lett.* **111** no. 15, (2013) 150403.

[50] N. Crawford, W. De Roeck, and M. Schütz, "Uniqueness regime for Markov dynamics on quantum lattice spin systems," *Journal of Physics A: Mathematical and Theoretical* **48** no. 42, (2015) 425203.

[51] S. Caspar, F. Hebenstreit, D. Mesterhazy, and U.-J. Wiese, "Dynamics of dissipative Bose-Einstein condensation," *Phys. Rev. A* **93** no. 2, (2016) 021602.

[52] S. Caspar, F. Hebenstreit, D. Mesterhazy, and U.-J. Wiese, "Dissipative Bose-Einstein condensation in contact with a thermal reservoir," *New journal of physics* **18** no. 7, (2016) 073015.

[53] M.-D. Choi, "Completely positive linear maps on complex matrices," *Linear algebra and its applications* **10** no. 3, (1975) 285–290.

[54] K. Kraus, *States, effects and operations: fundamental notions of quantum theory*. Springer, 1983.

[55] S. Bochner, *Vorlesungen über Fouriersche Integrale: von S. Bochner*, vol. 12. Akad. Verl.-Ges., 1932.

[56] D. Banerjee, F.-J. Jiang, M. Kon, and U.-J. Wiese, "Real-time simulation of large open quantum spin systems driven by dissipation," *Phys. Rev. B* **90** no. 24, (2014) 241104.

[57] F. Hebenstreit, D. Banerjee, M. Hornung, F.-J. Jiang, F. Schranz, and U.-J. Wiese, "Real-time dynamics of open quantum spin systems driven by dissipative processes," *Phys. Rev. B* **92** no. 3, (2015) 035116.

[58] D. Banerjee, F. Hebenstreit, F.-J. Jiang, and U.-J. Wiese, "Real-time simulation of nonequilibrium transport of magnetization in large open quantum spin systems driven by dissipation," *Phys. Rev. B* **92** no. 12, (2015) 121104.

[59] D. Mesterhazy and F. Hebenstreit, "Solvable Markovian dynamics of lattice quantum spin models," *Phys. Rev. A* **96** no. 1, (2017) 010104.

[60] P. L. Krapivsky, S. Redner, and E. Ben-Naim, *A kinetic view of statistical physics*. Cambridge University Press, 2010.

[61] H. Wichterich, M. J. Henrich, H.-P. Breuer, J. Gemmer, and M. Michel, "Modeling heat transport through completely positive maps," *Phys. Rev. E* **76** no. 3, (2007) 031115.

[62] T. Prosen, "Third quantization: a general method to solve master equations for quadratic open Fermi systems," *New Journal of Physics* **10** no. 4, (2008) 043026.

[63] R. Kubo, "Statistical-mechanical theory of irreversible processes. i. general theory and simple applications to magnetic and conduction problems," *Journal of the Physical Society of Japan* **12** no. 6, (1957) 570–586.

[64] R. Kubo, "The fluctuation-dissipation theorem," *Reports on progress in physics* **29** no. 1, (1966) 255.

[65] P. Benioff, "The computer as a physical system: A microscopic quantum mechanical hamiltonian model of computers as represented by turing machines," *Journal of Statistical Physics* **22** (1980) 563–591.

[66] R. P. Feynman, "Simulating Physics with Computers," *Int. J. Theor. Phys.* **21** (1982) 467.

[67] D. Deutsch, "Quantum theory, the church–turing principle and the universal quantum computer," *Proc. Royal Soc. A* **400** (1985) 97–117.

[68] T. Toffoli, "Reversible computing," in *Automata, Languages and Programming*, pp. 632–644. Springer Berlin Heidelberg, 1980.

[69] A. Barenco, C. H. Bennett, R. Cleve, D. P. DiVincenzo, N. Margolus, P. Shor, T. Sleator, J. A. Smolin, and H. Weinfurter, "Elementary gates for quantum computation," *Phys. Rev. A* **52** (1995) 3457–3467.

[70] P. W. Shor, "Polynomial-time algorithms for prime factorization and discrete logarithms on a quantum computer," *SIAM Journal on Computing* **26** (1997) 1484–1509.

[71] I. Bloch, J. Dalibard, and W. Zwerger, "Many-body Physics with Ultracold Gases," *Rev. Mod. Phys.* **80** (2008) 885.

[72] M. Lewenstein, A. Sanpera, and V. Ahufinger, *Ultracold Atoms in Optical Lattices: Simulating Quantum Many-Body Systems*. Oxford University Press, 2012.

[73] A. Kitaev, "Fault Tolerant Quantum Computation by Anyons," *Annals Phys.* **303** (2003) 2, `arXiv:quant-ph/9707021`.

[74] P. W. Shor, "Fault Tolerant Quantum Computation," `arXiv:quant-ph/9605011`.

[75] D. Gottesman, "A Theory of Fault Tolerant Quantum Computation," *Phys. Rev.* **A57** (1998) 127, arXiv:quant-ph/9702029.

[76] J. Preskill, "Fault Tolerant Quantum Computation," arXiv:quant-ph/9712048.

[77] A. Kitaev, "Anyons in an Exactly Solved Model and Beyond," *Annals Phys.* **321** (2006) 2.

[78] C. Nayak, S. H. Simon, A. Stern, M. Freedman, and S. Das Sarma, "Non-Abelian Anyons and Topological Quantum Computation," *Rev. Mod. Phys.* **80** (2008) 1083.

[79] F. Wilczek and A. Zee, "Linking Numbers, Spin, and Statistics of Solitons," *Phys. Rev. Lett.* **51** (1983) 2250.

[80] J. Fröhlich and P. A. Marchetti, "Quantum Field Theory of Anyons," *Lett. Math. Phys.* **16** (1988) 347.

[81] J. Fröhlich and P. A. Marchetti, "Quantum Field Theories of Vortices and Anyons," *Commun. Math. Phys.* **121** (1989) 177.

[82] F. Wilczek, ed., *Fractional Statistics and Anyon Superconductivity.* World Scientific, 1990.

[83] S.-S. Chern and J. Simons, "Characteristic Forms and Geometric Invariants," *Annals Math.* **99** (1974) 48.

[84] S. C. Zhang, T. H. Hansson, and S. Kivelson, "Effective-field-theory model for the fractional quantum hall effect," *Phys. Rev. Lett.* **62** (1989) 82–85.

[85] J. K. Jain, "Composite-fermion approach for the fractional quantum hall effect," *Phys. Rev. Lett.* **63** (1989) 199–202.

[86] S.-C. Zhang, "The Chern-Simons-Landau-Ginzburg theory of the fractional quantum Hall effect," *Int. J. Mod. Phys.* **B6** (1992) 25–58.

[87] P. Fendley and E. Fradkin, "Realizing non-Abelian statistics in time-reversal-invariant systems," *Phys. Rev.* **B72** (2005) 024412.

[88] S.-P. Kou, M. Levin, and X.-G. Wen, "Mutual chern-simons theory for Z_2 topological order," *Phys. Rev. B* **78** (2008) 155134.

[89] G. Palumbo and J. K. Pachos, "Abelian chern-simons-maxwell theory from a tight-binding model of spinless fermions," *Phys. Rev. Lett.* **110** (2013) 211603.

[90] K. G. Wilson, "Confinement of Quarks," *Phys. Rev.* **D10** (1974) 2445.

[91] R. Kantor and L. Susskind, "A Lattice Model of Fractional Statistics," *Nucl. Phys.* **B366** (1991) 533.

[92] D. Eliezer and G. W. Semenoff, "Anyonization and Novel Braid Structure in Dumbbell Chern-Simons Theory," *Phys. Lett.* **B266** (1991) 375.

[93] D. Eliezer and G. W. Semenoff, "Anyonization of Lattice Chern-Simons Theory," *Annals Phys.* **217** (1992) 66.

[94] D. Eliezer and G. W. Semenoff, "Intersection Forms and the Geometry of Lattice Chern-Simons Theory," *Phys. Lett.* **B286** (1992) 118, arXiv:hep-th/9204048.

[95] D. S. Freed and F. Quinn, "Chern-Simons Theory with Finite Gauge Group," *Commun. Math. Phys.* **156** (1993) 435, arXiv:hep-th/9111004.

[96] F. A. Bais, P. van Driel, and M. de Wild Propitius, "Quantum Asymmetries in Discrete Gauge Theories," *Phys. Lett.* **B280** (1992) 63, arXiv:hep-th/9203046.

[97] F. A. Bais, P. van Driel, and M. de Wild Propitius, "Anyons in Discrete Gauge Theories with Chern-Simons Terms," *Nucl. Phys.* **B393** (1993) 547, arXiv:hep-th/9203047.

[98] F. A. Bais and J. C. Romers, "Anyonic Order Parameters for Discrete Gauge Theories on the Lattice," *Annals Phys.* **324** (2009) 1168, arXiv:0812.2256 [cond-mat.mes-hall].

[99] J. B. Kogut and L. Susskind, "Hamiltonian Formulation of Wilson's Lattice Gauge Theories," *Phys. Rev.* **D11** (1975) 395.

[100] J. B. Kogut, "An Introduction to Lattice Gauge Theory and Spin Systems," *Rev. Mod. Phys.* **51** (1979) 659.

[101] J. B. Kogut, "A Review of the Lattice Gauge Theory Approach to Quantum Chromodynamics," *Rev. Mod. Phys.* **55** (1983) 775.

[102] Y.-H. Chen, F. Wilczek, E. Witten, and B. I. Halperin, "On Anyon Superconductivity," *Int. J. Mod. Phys.* **B3** (1989) 1001.

[103] X. G. Wen, F. Wilczek, and A. Zee, "Chiral Spin States and Superconductivity," *Phys. Rev.* **B39** (1989) 11413.

[104] G. W. Semenoff and N. Weiss, "3-D Field Theory Model of a Parity Invariant Anyonic Superconductor," *Phys. Lett.* **B250** (1990) 117.

[105] D. H. Adams, "A Doubled Discretization of Abelian Chern-Simons Theory," *Phys. Rev. Lett.* **78** (1997) 4155, arXiv:hep-th/9704150.

[106] M. Blau and G. Thompson, "Topological Gauge Theories of Antisymmetric Tensor Fields," *Annals Phys.* **205** (1991) 130.

[107] F. Berruto, M. C. Diamantini, and P. Sodano, "On Pure Lattice Chern-Simons Gauge Theories," *Phys. Lett.* **B487** (2000) 366, arXiv:hep-th/0004203.

[108] B. Douçot, L. B. Ioffe, and J. Vidal, "Discrete Non-Abelian Gauge Theories in Two-Dimensional Lattices and their Realizations in Josephson-Junction Arrays," *Phys. Rev.* **B69** (2004) 214501, arXiv:cond-mat/0302104.

[109] B. Douçot and L. B. Ioffe, "Non-Abelian Chern-Simons Models with Discrete Gauge Groups on a Lattice," *New J. Phys.* **7** (2005) 187, arXiv:cond-mat/0510612.

[110] E. Witten, "Quantum Field Theory and the Jones Polynomial," *Commun. Math. Phys.* **121** (1989) 351.

[111] M. Atiyah, "Topological Quantum Field Theories," *Inst. Hautes Etudes Sci. Publ. Math.* **68** (1989) 175.

[112] J. F. Schonfeld, "A Mass Term for Three-Dimensional Gauge Fields," *Nucl. Phys.* **B185** (1981) 157.

[113] R. Jackiw and S. Templeton, "How Superrenormalizable Interactions Cure their Infrared Divergences," *Phys. Rev.* **D23** (1981) 2291.

[114] S. Deser, R. Jackiw, and S. Templeton, "Topologically Massive Gauge Theories," *Annals Phys.* **140** (1982) 372. [Annals Phys. 281:409, 2000].

[115] S. Deser, R. Jackiw, and S. Templeton, "Three-Dimensional Massive Gauge Theories," *Phys. Rev. Lett.* **48** (1982) 975.

[116] W. M. Fairbairn, T. Fulton, and W. H. Klink, "Finite and Disconnected Subgroups of $SU(3)$ and their Application to the Elementary-Particle Spectrum," *J. Math. Phys.* **5** (1964) 1038.

[117] W. M. Fairbairn and T. Fulton, "Some Comments on Finite Subgroups of $SU(3)$," *J. Math. Phys.* **23** (1982) 1747.

[118] C. Luhn, S. Nasri, and P. Ramond, "The Flavor Group $\Delta(3n^2)$," *J. Math. Phys.* **48** (2007) 073501, arXiv:hep-th/0701188.

[119] P. O. Ludl, "Comments on the Classification of the Finite Subgroups of $SU(3)$," *J. Phys.* **A44** (2011) 255204, arXiv:1101.2308 [math-ph]. [Erratum: *J. Phys.* **A45** (2012) 069502].

[120] H. Bombin and M. A. Martin-Delgado, "A Family of Non-Abelian Kitaev Models on a Lattice: Topological Confinement and Condensation," *Phys. Rev.* **B78** (2008) 115421, arXiv:0712.0190 [cond-mat.str-el].

[121] M. A. Levin and X.-G. Wen, "String-Net Condensation: A Physical Mechanism for Topological Phases," *Phys. Rev.* **B71** (2005) 045110, arXiv:cond-mat/0404617.

[122] M. Aguado, G. K. Brennen, F. Verstraete, and J. I. Cirac, "Creation, Manipulation, and Detection of Abelian and Non-Abelian Anyons in Optical Lattices," *Phys. Rev. Lett.* **101** (2008) 260501, arXiv:0802.3163 [quant-ph].

[123] G. K. Brennen, M. Aguado, and J. I. Cirac, "Simulations of quantum double models," *New Journal of Physics* **11** (2009) 053009, arXiv:0901.1345 [quant-ph].

[124] E. Dennis, A. Kitaev, A. Landahl, and J. Preskill, "Topological Quantum Memory," *J. Math. Phys.* **43** (2002) 4452, arXiv:quant-ph/0110143.

[125] R. Alicki, M. Fannes, and M. Horodecki, "A Statistical Mechanics View on Kitaev's Proposal for Quantum Memories," *J. Phys. A: Math. Gen.* **40** (2007) 6451, arXiv:quant-ph/0702102.

[126] C. Castelnovo and C. Chamon, "Entanglement and Topological Entropy of the Toric Code at Finite Temperature," *Phys. Rev.* **B76** (2007) 184442, arXiv:0704.3616 [cond-mat.str-el].

[127] S. Chesi, B. Röthlisberger, and D. Loss, "Self-Correcting Quantum Memory in a Thermal Environment," *Phys. Rev.* **A82** (2010) 022305, arXiv:0908.4264 [quant-ph].

[128] C. G. Brell, S. Burton, G. Dauphinais, S. T. Flammia, and D. Poulin, "Thermalization, Error-Correction, and Memory Lifetime for Ising Anyon Systems," *Phys. Rev.* **X4** (2014) 031058, arXiv:1311.0019 [quant-ph].

[129] B. J. Brown, D. Loss, J. K. Pachos, C. N. Self, and J. R. Wootton, "Quantum Memories at Finite Temperature," arXiv:1411.6643 [quant-ph].

[130] T. Z. Olesen, N. D. Vlasii, and U.-J. Wiese, "From Doubled Chern-Simons-Maxwell Lattice Gauge Theory to Extensions of the Toric Code," *Annals Phys.* **361** (2015) 303, arXiv:1503.07023 [hep-lat].

[131] S. Caspar, D. Mesterházy, T. Z. Olesen, N. D. Vlasii, and U.-J. Wiese, "Doubled lattice Chern–Simons–Yang–Mills theories with discrete gauge group," *Annals Phys.* **374** (2016) 255–290, arXiv:1607.08825 [hep-lat].

[132] G. V. Dunne, "Aspects of Chern-Simons theory," in *Topological Aspects of Low-Dimensional Systems: Proceedings, Les Houches Summer School of Theoretical Physics*. 1998. arXiv:hep-th/9902115.

[133] M. Al-Hashimi and U.-J. Wiese, "Discrete accidental symmetry for a particle in a constant magnetic field on a torus," *Annals of physics* **324** no. 2, (2009) 343–360.